

PROTECTION AGAINST UNGROUNDED SINGLE PHASE OPEN CIRCUIT
FAULTS IN 3-PHASE DISTRIBUTION TRANSFORMERS

A Thesis

presented to

the Faculty of California Polytechnic State University,

San Luis Obispo

In Partial Fulfillment

of the Requirements for the Degree

Masters of Science in Electrical Engineering

by

Higinio Ariel Montoya

May 2018

© 2018

Higinio Ariel Montoya

ALL RIGHTS RESERVED

COMMITTEE MEMBERSHIP

TITLE: Protection Against Ungrounded Single Phase
Open Circuit Faults in 3-Phase Distribution
Transformers

AUTHOR: Higinio Ariel Montoya

DATE SUBMITTED: 5/2018

COMMITTEE CHAIR: Ali Shaban, Ph.D.
Professor of Electrical Engineering

COMMITTEE MEMBER: Taufik, Ph.D.
Professor of Electrical Engineering

COMMITTEE MEMBER: Ahmad Nafisi, Ph.D.
Professor of Electrical Engineering

ABSTRACT

Protection Against Ungrounded Single Phase Open Circuit Faults in 3-Phase Distribution Transformers

Higinio Ariel Montoya

This thesis explores the impacts and behavior of 3-phase distribution transformers when subject to ungrounded single phase open circuit faults. A simple 3-phase system is modeled using MATLAB Simulink and operation under fault conditions are simulated and studied. Simulation results are confirmed via lab experimentation. Finally, a robust detection and protection method using neutral current injection (as proposed in industry literature) is built and demonstrated.

Electric utility operating experience has demonstrated that all too often, loads on 3-phase distribution transformers are not adequately protected against an ungrounded single phase open circuit fault (commonly called “single phasing”). This type of fault is amongst the least understood and hence the least protected against. This is especially true at end of transmission system radial feeds where 3-phase transformers can re-create the opened phase voltage due to a variety of effects including magnetic coupling, voltage loops and loading effects. Operating experience in the nuclear power industry has shown that the results can be catastrophic especially considering the impacts to motor loads. Impacts can result in unavailability of emergency loads, tripping of motor protection circuits or even motor damage and failure.

Keywords: single phasing, open phase condition, transformer, MATLAB, three phase

ACKNOWLEDGMENTS

I dedicate this thesis to my wife Flor and our four sons Marcos, Rocky, Tony and Roberto who never let me give up and provided unconditional support and encouragement through long hours spent in the laboratory and libraries. I love you all very much.

I also dedicate this work to the memory of my mother Hortensia C. Montoya and to my father and siblings all of whom taught me that learning is the most precious gift in the world. They instilled in me the perseverance I needed to complete my graduate work despite the many challenges we faced together.

I want to thank Dr. Ali Shaban for his guidance, patience and kindness as I slowly completed this thesis in what time I could. Without his knowledge of power systems and suggestions in bounding this work, it would not have been possible to complete this thesis.

Thank you also to Cheryl-Anne Alfred. She came in to my life as a mentee but quickly became a mentor in completing this thesis.

Finally, I especially thank my employer, the Pacific Gas and Electric Company for assisting me with funding my graduate studies.

TABLE OF CONTENTS

	Page
LIST OF TABLES.....	viii
LIST OF FIGURES	ix
CHAPTER 1: INTRODUCTION	1
1.1 BACKGROUND OF PROBLEM STATEMENT (BYRON UNIT 2).....	3
1.2 PROBLEM STATEMENT	7
CHAPTER 2: LITERATURE REVIEW	8
2.1 CONCEPTUAL UNDERSTANDING OF OPEN PHASE CONDITION.....	10
2.2 EXISTING MODELING AND ANALYSIS TECHNIQUES	14
2.3 STANDARD DISTRIBUTION TRANSFORMER PROTECTION SCHEMES	21
2.4 METHOD FOR DETECTION OF OPEN PHASE FAULTS	27
CHAPTER 3: SYSTEM DESIGN AND ANALYSIS	30
3.1 SYSTEM ANALYSIS BY SYMMETRICAL COMPONENTS	31
3.2 SYSTEM ANALYSIS BY MATLAB SIMULINK	41
3.3 CURRENT INJECTION METHOD ANALYSIS BY COMPUTER SIMULATION.....	59
3.4 SUMMARY OF ANALYTICAL RESULTS.....	95
CHAPTER 4: SYSTEM TESTING, EVALUATION AND DISCUSSION.....	97
4.1 LABORATORY EXPERIMENTS FOR OBTAINING EQUIPMENT PARAMETERS ..	98
4.2 LABORATORY TESTING OF CURRENT INJECTION SYSTEM.....	104

CHAPTER 5: CONCLUSION	116
REFERENCES	119
APPENDIX 1: BENCH TRANSFORMER IMPEDANCE DATA	121
APPENDIX 2: MATLAB SIMULATION MODEL INFORMATION AND SETTINGS	127
APPENDIX 3: LABORATORY DATA ON CURRENT TRANSFORMER TESTING	142

LIST OF TABLES

	Page
Table 1: Laboratory Results of Case 1 Unloaded XFMR Secondary	110
Table 2: Laboratory Results for Case 2 Balanced Load on XFMR Secondary	112
Table 3: Laboratory Results of Case 3 Unbalanced XFMR Loading	115
Table 4: Bench 10 Transformer Open Circuit Data.....	121
Table 5: Bench 10 Transformer Base Parameters.....	122
Table 6: Bench 10 Transformer Short Circuit Test Data	123
Table 7: Bench 10 Transformer Zero Sequence Test Data	125
Table 8: CT Experiment 1 Data	143
Table 9: CT Experiment 2 Data	145
Table 10: CT Experiment 3 Data	147

LIST OF FIGURES

	Page
Figure 1: Typical Nuclear Power Plant Distribution Single Line Diagram	4
Figure 2: Diagram of Yg-D Distribution Transformer under Open Phase Fault	7
Figure 3: Voltage Re-Generation in a Yg-D Transformer During Open Phase Condition [5]	11
Figure 4: Voltage unbalance for a Y-D-Y transformer [6]	16
Figure 5: Standard Distribution Transformer Protection Scheme [9]	23
Figure 6: Schematic of Current Injection System under Open Phase Fault [10]	29
Figure 7: Schematic Diagram of 3-Phase Transformer with Open "A" Phase	31
Figure 8: Sequence Networks of the Ideal Voltage "Grid" Supply	34
Figure 9: Magnetic Circuit for Zero Sequence Flux	35
Figure 10: Sequence Networks for Unloaded Yg-D Transformer	36
Figure 11: Connected Sequence Network for Single Open Phase Fault on XFMR Primary	37
Figure 12: Simplified Sequence Network for Open Phase Fault	38
Figure 13: Simulink Model of Unloaded Transformer	42
Figure 14: XFMR Primary Terminal Voltage Open Phase at 0.05s	45
Figure 15: XFMR Primary Currents with Single Open Phase at 0.05s	46
Figure 16: XFMR Primary Side Neutral Current	48
Figure 17: Delta Winding Circulating Current Waveform (Amps)	48
Figure 18: RMS and Waveform Traces of XFMR Terminal Voltage 30% Load	50
Figure 19: RMS and Waveform Traces of XFMR Primary Currents 30% Load	51
Figure 20: RMS and Waveform Traces of XFMR Neutral Currents 30% Load	52
Figure 21: XFMR Secondary Side Voltage for 30% Loading	54
Figure 22: Secondary Side Coil Currents for 30% XFMR Loading (Amps)	55
Figure 23: Secondary Side RMS and Waveform Currents 30% XFMR Loading	57
Figure 24: MATLAB Model Focus on Current Injection Source	61

Figure 25: Primary XFMR Neutral Current with 180Hz Current Injection.....	63
Figure 26: Primary Side XFMR Terminal Voltage with Current Injection	64
Figure 27: XFMR Primary Side Currents with Current Injection.....	65
Figure 28: Secondary Side Voltage Traces for Unloaded XFMR with Current Injection	68
Figure 29: Secondary Winding Coil Currents Unloaded Including Current Injection	69
Figure 30: Primary Side Voltages for Balanced 30% Loaded XFMR with Current Injection	71
Figure 31: Primary Line Currents for 30% Loaded XFMR with Current Injection	72
Figure 32: Neutral Injection Current During 30% Loaded Scenario	73
Figure 33: 30% Loaded XFMR Secondary Voltages with Current Injection	74
Figure 34: 30% Loaded XFMR Secondary Side Currents with Current Injection	75
Figure 35: 30% Loaded XFMR Secondary Side Coil Currents with Current Injection	76
Figure 36: MATLAB Model for Unbalanced Loading (30%) on XFMR Secondary.....	77
Figure 37: Primary Side Voltages for Unbalanced Loaded XFMR with Current Injection	79
Figure 38: Primary Side Currents, Unbalanced Loaded XFMR with Current Injection.....	80
Figure 39: Neutral Injected Current, Unbalanced XFMR Loaded Scenario.....	81
Figure 40: Secondary Side Voltages, Unbalanced Loaded XFMR with Current Injection	82
Figure 41: Secondary Side Currents, Unbalanced Loaded Transformer with Current Injection...	83
Figure 42: Secondary Side Coil Currents, Unbalanced Loaded XFMR with Current Injection....	84
Figure 43: MATLAB Load Change for Balanced Resistive Loading on XFMR Secondary	85
Figure 44: Primary Side Voltages for Balanced Resistance Loading with CI.....	86
Figure 45: Supply Side XFMR Currents for Balanced Resistance Loading.....	87
Figure 46: Neutral Injection Current for Balanced Resistive Loaded XFMR (900W)	88
Figure 47: Secondary Side Voltages for Balanced Resistance Loaded XFMR (900W).....	89
Figure 48: Secondary Side Currents for Balanced Resistance Loaded XFMR (900W)	89
Figure 49: Supply Side Voltages for Unbalanced Resistance Supply Load (900W).....	90
Figure 50: Supply Side Currents for Unbalanced Resistance Loaded XFMR (900W)	91

Figure 51: Neutral Injection Current for Unbalanced Resistance Loaded XFMR (900W)	92
Figure 52: Secondary Side Voltages for Unbalanced Resistance Loaded XFMR (900W)	93
Figure 53: Secondary Side Load Currents for Unbalanced Resistance Loading	94
Figure 54: 9000VA Bench Transformer Configured in Wye-G:Delta	99
Figure 55: Bench Current Transformer	101
Figure 56: CT Connected for Current Injection and 180Hz Function Generator Source	103
Figure 57: Current Injection Test Set Up	106
Figure 58: Power Supply through Bench Switches	107
Figure 59: Delta Connected 10 Ohm Rheostat Load	108
Figure 60: Individual 10 Ohm Rheostat	108
Figure 61: Ammeter Measuring 180Hz Injection Current	109
Figure 62: Function Generator Exhibiting Output Overvoltage	113

CHAPTER 1: INTRODUCTION

Detection of fault conditions in power distribution systems is extremely important to ensuring reliable and safe delivery of power. The inability to detect certain fault conditions can quickly result in equipment damage or personnel harm, not to mention the disruption of power to customers served by the energy utility. This is especially true as it pertains to faults categorized as “shunt faults”. Shunt faults include the well-known and well-studied faults such as line-to-ground faults and line-to-line or phase-to-phase faults. Most utilities follow industry standards for the proper detection methods/devices and to establish protection settings against shunt faults. However, the ungrounded single open phase fault is not as well understood or protected against. This is complicated by the fact that standard devices are not as readily available to detect this type of fault. The ungrounded single open phase fault is classified as a “series fault” and is defined as the complete disconnection of a conductor without making contact to ground and maintaining high impedance between the conductor and the ground plane. This is also called an “open phase condition”. This type of fault can present itself in a variety of ways including: a spuriously blown fuse in a single phase of a 3-phase circuit, the failure of a single pole of a 3-phase circuit breaker to close or the inadvertent disconnection or failure of a single phase of a three phase bolted connection.

Depending on the location of an open phase fault and the topography of the power system, the fault may or may not be easy to detect and protective actions taken. For example if the open phase occurs on the secondary side of a distribution transformer between the transformer terminals and a voltage monitored bus, the fault will result in a loss of voltage signal to an under-voltage relay and protective measures can be taken.

However this thesis will show that when the open phase occurs on the primary side of 3-phase distribution transformers with primary windings connected in Wye with grounded neutral and secondary windings connected in Delta (hereafter called Yg-D in this thesis), standard protective elements in today's common distribution systems will not always detect such a condition. If a fault cannot be detected, it cannot be protected against. Analysis of actual industry events involving ungrounded open phase faults show that power quality can suffer resulting in an unreliable power system.

This thesis explores the problem of reliably detecting open phase faults on the primary side of 3-phase distribution transformers. The condition is first modelled using the MATLAB Simulink platform in order to better understand the behavior of 3-phase distribution transformers operating under open phase conditions. A solution is proposed based on industry literature utilizing neutral connection current injection and is modeled in MATLAB. The simulations and protection method are finally tested in a small-scale physical system set up in a lab.

1.1 BACKGROUND OF PROBLEM STATEMENT (BYRON UNIT 2)

On January 30th, 2012 an event occurred at Byron Station Unit 2 Nuclear Power Plant which brought to light vulnerability in the protection of many North American power systems. [1] Specifically it was identified that the on-site distribution system (which feeds normal and emergency operations loads) was not protected against an ungrounded single open phase condition on the transmission network that fed the station Start-Up power distribution transformers.

Byron Station is a 2300 Mega Watt electric Nuclear Power Plant consisting of two generation units and located in Ogle county Illinois. The plant is owned and operated by the Exelon corporation. Nuclear power plants are typically designed such that house loads required for plant operation are powered by the generation unit via an auxiliary step-down transformer. Upon a unit trip, the main generator is separated from the grid and station loads required for cooling and maintaining the reactor in a safe shutdown configuration are immediately transferred to an alternate off-site source of power (commonly called the “Start-Up” source). A typical single line diagram is shown in Figure 1. Byron Station receives its start-up power from a 3-phase 345kV transmission line. The Start-Up transformers step the voltage down to feed 6.9kV busses and 4.16kV busses.

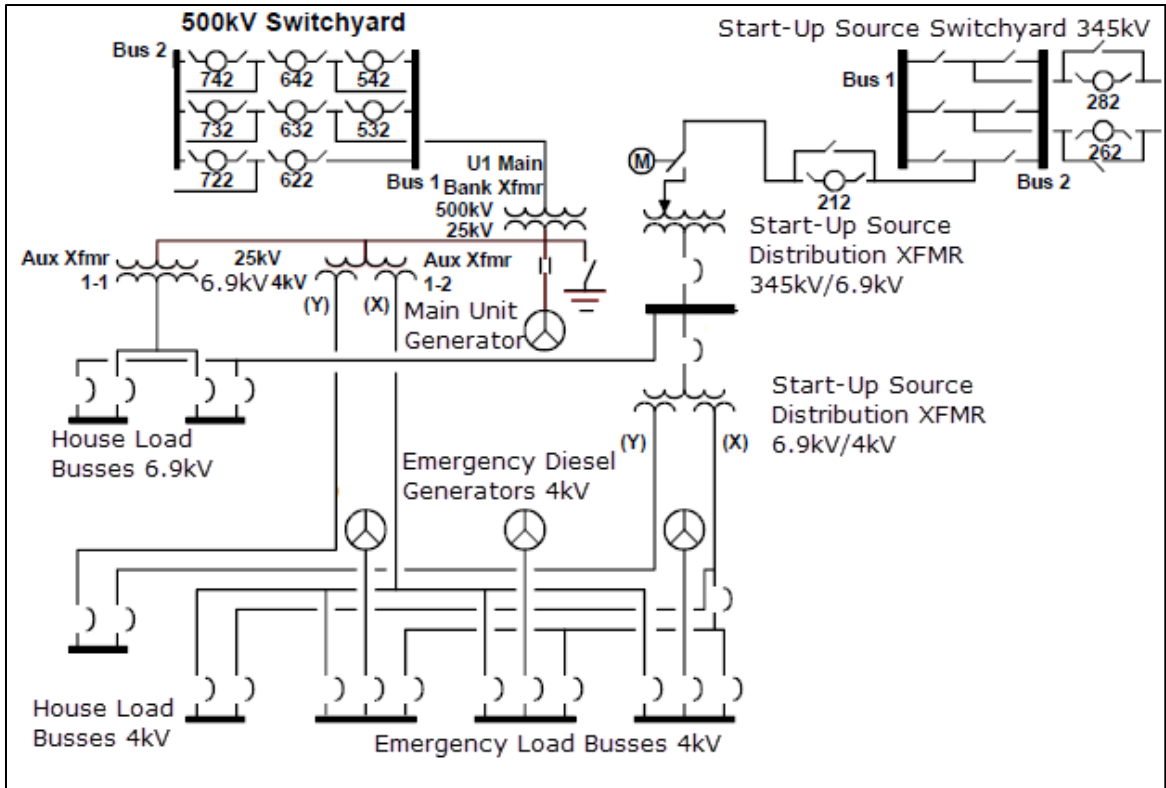


Figure 1: Typical Nuclear Power Plant Distribution Single Line Diagram

The subject event at Byron Station Unit 2, began when a Section of 345kV bus broke off due to failure of its insulator supports. This separation of the 345kV bus bar occurred on the “C” phase of the 3-phase supply and resulted in an ungrounded open circuit condition of the “C” phase. With only two of the three phases of 345kV power remaining, the secondary side of the Start-Up transformers fed unbalanced power supply to their loads. Two of these loads were the very large 6.9kV Reactor Coolant Pump (RCP) motors. These pumps are responsible for forcing coolant flow through the reactor to keep the nuclear fuel cool and to pump coolant through the steam generators which produce the steam driving the main turbine. Byron’s design consists of four RCP’s, each with undervoltage (UV) relaying that provide tripping signals to protect the motors on a UV event. When these relays sensed the low voltage on the “C” phase at the 6.9kV level,

they initiated the tripping of two RCP motors as designed. The other two RCP motors were being fed directly by the Main Unit generator and hence did not sense the loss of phase that occurred on the Start-Up source.

Byron's design is to initiate a Reactor Trip and a Main Generator Unit Trip upon the loss of two Reactor Coolant Pumps. This is done because without sufficient forced coolant flow, the reactor can heat up to unsafe levels in a short time period. The Reactor Trip occurred immediately after the two RCP motors tripped and shortly thereafter, the Main Generator Unit tripped. The Main Generator trip causes the on-site emergency diesel generators to start in preparation for accepting station loads, should the Start-Up source of power be deficient. Following the Main Generator trip, a design flaw allowed required station loads to transfer to the Start-Up transformer which had the single open primary phase. Because the system was not designed to detect and protect against an ungrounded single open circuit on the primary side of the Start-Up transformer, the remaining two RCP motors as well as the safety related 4.16kV busses stayed on the deficient Start-Up power source.

Induction motors are largely intolerant to unbalanced voltage sources and single phasing. This is because the motors are constant power loads and attempt to continue driving the same power output regardless of variations on the power input. They do so by drawing more or less current depending on voltage source conditions. In the case of the Byron event, the large induction motor loads from the RCP motors and the safety related busses transferred onto the now un-balanced Start-Up power source. They immediately began drawing much more current on the remaining two phases. As a result within minutes the RCP motors and many of the safety related loads began to trip due to their

over-current protection. It took eight minutes for Control Room operators to diagnose the problem. Upon realizing what had happened to the Start-Up source of power, operators manually tripped the Start-Up transformer feeder breakers to the station busses and forced busses to transfer to the Emergency Diesel Generators. Operators proceeded to cool the plant into a safe shutdown condition.

Following the Byron event, the United States Nuclear Regulatory Commission and the Nuclear Industry recognized the severity of the design deficiency presented with inadequate open phase condition. A significant amount of analysis work and research was performed at a majority of the various nuclear power plants around the world to bound the scope of the problem. As will be discussed in the literature Section, several sources have identified that standard undervoltage relay elements are adequate for detecting and protecting against this condition when the transformer winding configuration is wye-wye (shell type core), wye-wye (five legged core) and delta-wye. However undervoltage protection alone will not be sufficient to detect this condition in transformers with Yg-D (wye with grounded neutral) and wye-wye windings. [3, 4, 5]

1.2 PROBLEM STATEMENT

The impacts of ungrounded single phase open circuit faults on 3-phase distribution transformers are not well understood. Additionally, standard commercially available protective elements are unable to detect this type of fault. As a result it is difficult to protect distribution system loads against the consequences of distribution transformer primary side ungrounded open phases. This thesis will provide a better understanding of this fault in transformers with a Yg-D (Yg-D) configuration as shown in Figure 2 below. Furthermore this thesis will demonstrate one potential detection scheme based on solutions described in the literature.

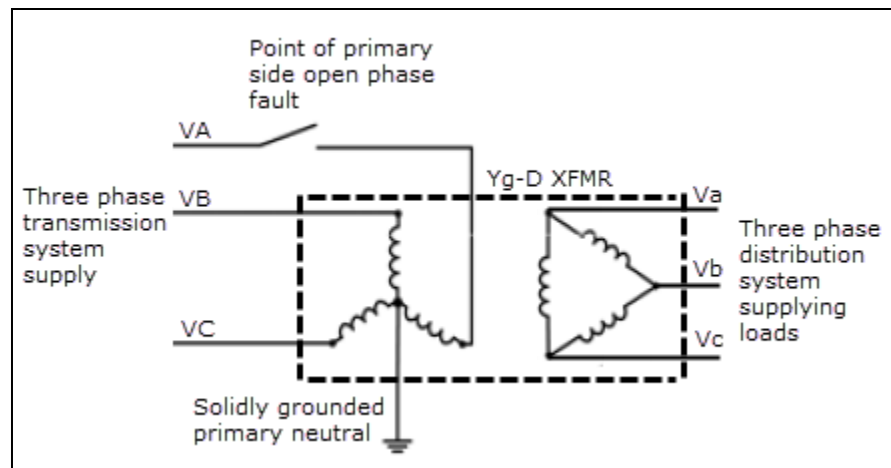


Figure 2: Diagram of Yg-D Distribution Transformer under Open Phase Fault

CHAPTER 2: LITERATURE REVIEW

The event at Byron station exposed a design vulnerability that exists in many of North America's generation facilities and substations. Recent electric utility operating experience has demonstrated that all too often loads on 3-phase distribution transformers are not adequately protected against an ungrounded single phase open circuit fault (commonly called "single phasing"). Following the Byron event, the US Nuclear Regulatory Commission (NRC) issued a bulletin citing similar events that happened at other generation facilities around the country and has requested all nuclear power plants in the country to evaluate the impacts of an ungrounded open phase event to the station power systems. [1]

This type of fault is amongst the least understood and hence the least protected against. In their paper titled "A Practical Guide for Detecting Single-Phasing on a Three-Phase Power System" authors Horak and Johnson stated, "Many papers have been presented on sequence quantities available during specific faults, but protection engineers will find fewer references deal exclusively with system conditions and resultant sequence quantities generated during a single phase condition." [2] As noted above, this problem is not restricted to generation facilities. Substations are equally vulnerable. True to the statement related to available literature on open phase conditions, there are not many older sources on protection against single phasing. Most literature is much more current and much of it is as a result of the Byron event and the mandate from the Nuclear Regulatory Commission for the Nuclear Industry to develop protection schemes. This Chapter will cover the literature that was read in preparation of this report. Focus will be placed on previous methods used for analysis of the open phase condition as well as

suggested protection methods. The literature review will compare and contrast the various analysis and protection solutions provided thus far in the literature and also state the advantages and/or limitations of each method.

2.1 CONCEPTUAL UNDERSTANDING OF OPEN PHASE CONDITION

In order to properly analyze and model three phase power transformers operating with a primary side open phase condition, one must have a conceptual understanding of how voltages, currents and fluxes interact under this condition. Several of the referenced articles discuss the operation of the Yg-D transformer under open phase conditions in great detail. From these references we learn that when an open phase occurs in one of the three high side phases, voltages on all three phases of the high and low side windings remain at or near the same magnitudes and phases as before the open phase condition existed. This is due to two different phenomena occurring at the same time. First, the three phases of voltage on the low side delta winding of the transformer are re-created due to Kirchhoff's Voltage law. Since two of the three high side windings remain energized from the two intact primary feeders, the corresponding low side windings also remain energized. The low side windings are arranged in a Delta configuration. Hence, a sum of the coil voltages around the delta loop must equal zero. To do so, the secondary side coil voltage associated with the primary side open phase must equal its pre-fault magnitude and phase. The second phenomenon is due to Faraday's law which states that flux in a coil is proportional to the voltage across that coil. Since a voltage is re-created in the secondary side of all three phases due to Kirchhoff's Voltage law, then flux will be induced in the corresponding leg of the primary side experiencing the open phase due to Faraday's law. As a result, this flux will induce a voltage on the open phase terminals of the transformer primary. [2, 4] This relationship during the open phase is demonstrated in the Figure below. Note that except for the line currents on the primary side of the transformer, the system represents an ideal and balanced condition.

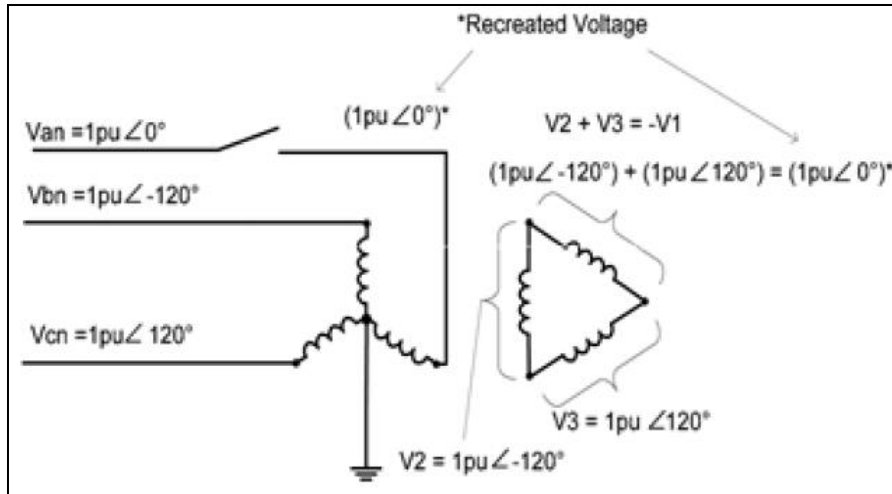


Figure 3: Voltage Re-Generation in a Yg-D Transformer During Open Phase Condition [5]

The relationships described above are true for a transformer operating under no load or lightly loaded secondary side conditions. However the transformer terminal voltages are affected by adding load to the distribution system. In [4], Norouzi describes how loading significantly impacts power quality as the system becomes more unbalanced with increasing load. While the primary and secondary side coils corresponding to the open phase remain energized due to the combination of Kirchhoff's voltage law and Faraday's law, these coils cannot transfer any power. The only currents flowing through these coils are the minute magnetizing currents which are supplied by the other two phases. When real load is added to the secondary side distribution circuit, the intact phases are the only ones that can provide the power to that load. As a result the intact phases must draw additional current from the primary side transmission supply and the corresponding secondary side transformer coils must deliver additional current to compensate for the incapacitated phase. This results in additional voltage drop on the intact secondary side phases due to the additional copper losses experienced by the

unbalanced currents. Three phases of currents are still delivered to the secondary side load due to the delta configuration; however it is all supplied by only two of the transformer coils. The voltage unbalance is negligible at zero loading and light loaded conditions. However the unbalance can become very severe when the transformer loading approaches levels closer to the name plate rating.

Voltage unbalance is especially problematic as it pertains to induction motors. The main effect of voltage unbalance is motor damage from excessive heat from negative sequence currents. As described in [1] during the Byron event, the actuation of individual motor load protective elements (also known as thermal overload relays or simply over current relays) preceded a systematic detection of open phase. The discussion above clarified that voltage unbalance is the result of load currents on the transformer secondary side causing voltage drop across the two intact phases. Much of the analytical research regarding the impacts of open phase conditions is summarized in Section 2.2 below. In general the research has found that while at low loading levels the unbalance is small, it can still easily approach greater than 5% [5,6]. NEMA MG1 specifies design standards for induction motors. This industry standard also describes the impacts of voltage unbalance on AC induction motors. Per MG-1, a small percentage voltage unbalance will result in a much larger percentage current unbalance. Consequently the temperature rise of the motor operating at a particular load and percentage voltage unbalance will be greater than for the motor operating under the same conditions with balanced voltage. This is true even if the balanced voltages are degraded as in an under voltage condition. Current rise during balanced under voltage conditions is inversely proportional to the per-unit under-voltage due to the motor maintaining constant power. However during an

unbalanced voltage condition the currents are on the order of approximately 6 to 10 times the voltage unbalance. This effect is caused by the fact that unbalanced voltages introduce a negative sequence voltage having opposite rotation of that occurring with balanced voltages. This negative sequence current produces a flux in the air gap rotating against the rotation of the rotor and will produce very high currents in the rotor windings. While MG-1 provides derating factors for anticipated levels of voltage unbalance, the standard does not recommend operating any motor where anticipated voltage unbalance exceeds 5% [7]. Therefore it is necessary to develop modeling techniques which cannot only accurately determine the consequences to the system of the open phase condition, but that can also simulate possible protective solutions.

2.2 EXISTING MODELING AND ANALYSIS TECHNIQUES

As stated previously, older sources that describe the analysis or modeling of a distribution transformer operating under open phase conditions are difficult to find. The Byron station event and the NRC bulletin have generated a significant amount of current publications documenting methods and studies for open phase conditions. Additionally, prior to the Byron event there was a lack of familiarity with analytical methods and tools that had the capability to analyze ungrounded open phase conditions. For example, the Electrical Transient Analysis Program (ETAP) developed and sold by Operation Technology, Inc. (OTI) did not contain a software package that could simulate open phase faults until requests poured in from the ETAP Nuclear Utility User's Group (NUUG) following the Byron Event. Today, ETAP contains an Unbalanced Load Flow (ULF) module which provides a steady state analysis of an open phase fault at transformer terminals. [6] The ETAP tool has been used not only to produce anticipated voltages and currents following the open phase fault, but also as a way to classify and identify general behaviors of distribution systems subject to open phase conditions.

In reference [5], engineers used the ETAP unbalanced load flow module to determine individual phase voltage and currents as well as symmetrical components for a generic Korean Power Plant distribution network. The paper analyzed 12 different cases of single and double open phase faults for low, medium and high loaded cases. Previous work was relied upon for dismissing the need to analyze certain transformer winding configurations due to the known inability to re-generate system voltages. However the Yg-D transformer was analyzed due to its known ability to re-generate voltages. ETAP can only generate steady state results so the ability to determine any transient effects at

the time of the fault is not available. The resulting voltage and current levels were manually compared to existing plant protective elements such as bus under voltage relays (27 devices), neutral time ground overcurrent relay (51N devices) and negative sequence over-voltage relays (59_2 devices). The paper concluded that in general, as load increases the amount of voltage unbalance also increases. However, at low loading conditions the unbalance is not severe enough to pick up bus undervoltage relays and cannot be detected using any of the standard available protective devices. Voltage values were often very near 1.0 pu following the open phase fault.

Reference [6] also utilized the ETAP load flow module however in contrast to the studies performed in reference [5], reference [6] determined a systematic way of utilizing the ETAP unbalanced load flow analysis tool in order to generate a 3-dimensional surface which is better at generalizing the corresponding voltage unbalance behavior with respect to transformer loading and fault impedance. This paper sought to not only analyze the case where the open phase faults in an ungrounded manner, but also where it grounds through various levels of impedance. The following Figure was produced which demonstrates that transformers with Wye primaries and incorporating a Delta winding (in this case as a buried delta) experience minimal voltage unbalance even at higher transformer loading. For this type of transformer, fault impedance has a much higher impact on resulting voltage values. However in general, this reference supports reference [5]'s conclusion that voltage unbalance can be undetectable by standard under voltage protection. This source did not simulate any protective elements.

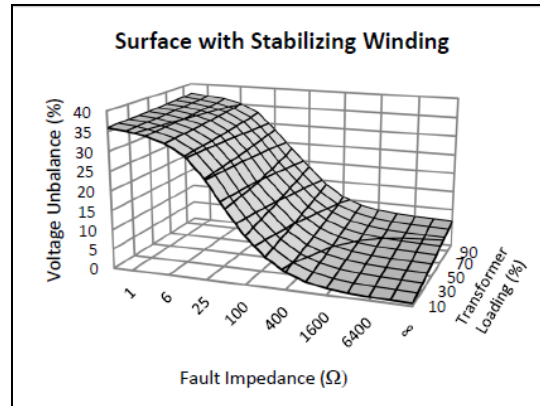


Figure 4: Voltage unbalance for a Y-D-Y transformer [6]

The ETAP tool is inhibited by the fact that it cannot simulate certain detection methods such as current injection or unique programmable logic. Also, while it can perform harmonic analysis it cannot perform Fourier transforms to allow for categorizing a fault signature by a frequency response. Nor can it display wave forms during a certain time interval. As a result, other papers have focused on the use of analysis tools that can provide a better level of detail and can provide results in the time domain.

References [4] and [8] both utilized MATLAB as the modeling and analysis tool of choice. MATLAB's Simulink software provides the Simscape Power Systems suite which has a full library of component and analysis tools. Components in the Simscape library include three phase core-type transformer models which incorporate all of the electro-magnetic interdependencies that allow secondary side voltage re-generation following an open phase fault of the transformer primary. The system is easily modeled using a schematic layout. Physical effects and component states of the system can be assigned at points of time. Data collection in terms of currents and voltages can be performed almost anywhere within the system model and can be analyzed in the time,

frequency or symmetrical component domain. Unlike ETAP, this tool allows you to develop a scope trace of currents or voltages at any point within the system. The latter is a powerful feature for attempting to derive a “signature” for detecting the open phase fault. Additionally MATLAB Simulink allows the modeling of unique or logic based protection systems with uniquely derived algorithms. This is a feature that is not offered in ETAP.

In reference [4], Norouzi primarily uses the MATLAB tool to model an open phase on a 1800kVA three phase Yg-D transformer in order to confirm the conceptual behavior described in Section 2.1 of this Chapter. This will also be done as part of this thesis and is described in Chapter 3. The simulation results confirm that secondary side voltages and currents remain fairly balanced although are not identical to their pre-fault values. Additionally the analysis confirms that the degree of unbalanced is proportional to the secondary side loading thereby validating the concept that the voltage unbalance is a result of the voltage drop across the coils contributing more load current. Simulations are performed at 60kW and 600kW. In the latter case the voltage unbalance exceeds the 5% limit for motor operation introduced by NEMA MG-1, however the voltage levels never degrade below 0.9% per unit which is the highest point at which most distribution systems set under voltage protection. Norouzi’s paper concludes with the use of MATLAB Simulink to simulate a proposed solution method which will be described in Section 2.3 of this Chapter.

Reference [8] used MATLAB Simulink to determine the type of impact that the primary to ground zero sequence impedance of the transformer has on the secondary side equipment during the primary open phase. This was done to further understand the effects

of large motor starting and running performance. Focus was placed on determining whether a large motor (6000HP reactor coolant pump motor) could successfully accelerate to rated speed, what the resulting acceleration time would be and what the voltage unbalance (determined as $V2/V1$) was after reaching steady state operation. The transformers modeled in this study were not strictly Yg-D but were instead primary and secondary side wye connected with grounded neutrals (known as Yg-Yg) with a buried Delta winding at 18MVA, 26MVA and 33MVA load ratings. As was previously demonstrated in reference [6], the buried delta allows the Yg-Yg transformer to behave very similarly to a Yg-D transformer due to the stabilizing effects of the delta winding. Simulations demonstrated that the motor was able to successfully accelerate following an open phase condition. Locked rotor current decreased slightly under open phase and acceleration time increased by various times depending on the transformer type and size. Voltage unbalance was largest at the instant of motor starting (8.6% unbalance) but steadied out at 1.2% once reaching steady state operation. Line currents at the load were unbalanced with some phases running lower than normal and some at higher values than normal. Motor heating decreased initially as compared to normal starting however increased once reaching steady state. A separate run was performed where all transformer parameters were equalized on a 33MVA base but the zero sequence impedance was allowed to vary. The author correlates zero sequence impedance as the major contributor to the open phase effects on load running. This further supports findings in reference [6] where it was demonstrated that fault impedance had a larger impact on the consequences of a primary side open phase than did the size of the load. Reference [8] did not simulate any potential detection or protection schemes.

The studies documented above demonstrate several key take aways that will be used in the analysis portion of this thesis and to support the detection and protection method of choice by this thesis. First, the MATLAB simulation tool provides a superior platform for analyzing the behavior of open phase conditions over the ETAP platform. While the ETAP platform is a simpler tool to use and is the industry standard for transmission and distribution system analysis, open phase faults produce unique system conditions that require a closer look at details such as single phase and zero sequence impedances. Additionally, the MATLAB tool allows for producing scope views of points of interest which can be very helpful in analyzing transient phenomena during an open phase fault. Second, all of the studies demonstrated that the use of secondary side voltages and currents alone for detection of the open phase condition is not highly reliable. This is because while the condition will provide some level of unbalance, the average degradation in voltage (which is typically used to trigger undervoltage protection) is typically not severe. It is the unbalance of the voltage which produces the hazardous effects to motors, not the degradation in average voltage. Hence existing standard protective elements are not highly reliable in detecting this system. Finally, these sources identify that zero sequence impedance has a heavy influence on the resulting secondary side behavior of the distribution transformer. As will be described in Section 2.3 of this Chapter the zero sequence impedance path provides a novel way of providing highly reliable detection of the open phase condition.

As a result of these findings, this thesis utilizes the MATLAB Simulink tool to model and analyze the open phase condition. This thesis advances the research in this

area by simulating a novel detection method as described in the literature summarized in Section 2.3.

2.3 STANDARD DISTRIBUTION TRANSFORMER PROTECTION SCHEMES

The primary purpose of this thesis (besides a better understanding of how a Yg-D transformer operates under open phase condition) is to identify a method of detecting this condition so as to initiate protective action. The narrative of the Byron event demonstrates that relying on human operators for detecting this condition and taking action, can lead to severe consequences. The literature identifies cases where the condition was not detected until consequences such as failed motors were experienced. In some cases the condition went undetected for weeks or months due to the fact that stand by Yg-D transformers will not present noticeable symptoms as described in Section 2.2 [1, 5]. Before we can discuss detection solutions discussed in the literature, it is helpful to understand how standard protection schemes are designed for protecting distribution transformers and why standard protection schemes are not effective in detecting the open phase condition for Yg-D transformers. The following discussion primarily comes from reviewing reference [9], although the concepts can be found in almost any source on electrical system protection and relaying.

Distribution transformers feeding low voltage distribution systems are sized according to their application and anticipated load. These transformers receive their supply from a transmission substation at voltages from 69kV and above. The secondary side typically feeds medium voltage loads at 2.4 to 13.8 kV. These loads can be secondary distribution transformers or large loads such as large station motors. At power generating stations the station service transformers are often wound in Yg-D configuration with the grounded wye winding connected to the high voltage transmission supply and the delta winding connected to a medium voltage bus. As the delta winding

has no neutral point, a neutral will typically be derived via a grounding transformer such as a zig-zag transformer. Standard protection schemes for these transformers have multiple objectives. Overload and fault protection are provided by phase over-current relays (device 50/51). Ground overcurrent protection is typically provided on the secondary side only using device 50-G or 50-N. Thermal protection of the windings is provided by thermal protective relays also called thermal overload relays (device 49). Protection of the transmission supply feeder against internal transformer faults is accomplished using differential protection relays (device 87). Finally, additional protection against transformer internal faults is provided by sudden-pressure relays (device 63). The standard transformer protection scheme is shown in Figure 5.

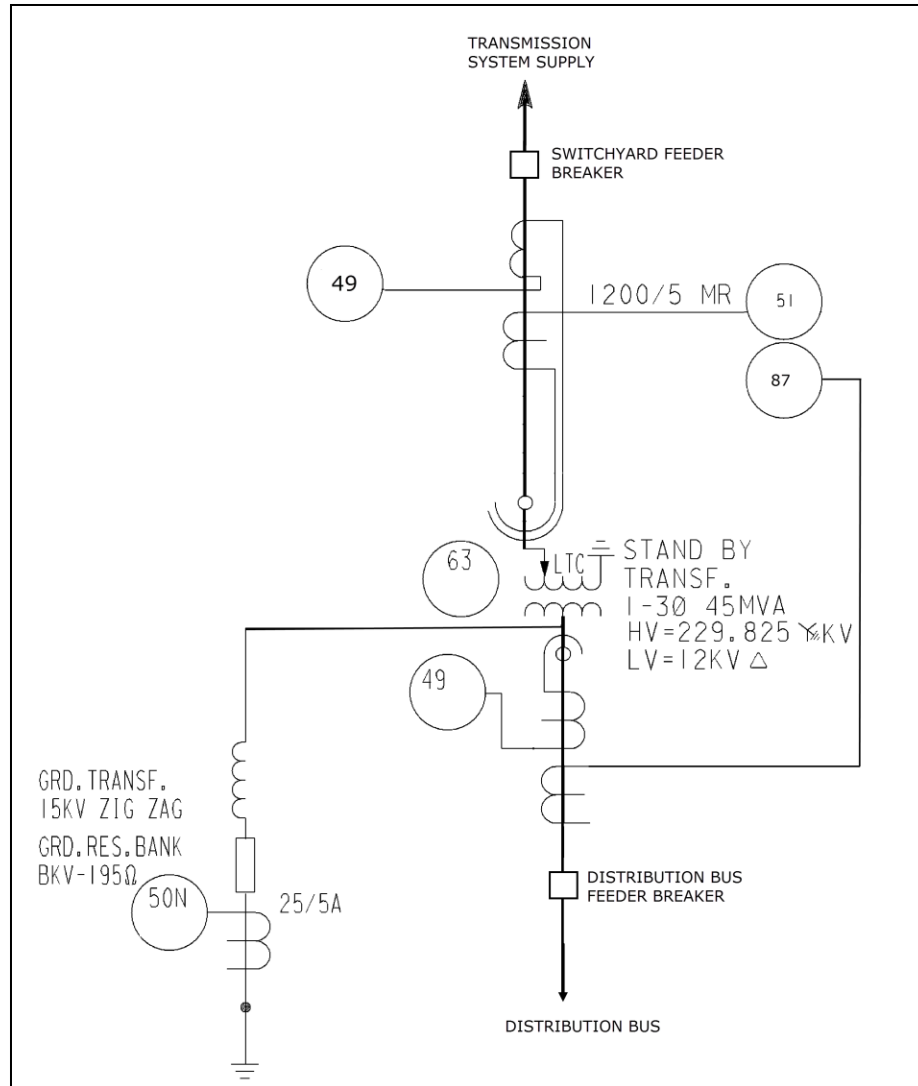


Figure 5: Standard Distribution Transformer Protection Scheme [9]

It is helpful to look at each of these protective devices and compare the manner in which they function to the results of open phase condition analyses described in Section 2.2. We can see that especially for the lightly loaded stand-by transformer, these devices cannot detect the condition. Thermal overload relays (device 49) are designed to mimic the heating that occurs either within the windings of the transformer, in the case of 49 devices upstream of the transformer, or of the downstream bus bars as in the case of the

49 device downstream of the secondary side winding. These devices respond to positive sequence current magnitude. These devices must allow the transformer to maintain nameplate rated load and are usually set at greater than 125% of the transformer nameplate rated current. As shown in studies documented in references [3, 4 & 5] an open phase condition does not result in a significant change to positive sequence current downstream of the transformer terminations. Current rises in the two individual transformer windings left intact to transfer power, however since the secondary side of the transformer is wound in delta, the current is allowed to more evenly distribute to all three phases and hence the increased current internal to the transformer windings is not detectable by the 49 devices. While a primary side 49 device would sense an increase in current draw in the two remaining transmission line phases, the ability to detect the overcurrent will depend on the following factors: 1) whether the transformer is loaded at or near the nameplate rating, 2) how sensitive the current transformer used to drop the measured current is and 3) the setpoint of the device. Reference [4] shows that the primary side currents can expect to increase by up to 50% however if the loading on the transformer is not at or near nameplate rating at the time of the open phase fault, the current value may not be sufficient to be detected. Therefore, the 49 devices cannot be relied upon for reliable open phase detection.

A similar argument is made for the 51 device (over-current) typically found on the primary side of the transformer. This device is also set to allow for 100% of nameplate rated current. During very light loading or no loading, the typical current transformer that is used for dropping the current down for measurement, does not have the appropriate accuracy for measuring the very small amount of current. This is

especially true for the no-load case. During the no load case the only current measured is the magnetizing current and even in very large transformers the total magnetizing current can easily be less than 1 amp per phase. When divided by the CT ratio, this magnitude of current is undetectable by the 51 device.

The differential relay (87 device) compares current levels entering the transformer via the transmission line feeder and compares to the current values exiting the transformer. The purpose of this protective element is as a prompt detection of faults internal to the transformer. However the open phase condition results in no difference between the sum of the currents entering the transformer as compared to those exiting the transformer. Currents are scaled using the current transformers such that the absolute values of the current are not being compared. Since there is no differential current during an open phase condition, the relay cannot detect the fault. Additionally, use of individual phase differential relays may not detect losses of a phase during unloaded or lightly loaded secondary's. This is because high power CT's are typically not very accurate at extremely low current levels and because differential relay sensitivity at such low levels may trigger nuisance alarms. Furthermore some utilities do not have the differential CT's right at the transformer terminals. Rather they take advantage of existing CT's at the nearest switching component which may leave Sections of power lines un-monitored for to detect an open phase. The 63 device (sudden pressure relay) is also ineffective to protect against this condition. This relay responds to increased pressure in the transformer tank due to arcing in the coil turns. This is also a condition that would not be encountered due to the open phase condition.

The final device that is part of the protection scheme for the distribution transformer is the 50N device. Since the secondary side of a Yg-D transformer is an ungrounded delta winding, a ground fault on the secondary side only draws fault current when two of the three phases fault to ground. This creates the potential for undetected ground faults that could become an industrial safety hazard. The introduction of a grounding transformer through a resistor bank allows for detection of a system ground. This is accomplished because during a secondary side ground fault, the neutral point in the delta winding will shift and result in current flow through the 50N device. As shown in reference [2] though, this does not occur during an open phase condition because of the extremely balanced voltage conditions at the secondary side terminals of the delta winding. Hence the grounding transformer would not experience a shift in neutral point and would not conduct ground current. We have demonstrated that the standard transformer protection scheme is ill equipped to protect a distribution transformer during an open phase condition.

2.4 METHOD FOR DETECTION OF OPEN PHASE FAULTS

As previously stated, current detection and protection methods for open phase faults at the primary connection of Yg-D distribution transformers are not adequately designed. Differential elements detect unbalances in power flow between the primary and secondary sides of a transformer to protect against internal transformer faults. An open phase fault does not result in such an imbalance. As a result of the significant current unbalance on the primary side of the Yg-D transformer, an open phase fault will result in ground current flowing through the primary neutral and circulating back to the grounded voltage supply. However, the magnitude of such a current (especially for a lightly loaded or un-loaded transformer) will not be large enough to actuate an overcurrent relay. Finally as documented in the resources above, primary and secondary side voltages will remain almost identical to pre-fault conditions. Slight unbalances will be noted (due to voltage drop across the secondary side transformer coils) however they are not great enough to actuate even downstream undervoltage or voltage unbalance relaying.

In a recent US patent application [11] and as documented in [10], the Electric Power Research Institute (EPRI) in collaboration with Power System Sentinel Technologies, LLC describe a method of protection using current injection into the primary side neutral connection. A three phase transformer operating in balanced condition will have a certain Zero-Sequence impedance. When looked at from the point of the transformer primary side neutral connection, the zero sequence impedance consists of the three transformer primary side winding impedances in parallel along with the transmission system's zero sequence impedance (see Figure 6 as an example of the flow path for zero sequence current). When the system is operating in balanced condition, the

total zero sequence impedance is small. The three balanced primary side transformer currents will sum to zero or very close to zero at the primary side neutral point. Per [10] and [11], a balanced three phase transformer will allow current to be injected via magnetic coupling onto the primary neutral connection. During balanced condition, because of the low zero sequence impedance, current will be allowed to flow through into the neutral connection and circulate through the transmission zero sequence network. The current is injected at a known frequency (nominal 90Hz) and is sensed via a secondary current sensing loop. It is important to utilize a frequency different from the nominal system frequency of 60 Hz because when the system is unbalanced, 60 Hz current will normally flow through the neutral. When a phase is opened on the primary side of the transformer, the zero sequence impedance transitions into a high impedance state and the injection current is significantly altered. The system described in [10] and [11] utilizes a measurement of 5th harmonic component and magnitude of injected frequency current. However based on operating experience at Diablo Canyon Power Plant, this system has experienced several false positives. This is believed to be due to the significant 5th harmonic noise created by normal anticipated switching in nearby switchyards. This thesis will show that a simpler approach is to look at the shift in fundamental frequency in the injected neutral current during an open phase. When a phase is opened, the injected current at a fundamental of 180 Hz will be reduced and overcome by 60Hz nominal unbalanced system current. See Figure 6 for a schematic representation of this system. This method of detection can be used regardless of how heavily or lightly loaded the transformer is.

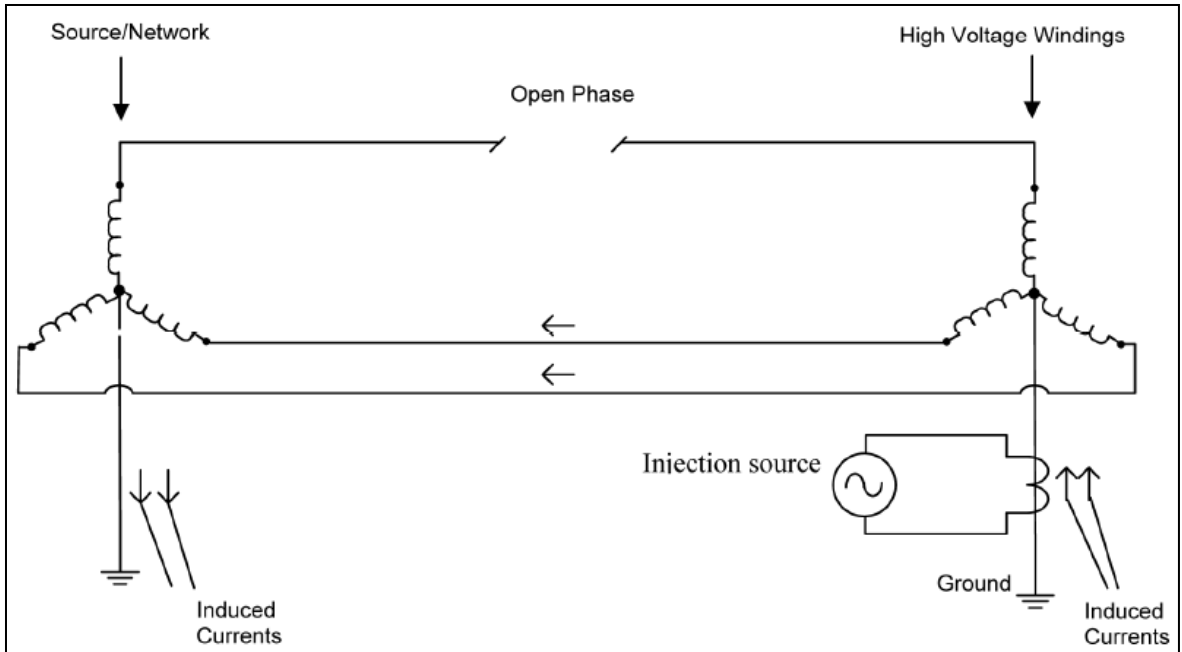


Figure 6: Schematic of Current Injection System under Open Phase Fault [10]

CHAPTER 3: SYSTEM DESIGN AND ANALYSIS

While references [10] and [11] provide a conceptual description of how the current injection detection method works, these references do not provide a mathematical analysis describing how the change in zero sequence impedance manifests itself. Furthermore a detailed symmetrical component analysis, showing how currents in an unloaded standby distribution transformer are impacted by an open phase condition, is difficult to find in the literature. A computer analysis demonstrating the current injection solution could not be identified in any of the literature researched by this thesis. This Chapter will perform several analyses of a transformer subject to an open phase condition to explore the validity of the current injection detection method and to demonstrate why other solutions such as neutral overcurrent relays are not effective in detecting and protecting against this type of fault. Section 3.1 provides an analysis using symmetrical components to show how line and neutral currents in a distribution transformer are impacted by the open phase condition. Section 3.2 provides a computer analysis using the MATLAB Simulink PowerScape environment to demonstrate by simulation the functionality of the current injection method.

3.1 SYSTEM ANALYSIS BY SYMMETRICAL COMPONENTS

The use of symmetrical components for determining power system responses to a variety of shunt type faults is well documented and familiar to most power engineers. References [12], [13] and [14] provide several examples of this type of analysis. However there is less familiarity with the analysis of a series type fault such as an ungrounded open circuit fault. Such an analysis assuming an unloaded secondary side of a distribution transformer is further complicated by the fact that the magnetizing branch of the transformer model cannot be ignored. This is because it is the principle reason for current draw on the power supply. This Section of the thesis documents the analysis using basic symmetrical component analysis. As this thesis focuses on the behavior of the Yg-D three phase transformer operating at lightly loaded or unloaded conditions, the system in Figure 7 below will be utilized for this analysis.

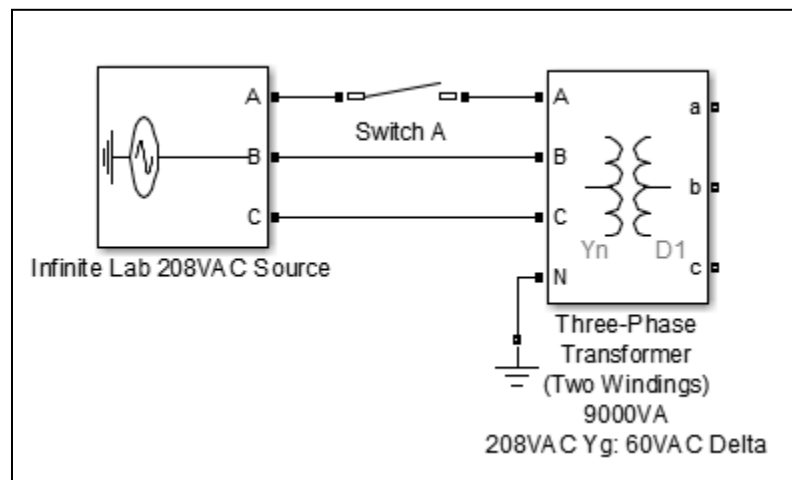


Figure 7: Schematic Diagram of 3-Phase Transformer with Open "A" Phase

The system in Figure 7 is based on real components used in Cal Poly's Energy Conversion laboratory. Single phase bench transformers of rating 3kVA were used and

connected in a Yg-D bank. Open circuit and short circuit tests were performed in order to obtain the transformer positive and negative sequence series impedances and shunt (magnetizing) impedances as described in [12] & [15]. Additionally, the zero sequence impedance was needed and could not be ignored due to the unloaded secondary. The zero sequence impedance allows for proper modeling and calculation of the neutral current during the open phase condition. Zero sequence impedance testing is more unfamiliar and involves a shorting of all three transformer primary terminals together and slowly energizing using a single phase source through a variac. The test procedure is described in [15]. The calculations and procedure results for the determination of the transformer parameters are documented in Appendix 1. For the purposes of these calculations and the computer modeling performed in Section 3.2, an ideal supply source is assumed with all impedances equal to zero. In a true distribution application the sequence impedances are necessary as they can impact the value of the zero sequence current and in turn the value of the line current. However for this thesis the assumption of an infinite source is conservative as it will best demonstrate the feasibility of using existing protection elements for detecting the fault currents.

From symmetrical component analysis, we know that we first must determine the sequence circuit for each element of the model shown in Figure 7. The sequence circuits allow us to determine the separate response of each element to the positive, negative and zero sequence voltages and currents determined by the pre-fault state and post-fault state of the system. Once the sequence circuits are known, they can be organized into three sequence networks whose topography is determined by the nature of the unfaulted and faulted states.

The elements of the network are the three phase transmission voltage supply and the three phase Yg-D distribution transformer. For simplicity and to avoid too many permutations, this analysis will only consider the completely unloaded distribution transformer condition as this is the most difficult condition to detect. Recall from symmetrical component analysis that the phase current of any bus or component is the sum of their respective symmetrical components as follows:

$$\begin{aligned}
 I_a &= I_a^{(0)} + I_a^{(1)} + I_a^{(2)} \\
 I_b &= I_b^{(0)} + I_b^{(1)} + I_b^{(2)} \\
 I_c &= I_c^{(0)} + I_c^{(1)} + I_c^{(2)}
 \end{aligned} \tag{1}$$

We can simplify equation (1) further by substituting the transposed “a-phase” vectors for the “b-phase” and “c-phase” values by virtue of using the “a” matrix and arrive at the following equation which will convert system symmetrical components to phase values:

$$\begin{bmatrix} I_a \\ I_b \\ I_c \end{bmatrix} = \begin{bmatrix} 1 & 1 & 1 \\ 1 & a^2 & a \\ 1 & a & a^2 \end{bmatrix} \begin{bmatrix} I_a^{(0)} \\ I_a^{(1)} \\ I_a^{(2)} \end{bmatrix} = A \begin{bmatrix} I_a^{(0)} \\ I_a^{(1)} \\ I_a^{(2)} \end{bmatrix} \tag{2}$$

where $A = \begin{bmatrix} 1 & 1 & 1 \\ 1 & a^2 & a \\ 1 & a & a^2 \end{bmatrix}$.

Furthermore we also have the inverse of equation (2) which will convert phase values to symmetrical components:

$$\begin{bmatrix} I_a^{(0)} \\ I_a^{(1)} \\ I_a^{(2)} \end{bmatrix} = \begin{bmatrix} 1 & 1 & 1 \\ 1 & a^2 & a \\ 1 & a & a^2 \end{bmatrix}^{-1} \begin{bmatrix} I_a \\ I_b \\ I_c \end{bmatrix} = \frac{1}{3} \begin{bmatrix} 1 & 1 & 1 \\ 1 & a & a^2 \\ 1 & a^2 & a \end{bmatrix} \begin{bmatrix} I_a \\ I_b \\ I_c \end{bmatrix} \quad (3)$$

From [12], [13] & [14] we know that the elements of the system in Figure 7 can be described in terms of their respective positive, negative and zero sequence networks. Since the voltage supply (grid or generation unit) is assumed to be ideal in this case and is assumed to be Wye connected with a solid ground, then all sequence impedances are zero and the sequence networks can be represented as shown in Figure 8 below.

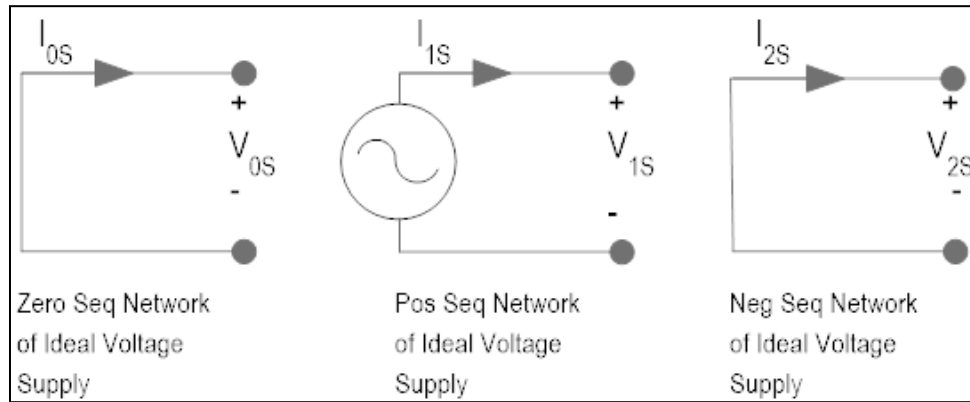


Figure 8: Sequence Networks of the Ideal Voltage "Grid" Supply

In this system the resultant currents and voltages will be largely determined by the transformer and its associated loading. For this analysis the transformer is assumed unloaded. Hence the magnetizing impedances cannot be ignored since they are what largely determine the transformers line current. As the transformer is loaded, the contribution of the magnetizing impedances can be ignored. Additionally, references [12], [13] & [14] all state that for a transformer, the positive and negative sequence impedances are equal as a transformers behavior is not determined by phase rotation

(unlike rotational machines). For the zero sequence impedance there are fewer sources providing clear direction on how to treat the zero sequence component of the magnetizing impedance. From a conceptual perspective, the zero sequence component of the magnetizing impedance can be ignored at low current levels such as unloaded transformers. However at much higher loading levels, this component cannot be ignored especially in core type transformers. This is because the flux from zero sequence current will cause the core to saturate as the current has no return path through the core except through the air gap or tank wall. This is shown in the magnetic circuit of Figure [9] below. The determination of how zero sequence magnetizing impedance impacts the system behavior is left for future work.

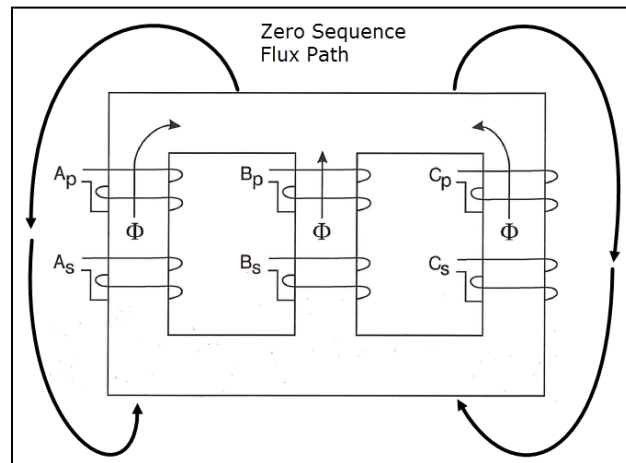


Figure 9: Magnetic Circuit for Zero Sequence Flux

The positive, negative and zero sequence networks for the lab bench transformers connected in a solidly grounded Yg-D configuration are shown in Figure [10] below. Impedance values are shown in per unit and are based on a 3kVA single phase apparent power base and 120VAC single phase voltage base. Parameter calculations from empirical data are shown in Appendix 1.

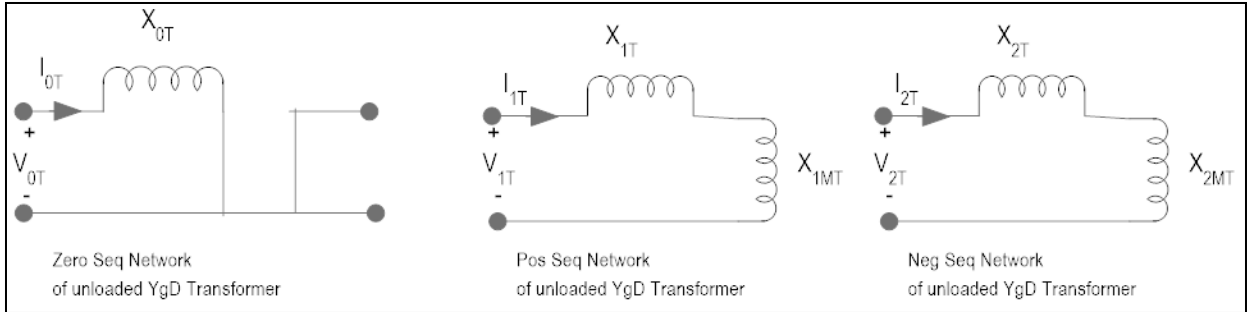


Figure 10: Sequence Networks for Unloaded Yg-D Transformer

References [12], [13] and [14] derived the method of connecting the sequence components together given the open phase fault. Per these references, given a single ungrounded open phase (assumed “A” phase open) the positive sides of the networks are all connected in parallel with no interconnection across the fault location while the negative or return sides are connected across elements but not between sequences. Note that since the transformer is unloaded, there is no current path across through to the secondary side and so for simplicity the voltage transformation across the transformer is not shown. The transformer network terminates with the magnetizing impedances for the positive and negative sequence networks. This is shown below in Figure 11.

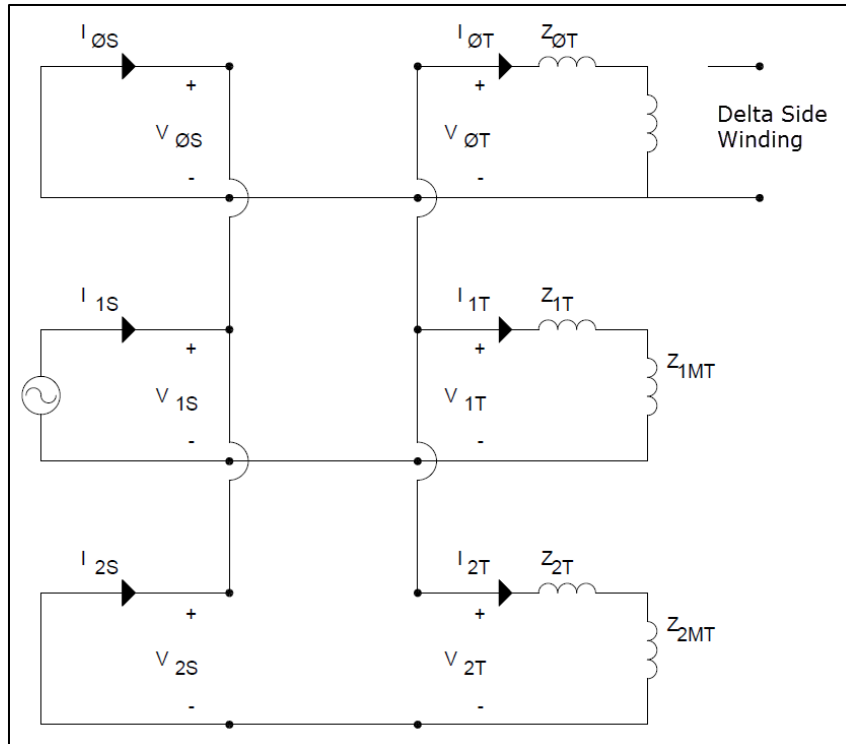


Figure 11: Connected Sequence Network for Single Open Phase Fault on XFMR

Primary

Figure 11 simplifies down to a simple impedance network with the zero sequence impedance and the negative sequence impedance connected in parallel with each other and in series with the positive sequence impedance. This is shown below in Figure 12. Note that the positive sequence and negative sequence transformer impedances are identical. For an unloaded secondary side transformer they consist of the transformer coil series impedance in series with the magnetizing impedance. The magnetizing impedance is very large as compared to the series impedance and so it dominates the impedance of the positive and negative sequence impedances. In contrast, the zero sequence impedance is very small. This is expected especially for an unloaded transformer where the core would be far from saturation. As a result a negligible amount of negative sequence

current will flow. For simplicity this analysis will assume it is zero. The vast majority of the current will flow strictly through the zero sequence path of the parallel portion of the circuit. Note that the zero sequence current will be negative with respect to the reference direction in Figure 11. This is important to note because the zero sequence current must be negative for the conversion from sequence domain currents to phase domain currents to occur correctly. Sequence current calculations are as follows:

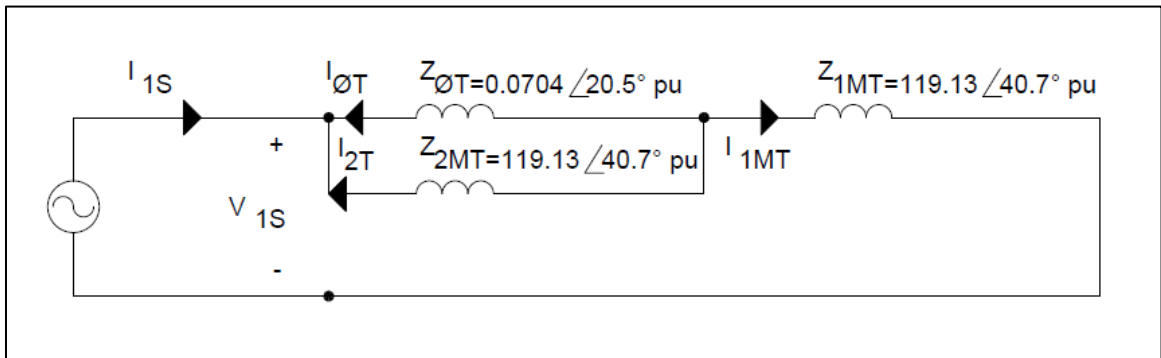


Figure 12: Simplified Sequence Network for Open Phase Fault

$$I_1 = \frac{1pu}{(0.0704 \angle 20.5^\circ + 119.13 \angle 40.7^\circ)}$$

$$I_1 = 0.00839 \angle -40.7^\circ pu \quad (4)$$

Per the discussion above we know that I_0 is equal to the negative of I_1 . Hence:

$$I_0 = -(0.00839 \angle -40.7^\circ pu)$$

$$I_0 = 0.00839 \angle 139.3^\circ pu \quad (5)$$

Using equation (2) we can determine the phase domain currents as follows:

$$\begin{bmatrix} I_a \\ I_b \\ I_c \end{bmatrix} = \begin{bmatrix} 1 & 1 & 1 \\ 1 & 1\angle -120 & 1\angle 120 \\ 1 & 1\angle 120 & 1\angle -120 \end{bmatrix} \begin{bmatrix} 0.00839\angle 139.3 \\ 0.00839\angle -40.7 \\ 0 \end{bmatrix}$$

$$\begin{bmatrix} I_a \\ I_b \\ I_c \end{bmatrix} = \begin{bmatrix} 0 \\ 0.145\angle 169.3 \\ 0.145\angle 109.3 \end{bmatrix} pu \quad (6)$$

Since the transformer primary is a grounded Wye, using equation (6) we can calculate the neutral current which goes to ground by either adding the three phase currents together or by using the known relationship:

$$I_N = 3 * I_0 = 0.025\angle 139.3^\circ pu \quad (7)$$

Converting these currents by multiplying by $I_{base} = 25$ amps we obtain the anticipated post rms fault currents:

$$I_a = 0 \text{ Amps}$$

$$I_b = 0.363\angle 169.3^\circ \text{ Amps}$$

$$I_c = 0.363\angle 109.3^\circ \text{ Amps}$$

$$I_N = 0.629\angle 139.3^\circ pu$$

These results intuitively make sense. For an ungrounded open phase on the “A” phase, we would expect the corresponding current to be zero. Additionally, we know from Appendix A that the unloaded balanced three phase current is 0.21 Amps per phase at a line to neutral voltage of 120VAC. For the three phase bank this is an equivalent three phase apparent power of $0.2A * 120V * 3 \text{ phases} = 75.6VA$. We would expect that apparent power would remain approximately the same after the fault and in order to do that the

remaining phases would have to contribute approximately 50% more power. In this case the post fault VA goes up to $0.363\text{A} \cdot 120\text{V} \cdot 2\text{phases} = 87.12 \text{ VA}$ most likely due to the additional losses experienced by the loss of 3 phase efficiency.

The above calculation demonstrates that for an unloaded transformer, the neutral ground current on the transformer will be very small despite the single open phase. This is due to the fact that the only contributions to the line current are the load due to magnetizing losses on the transformer. These are very small even in very large distribution transformers. Typical settings of neutral ground current relays on distribution transformers with solidly grounded neutrals are 100% of nameplate rating or higher. While even at moderate loading, the ground current may not be significant enough to trigger a neutral overcurrent relay, the impacts to secondary side voltage drop are significant as is seen in Section 3.2 of this thesis. A computer analysis for open phase loading of this system to 30% of the transformer name plate rating on the secondary side is documented in Section 3.2.

3.2 SYSTEM ANALYSIS BY MATLAB SIMULINK

At the time of the start of this thesis work, few analytical tools were available to study the consequences of open phase conditions on three phase systems. ETAP (which is the most popularly used electrical system analysis tool) did not have a module that could perform analyses of series faults such as open phase. This was added eventually into the ETAP Suite as part of the Unbalanced Load Flow Analysis module included in Revision 12. Reference [5] performed a sensitivity analysis on the impact to voltage unbalance caused by various open phase fault impedances and transformer loading profiles using the ETAP unbalanced load flow analysis. Additional tools such as EMTP-RV have been used in studies such as that documented in [16]. EMTP-RV is a time domain based analysis tool which is much more powerful than ETAP. However this tool is unfamiliar to this thesis author and is very expensive to use. The MATLAB Simulink tool with Power Systems module allows simulation of many power system faults in the time domain and allows views down to individual component phase currents that are not available in ETAP. The tool is also much more inexpensive for academic use. Therefore this thesis utilized MATLAB in performing simulations to validate the calculations performed in Section 3.1. This validation was also used as a means to simulate the faults prior to performing laboratory validations thereby ensuring the laboratory equipment would not be subject to dangerously high currents or voltages.

The model used by this thesis employed the simple simulation blocks available in the Simscape Power systems library of Simulink. Blocks are dragged and dropped and connected in schematic style. Voltage and current measurements can be made at almost any point in the system topography including internal to the transformer windings. Figure

13 below represents the simplified Simulink model. The full network connections, list of components and block settings are shown in Appendix 2. The model was designed using empirical transformer data from the Cal Poly energy conversion laboratory equipment. An ideal breaker was used in the computer model to represent the point at which an open phase fault could occur. In the laboratory the bench supply switches were used to perform this function.

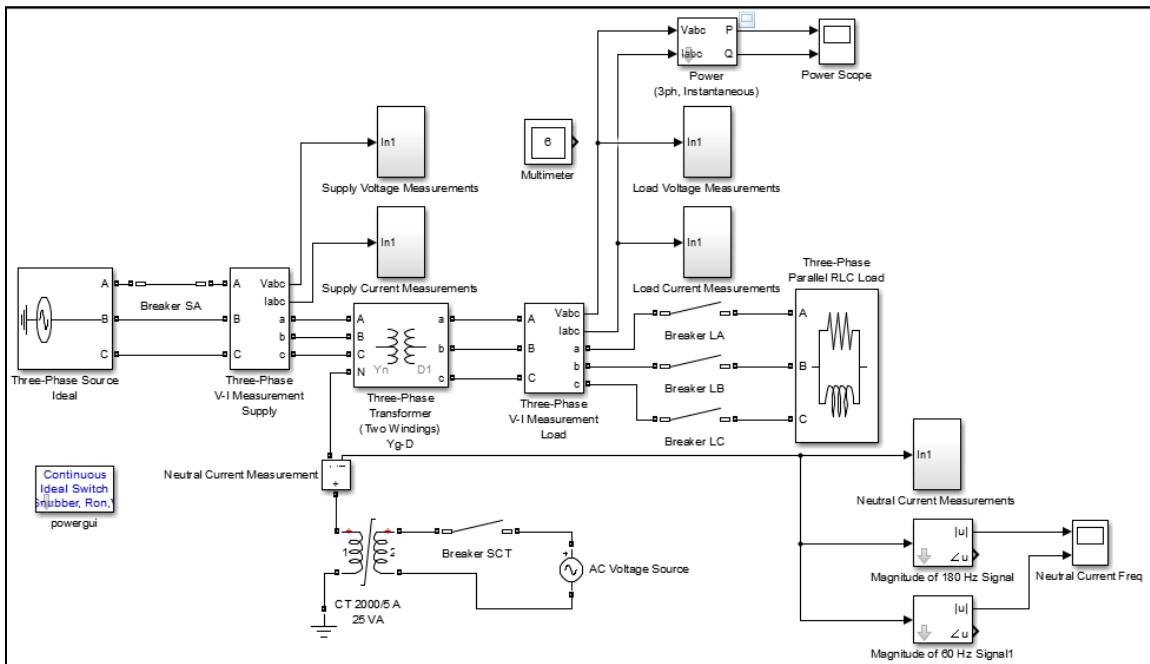


Figure 13: Simulink Model of Unloaded Transformer

Once the model was built and configured, the simulation was set up. Two cases were simulated initially, an unloaded case and a loaded case. The first case was for an unloaded laboratory bench transformer energized via a 3-phase Wye connected ideal supply with a solidly grounded neutral. The voltage supply was at 208VAC line-to-line. The system transformer consisted of a 9kVA transformer bank connected in a Wye primary with solidly grounded neutral. The secondary side of the transformer is

connected in Delta and for the first simulation case is left open circuited with no load as would be the case with a stand-by transformer. The secondary side of the transformer generates 60VAC line-to-line due to the 2:1 ratio of the bench transformers. The simulation measures supply voltages and currents at the terminals of the primary side of the system transformer as well as secondary side of the transformer and the neutral current. Additionally, the transformer coil and excitation currents can also be seen and plotted. The simulation was programmed to allow for a 100ms (6.25cycles) real time simulation. The circuit breaker in the “A” phase voltage supply to the transformer is programmed to open after 50ms or 3.125 cycles. This is seen as sufficient time to allow the system to reach steady state. Additionally, all measurement channels were placed on a 0.1ms sample time or 160 samples per cycle. The simulation time was limited to 100ms to allow for a more expeditious simulation run as well as to limit the large amount of data that was provided.

The simulation for case 1 (unloaded case) matched well with the symmetrical component analysis of Section 3.1. As described in the literature review of Chapter 2, the line side voltages at the terminals of the transformer are for the most part unaffected by the open phase condition on the “A” phase. RMS voltage on the “A” phase terminal dips very slightly to a value of 119.875VAC while “B” and “C” phases are slightly elevated at 120.75VAC RMS. The negligible change in transformer terminal RMS voltage would not be detectable with most conventional undervoltage relays. The scope wave form shows the voltages completely undisturbed by the event as shown below in Figure 14. As can be seen, any attempt to use changes in voltage as a form of detection will not work on the primary side of the transformer. Contrary to the balanced transformer terminal

voltage, the primary side currents experience significant unbalance with “A” phase at 0 Amps as expected and “B” and “C” phase at approximately 50% higher and closely matching the calculated values of Section 3.1. Pre-fault currents were all balanced at 0.21 Amps RMS as expected and according to the open circuit test of the transformer. Post fault “B” and “C” phase currents matched at 0.363 Amps RMS in accordance with the calculations of Section 3.1. Additionally as predicted by the symmetrical component analysis, the waveform as shown in Figure 15 below shows that the phase angle between the “B” and “C” phase currents is no longer 120 degrees. Rather the phase angle narrows and brings the currents closer in phase.

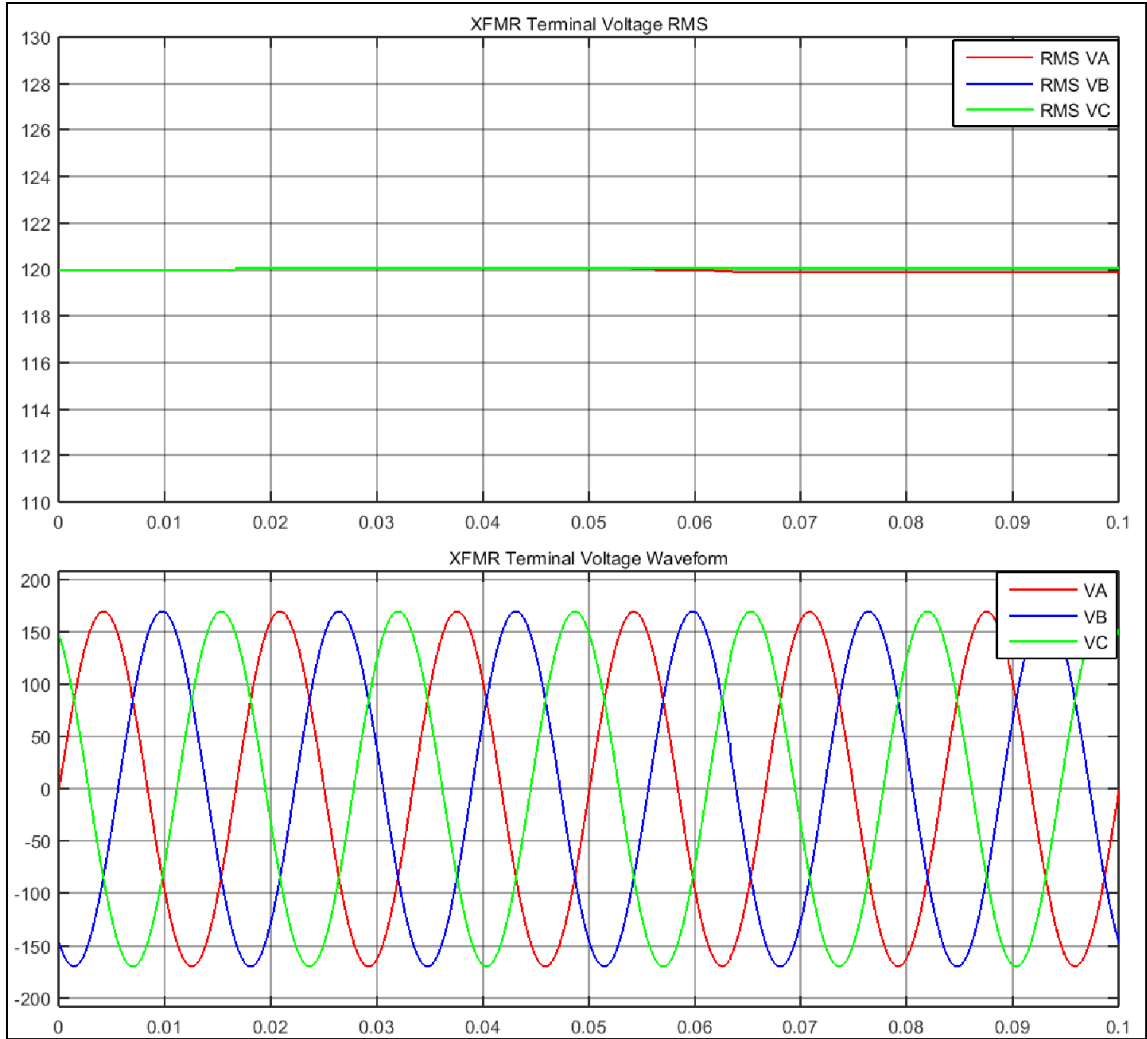


Figure 14: XFMR Primary Terminal Voltage Open Phase at 0.05s

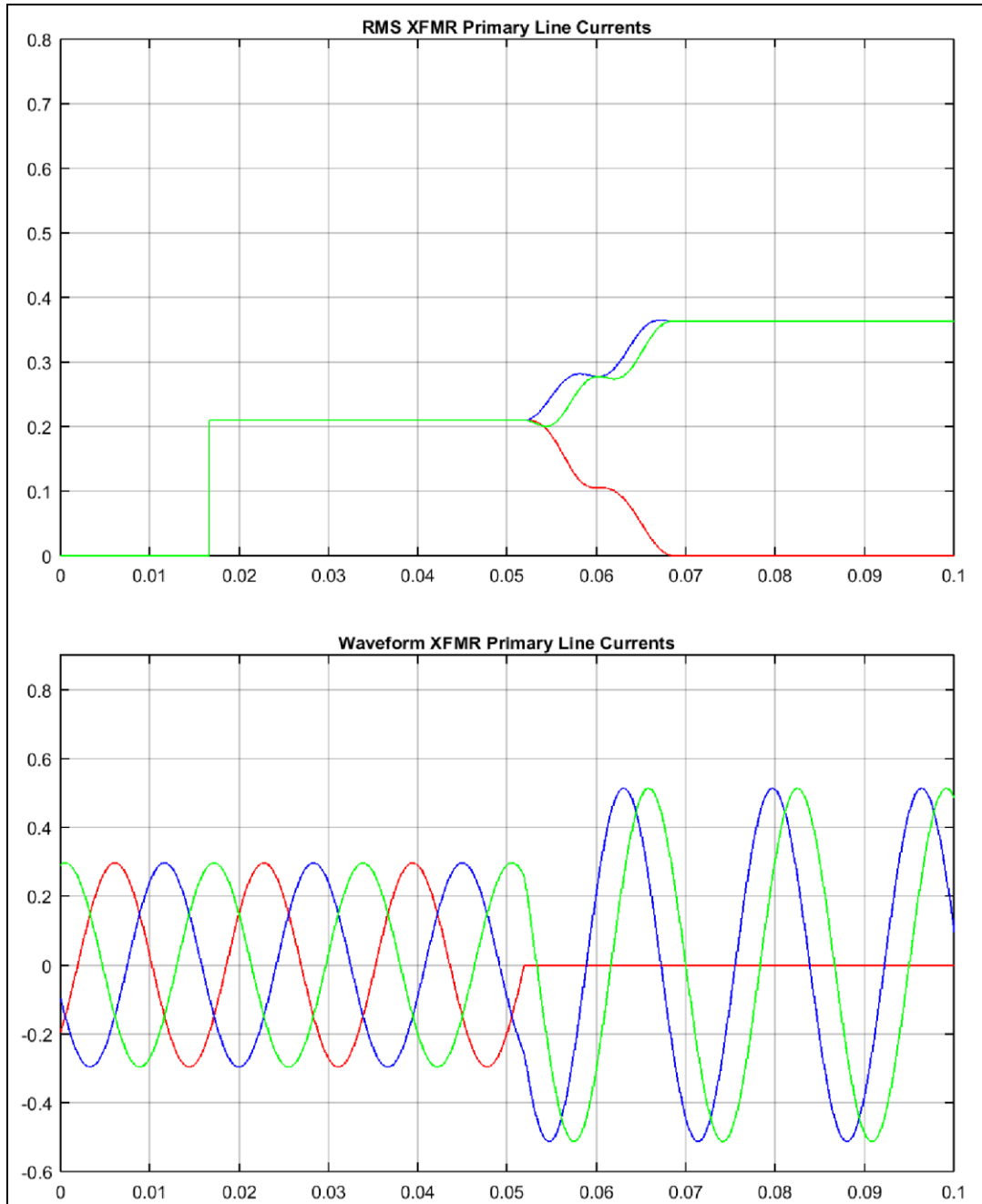


Figure 15: XFMR Primary Currents with Single Open Phase at 0.05s

The primary side transformer neutral current as shown below in Figure 16 is also in accordance with the symmetrical component analysis. Post fault simulation results show that the RMS value of the neutral current is 0.63 Amps where it is zero prior to the

fault. This level of fault current would not be enough to trigger even the most sensitive of overcurrent relays. Furthermore any relay set this low would struggle to distinguish between a true faulted situation and normal system imbalances. Transformer winding currents on the primary side winding mirror the line currents as would be expected with a Wye wound primary. The secondary side voltages remain fairly balanced also as described in the literature sources of Chapter 2. This is again due to the voltage being re-created by a combination of Kirchhoff's voltage loop law (sum of the voltages around the Delta winding are zero) and Faraday's law (the flux in a transformer is related to the voltage induced in the winding). More interesting is the presence post fault of a circulating current within the delta winding. Since the secondary side is an unloaded delta, current will not flow out of the transformer terminals to a load. However, due to the neutral current on the primary side a proportional current will circulate through the delta connected windings (Figure 17).

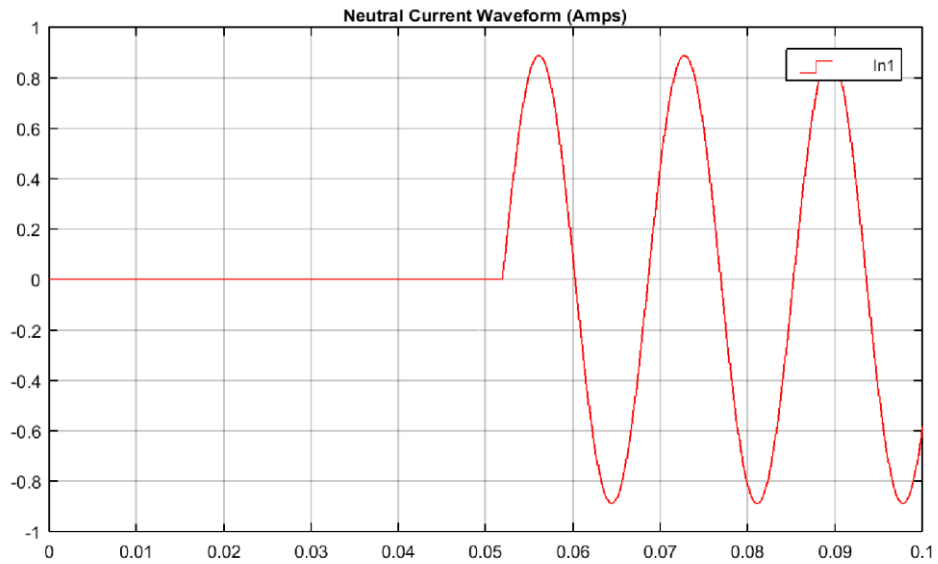
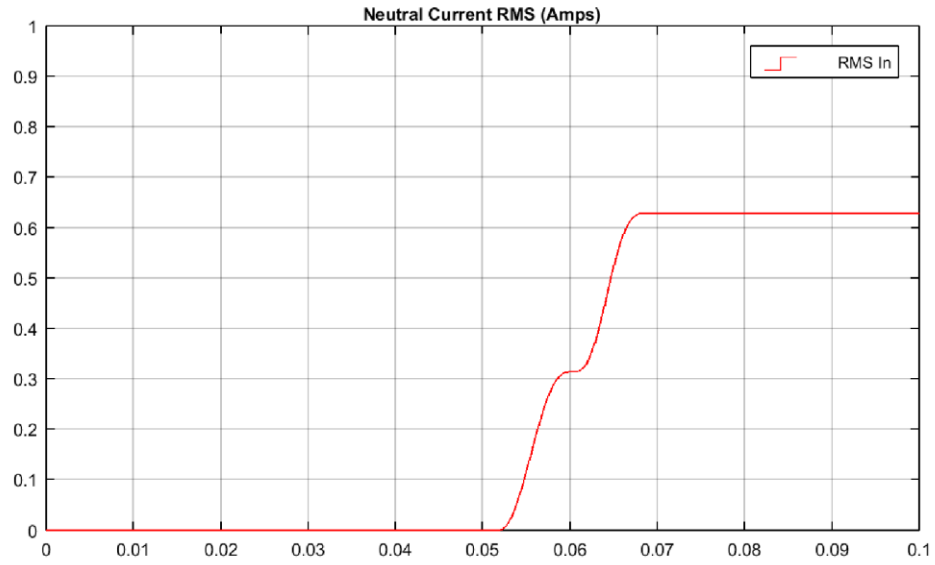


Figure 16: XFMR Primary Side Neutral Current

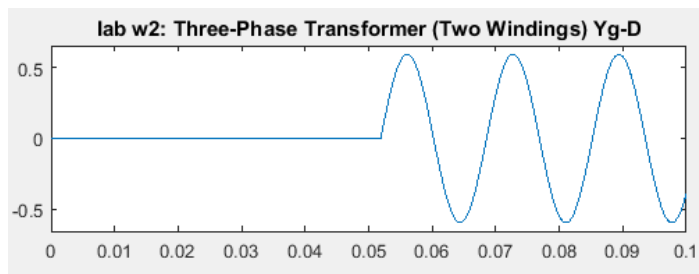


Figure 17: Delta Winding Circulating Current Waveform (Amps)

The analysis for a loaded transformer follows. This analysis assumed 30% (3000VA) loading on the secondary side with a power factor of 0.8 inductive to mimic loading of primarily motor loads. Loading was simulated using the *Three Phase Parallel RLC Load* block from the powerscapes library. The line side voltages at the terminals of the transformer are (as the case for the unloaded transformer) mainly unaffected by the open phase condition on the “A” phase. RMS voltage on the “A” phase terminal dips a little more than the unloaded case to a value of 114VAC while “B” and “C” phases are steady at approximately 120VAC RMS. The greater voltage drop in the A phase is primarily due to the drop in voltage on the secondary side as it is reflected back on the primary. However, this condition would also not be detectable with conventional undervoltage relays which are typically set to actuate at greater than a 10% drop in voltage. Scope and waveform signals for the transformer primary terminals are shown in Figure 18 below. The primary side currents prior to the fault are approximately 6.5 Amps and balanced. After the fault the intact “B” and “C” phases deliver 11.75 amps while “A” phase is zero. Current traces are shown in Figure 19.

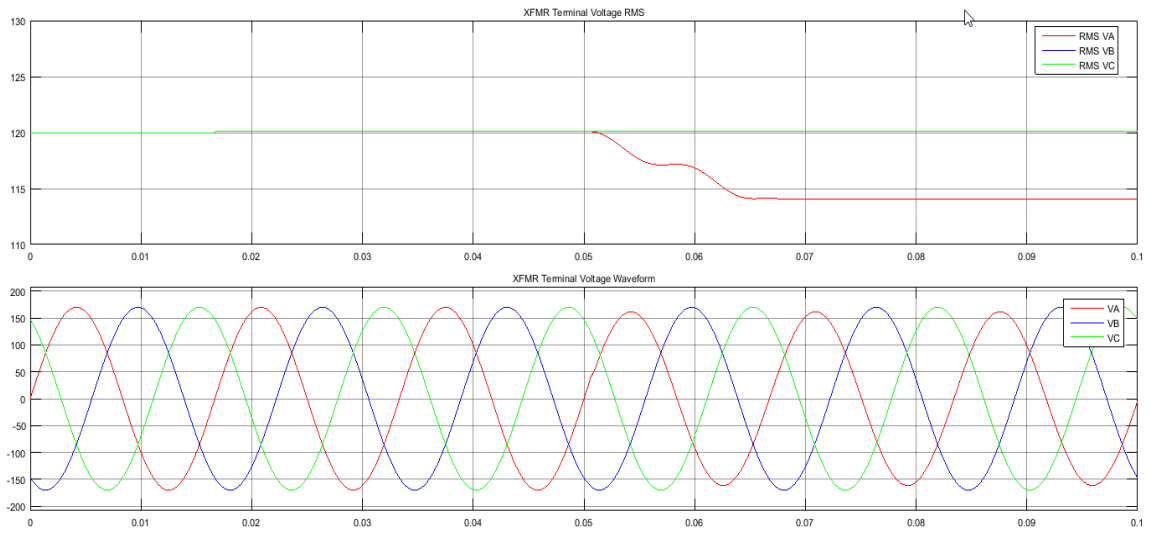


Figure 18: RMS and Waveform Traces of XFMR Terminal Voltage 30% Load

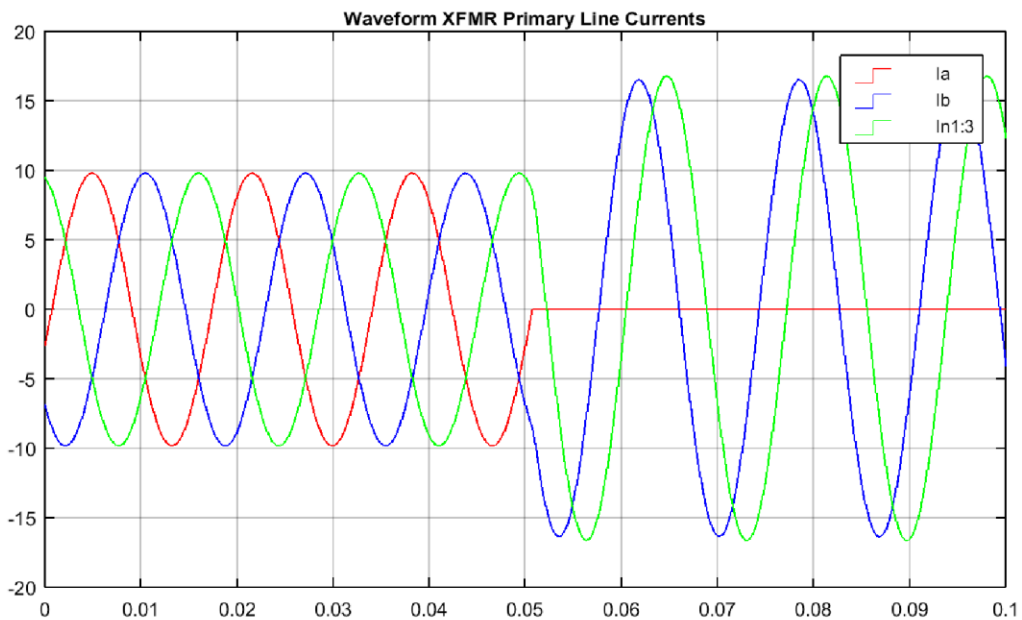
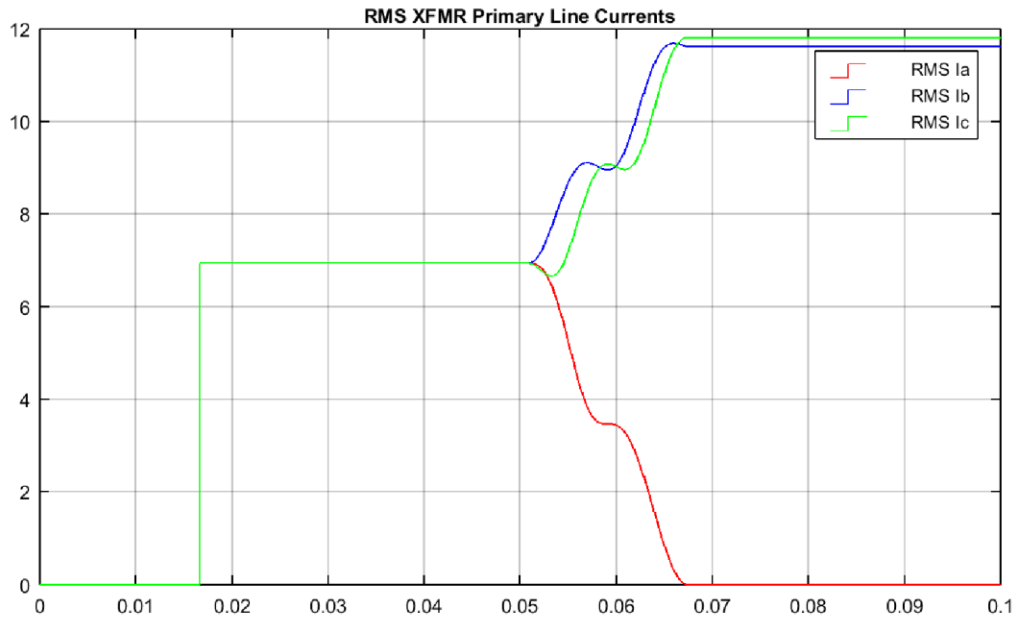


Figure 19: RMS and Waveform Traces of XFMR Primary Currents 30% Load

At this loading level the primary side transformer neutral current significantly increases as shown below in Figure 20. Post fault simulation results show that the RMS value of the neutral current is 20 Amps where it is zero prior to the fault. This level of neutral current begins to approach the nameplate rating of the primary side of the

3000VA single phase transformers (25Amps). However it still would not set off most neutral ground overcurrent relays as the neutral is typically sized to handle maximum transformer unbalance.

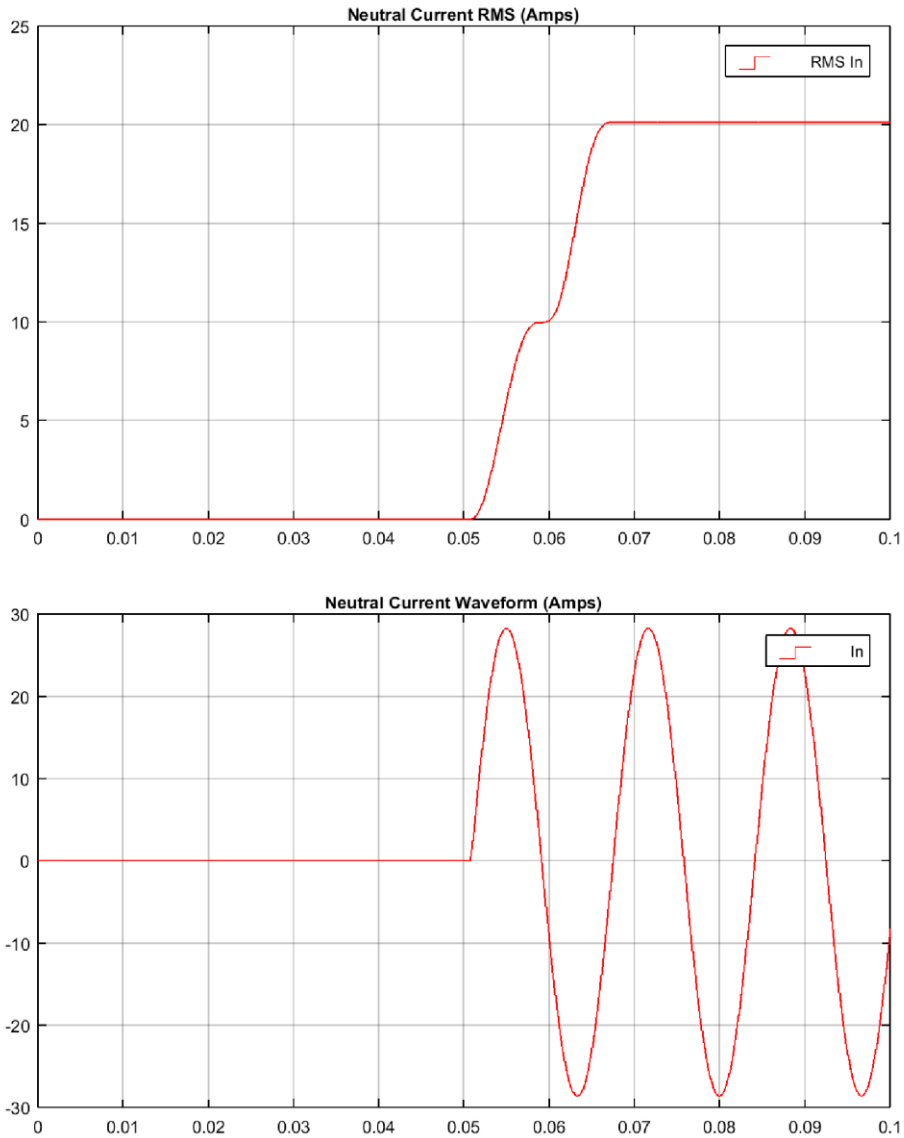


Figure 20: RMS and Waveform Traces of XFMR Neutral Currents 30% Load

The secondary side voltages as with the unloaded case, remain fairly balanced. See Figure 21. The largest drop is on “A” phase which drops from a nominal 60VAC to

57VAC. This drop is primarily due to the drop in “B” and “C” phase. Recall that the voltage at secondary terminal “A” will be a result of the sum of the voltages at “C” and “B” terminals. The voltages at “C” and “B” terminals drop from the nominal 60VAC to 59VAC and 58VAC respectively. This is due to voltage drop across the coil. As is seen in Figure 22 below, the secondary side coils corresponding to phases “C” and “B” carry substantially more current. This is due to the fact that the “A” phase coil does not transfer power and therefore does not carry current other than the magnetizing current and any circulating current due to the primary neutral current. The coil current unbalance poses a significant risk for the secondary side transformer “B” and “C” phase coils which will carry significantly more current as they compensate in power delivery for the lack of power contributed by the “A” phase. Higher loading levels could overheat secondary side transformer coils. This would go undetected because few distribution transformers are provided with coil current transformers.

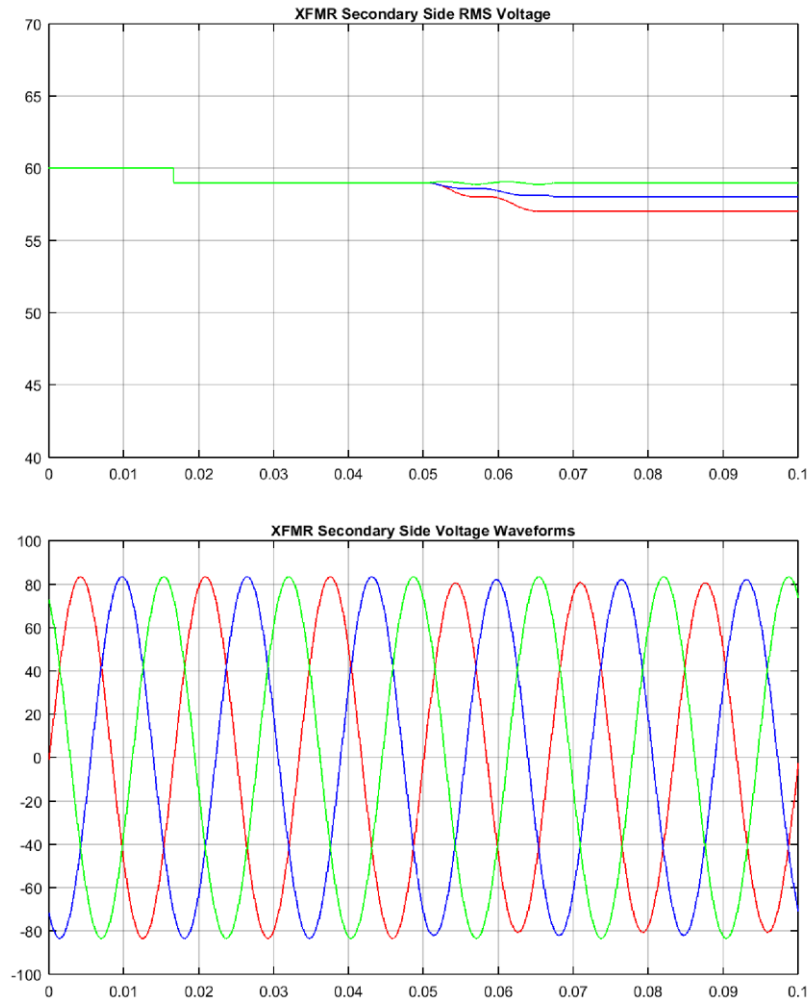


Figure 21: XFMR Secondary Side Voltage for 30% Loading

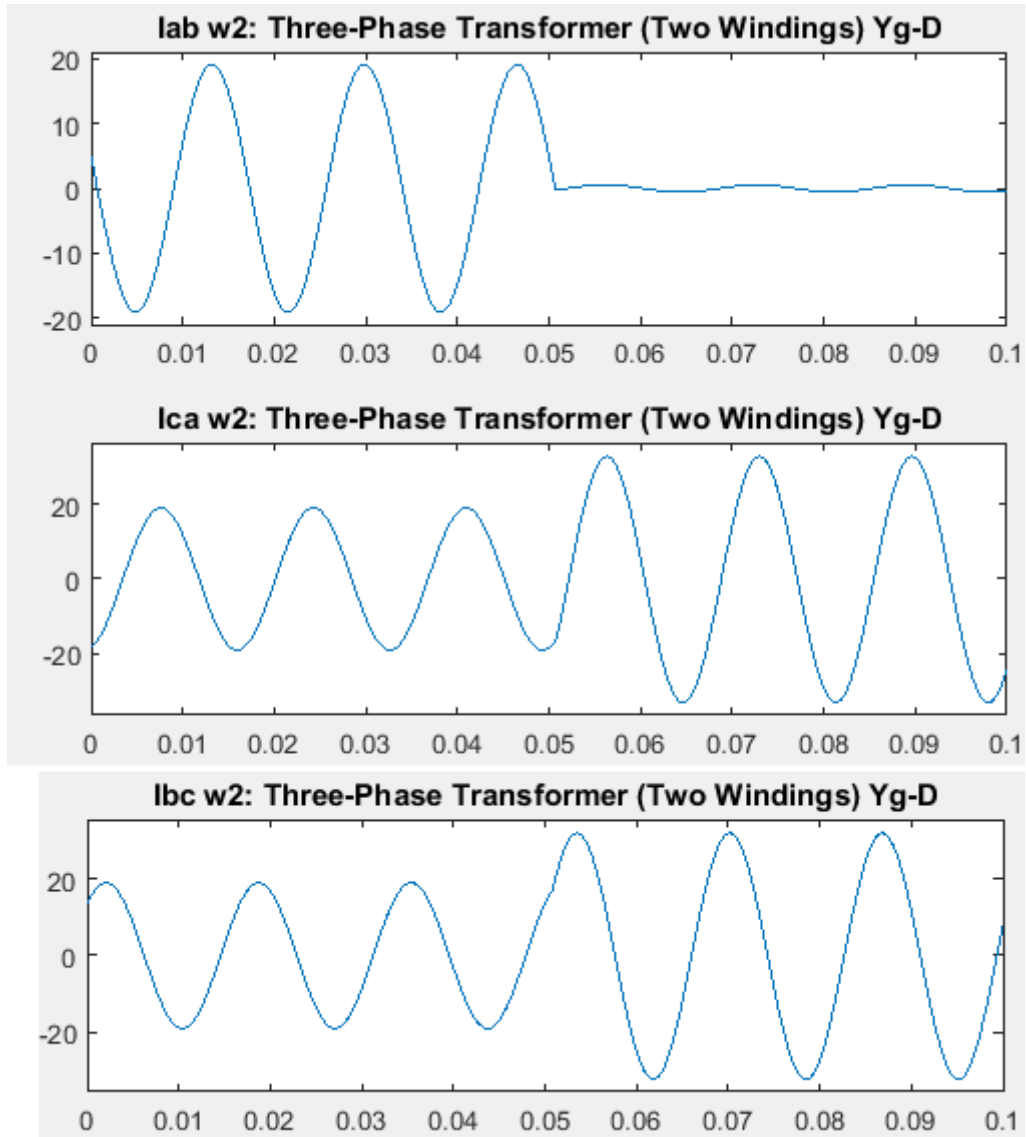


Figure 22: Secondary Side Coil Currents for 30% XFMR Loading (Amps)

While the secondary coil currents show significant current unbalance, the secondary side terminal currents are fairly balanced. Pre-fault supply current to the load was a balanced 23.5 amps nominal. Following the open phase the “A” phase line current to the load drops to 23 amps, the “B” phase line current drops to 22.5 amps and the “C” phase line current remains steady at 23.5 amps. This change in load current would not be detectable to any overcurrent protection. While the most significant unbalance is in the

secondary side coil currents, the secondary side terminal voltages experience a slight voltage unbalance. At this level of voltage unbalance we begin to encroach on the 5% limit set by NEMA MG-1 [7] and while the line currents may not present a risk to motor stators, the negative sequence currents that this can produce on the secondary side of the transformer could result in significant rotor damage and potential damage to motor loads. Hence a significant risk can go undetected by conventional protection standards.

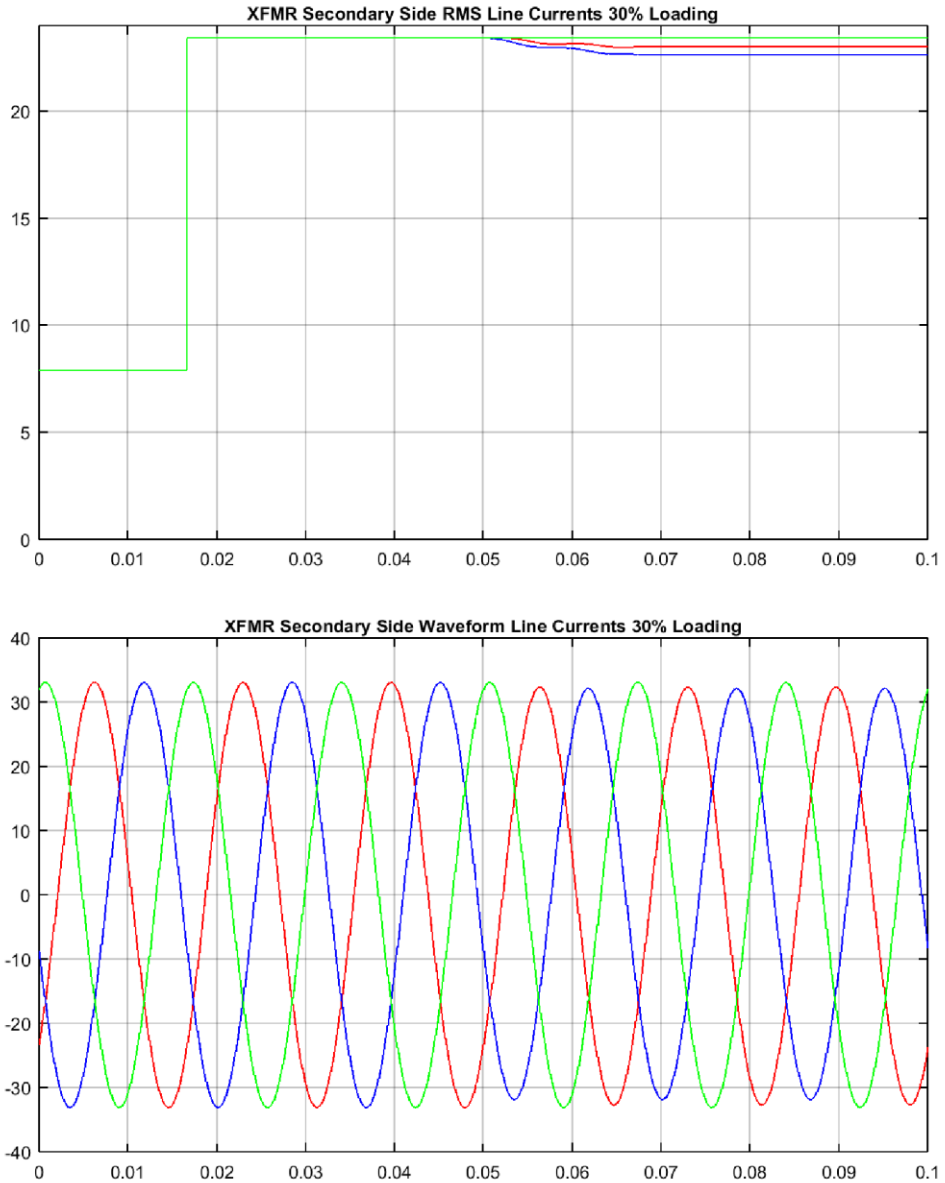


Figure 23: Secondary Side RMS and Waveform Currents 30% XFMR Loading

In conclusion, the system modeling in this Section has demonstrated that for unloaded and lightly loaded conditions on a distribution transformer an open phase fault on the primary side transformer will produce line voltages and currents that can present normal conditions and yet produce a risk to secondary side transformer coils and motor loads. Hence an alternative method of active detection and protection is necessary. In the

next Section we will utilize the MATLAB model to simulate the protection method of current injection described in [10, 11].

3.3 CURRENT INJECTION METHOD ANALYSIS BY COMPUTER

SIMULATION

The symmetrical component analysis documented in Section 3.1 shows that system currents can easily be calculated for an open phase condition. However, symmetrical component analysis assumes that the entire system is operating at the same frequency. Any change in signal frequency will change the phasor interaction and hence the method of symmetrical components cannot evaluate a mixed signal system. Additionally, as discussed in Section 3.2, many computer analysis tools are unable to model effects of faults and system interactions down to the individual phase node. ETAP as an example can show steady state 3-phase load flow for balanced and unbalanced conditions but cannot show individual transformer coil or device phase currents in the manner that MATLAB can. Other electrical system tools also do not have the capability of analyzing a mixture of signal frequencies within a power system. For example, they may be able to evaluate and determine the 60Hz voltages, currents and power flows in a system. However once an off nominal frequency signal is injected at a given point, the system may not be able to determine how the system is affected by it. This is especially crucial when analyzing the detection method of neutral current injection. The MATLAB model developed as part of this thesis has the capability of accurately modeling the neutral currents. Simulink is capable of handling and evaluating multiple frequency signals within a power system. This model will be used to model neutral current injection as a method of active detection of an open phase condition.

The method of neutral current injection is based on the concept that the zero sequence impedance as viewed from the transformer grounded neutral, through the

transformer windings and through the transmission system will be small in the balanced system. Once a phase opens the combination of reduction from three intact phases to two, as well as the potential zero sequence saturation of the transformer core will create significant resistance to current attempting to enter the neutral point. At this point small levels of injected current will be overcome by the natural unbalanced 60Hz neutral ground current that results from the sum of the intact phases in the transformer primary neutral. This principle can be harnessed as a detection method using the system design shown below in Figure 24. Using a function generator, a 180Hz voltage will be applied to a current transformer (CT) secondary with a current ratio of 100:1. The primary side of the CT is connected between the distribution transformer neutral and ground. This is done for two reasons. First, because a practical function generator can typically only produce an output current of 200mA. By applying the current to the secondary side of the CT the CT will act as a current amplifier and increase the current according to the CT ratio to a measurable level. This was tested in the Cal Poly laboratory and is documented in Appendix 3. In actuality the amplification factor did not match the CT ratio but instead was much less. It became even smaller when the primary was connected to the distribution transformer neutral and the transformer was energized. The second reason for injecting the current via a CT is to allow any normal neutral current due to system unbalance to flow un-impeded. Not doing so can result in dangerous neutral voltages and possibly damage the transformer as the transformer would essentially become ungrounded.

While current is being injected at 180Hz, a second CT will measure the injected current. When the system is balanced, only the 180Hz current will flow through the

transformer neutral and will be sensed. As the system becomes more unbalanced, 60Hz neutral current will flow and begin to overcome the injected current. An open phase represents maximum unbalance and will produce a high enough zero sequence impedance path so as to significantly reduce the 180Hz injected current. By analyzing the frequency signature of the neutral current we can detect the shift from primarily 180Hz neutral current to 60Hz current and declare an open phase.

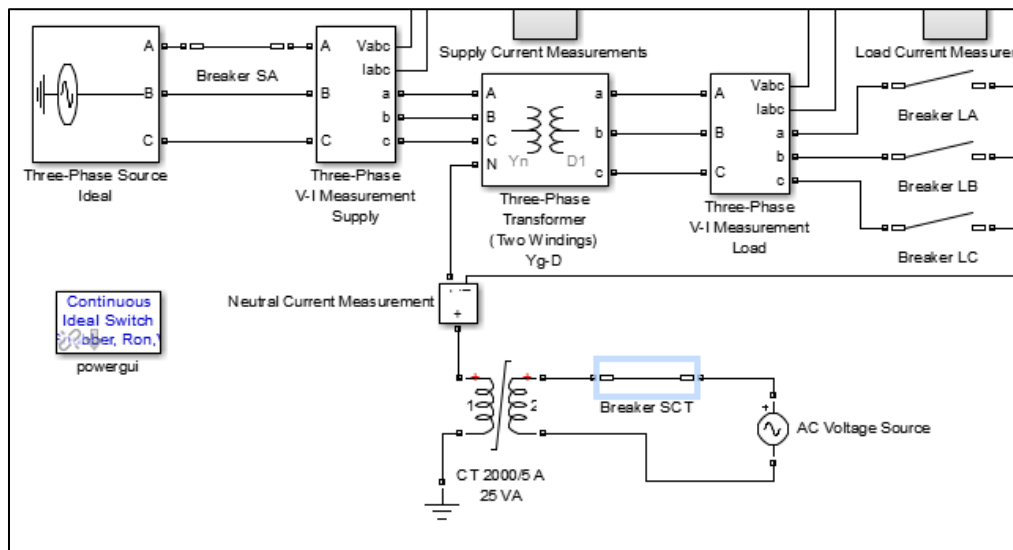


Figure 24: MATLAB Model Focus on Current Injection Source

The system model was modified to support the current injection method by placing a saturable transformer between the transformer neutral connection and the ground point. MATLAB Simulink does not have a current transformer block and also does not allow the introduction of a current source injecting directly into the transformer neutral point. However a model for a saturable CT is included as a demo in the Simulink program by typing in the *power_ctsat* command. This transformer was used as part of the current injection simulation. The transformer was introduced downstream of the current

measurement point to allow for detection of the shift from 180Hz dominant injection current to 60Hz ground current. A 180Hz voltage source was placed on the secondary side of the current transformer. The voltage source was adjusted in Simulink until results similar to the CT laboratory data of Appendix 3 were obtained. Additionally, the output of the neutral current measurement CT was run through a Fourier transform both at a 60Hz fundamental and a 180Hz fundamental to obtain frequency domain amplitudes of the signal.

The first case run was for the completely unloaded condition. The circuit breakers feeding the load were all set to open. The results are as predicted in references [10] and [11]. Measured primary neutral current is initially dominated by the 180Hz injection signal with an RMS value of approximately 420mA (see Figure 25 below). The current injection does not seem to impact the primary transformer supply voltage as prior to the fault the supply is stable and balanced at a nominal 120VAC RMS as shown in Figure 26 below. The supply current though is impacted as it shows a distorted waveform due to the superimposed 180Hz current injected (Figure 27). The magnitude of this current though is an average 220mA RMS and so it is assumed that the change in frequency will not cause harmful effects to the transformer at this low of a magnitude. The significant impact to the current waveform is due to the fact that the transformer is unloaded and so the only current flowing from the supply is the magnetizing current.

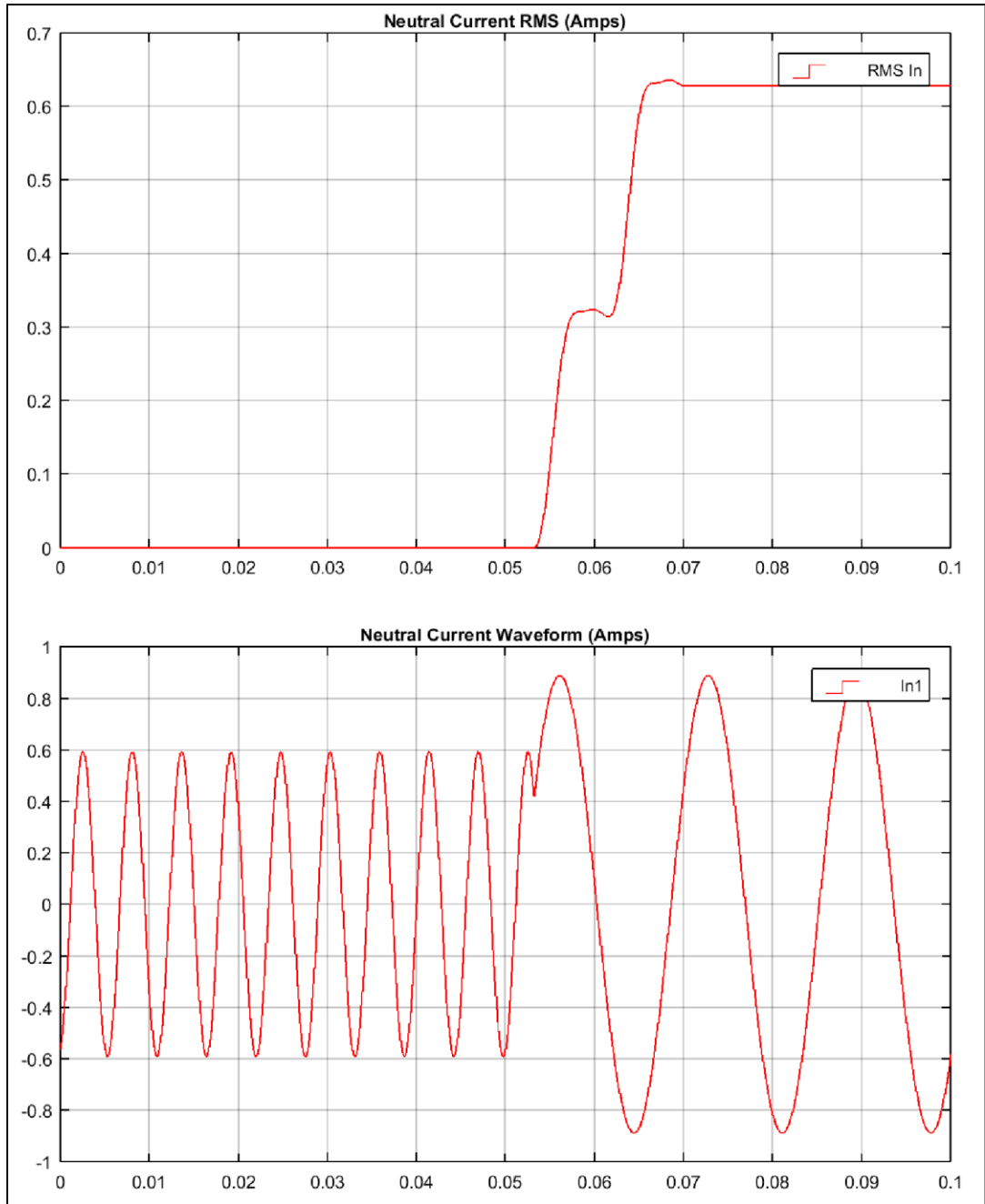


Figure 25: Primary XFMR Neutral Current with 180Hz Current Injection

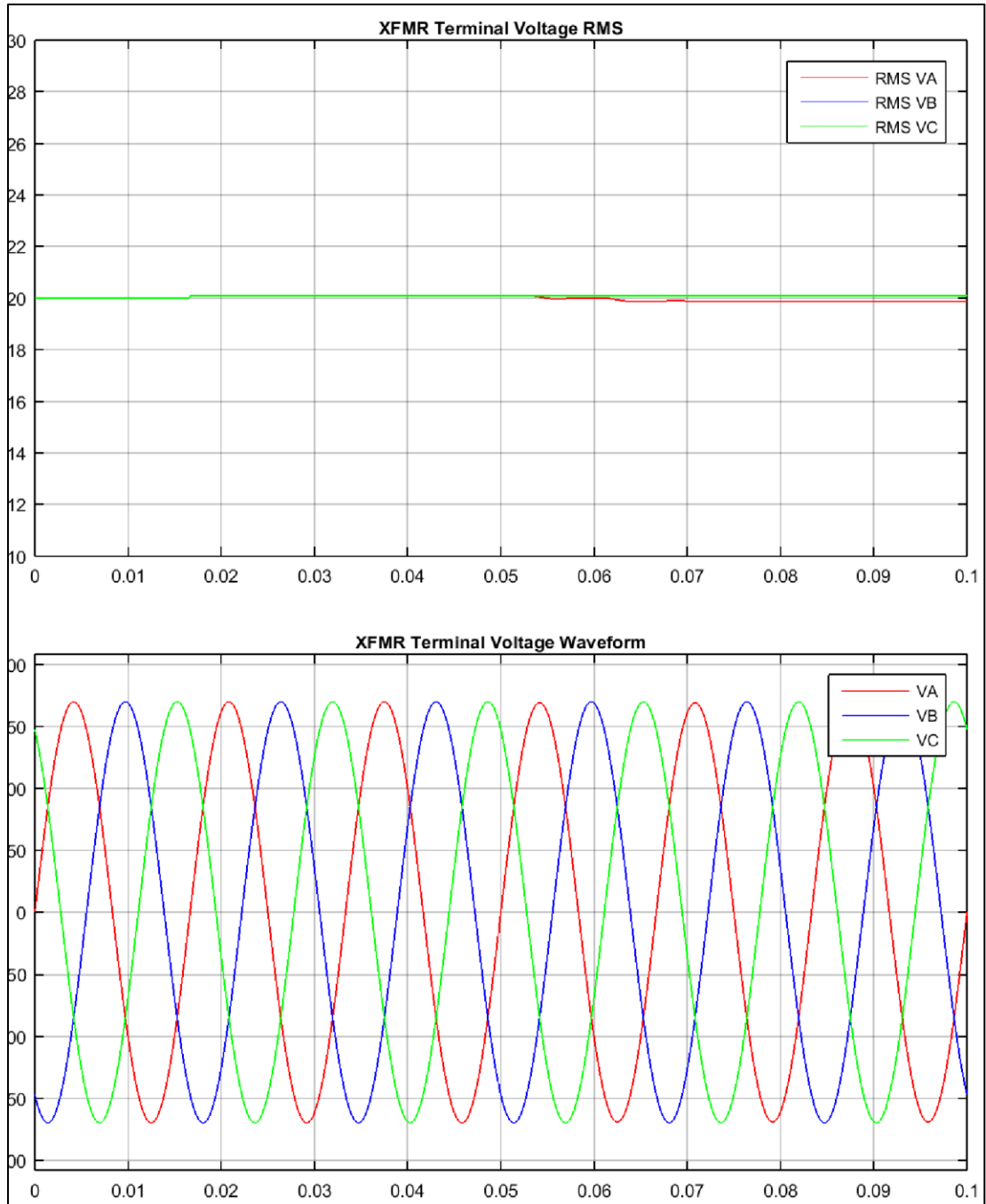


Figure 26: Primary Side XFMR Terminal Voltage with Current Injection

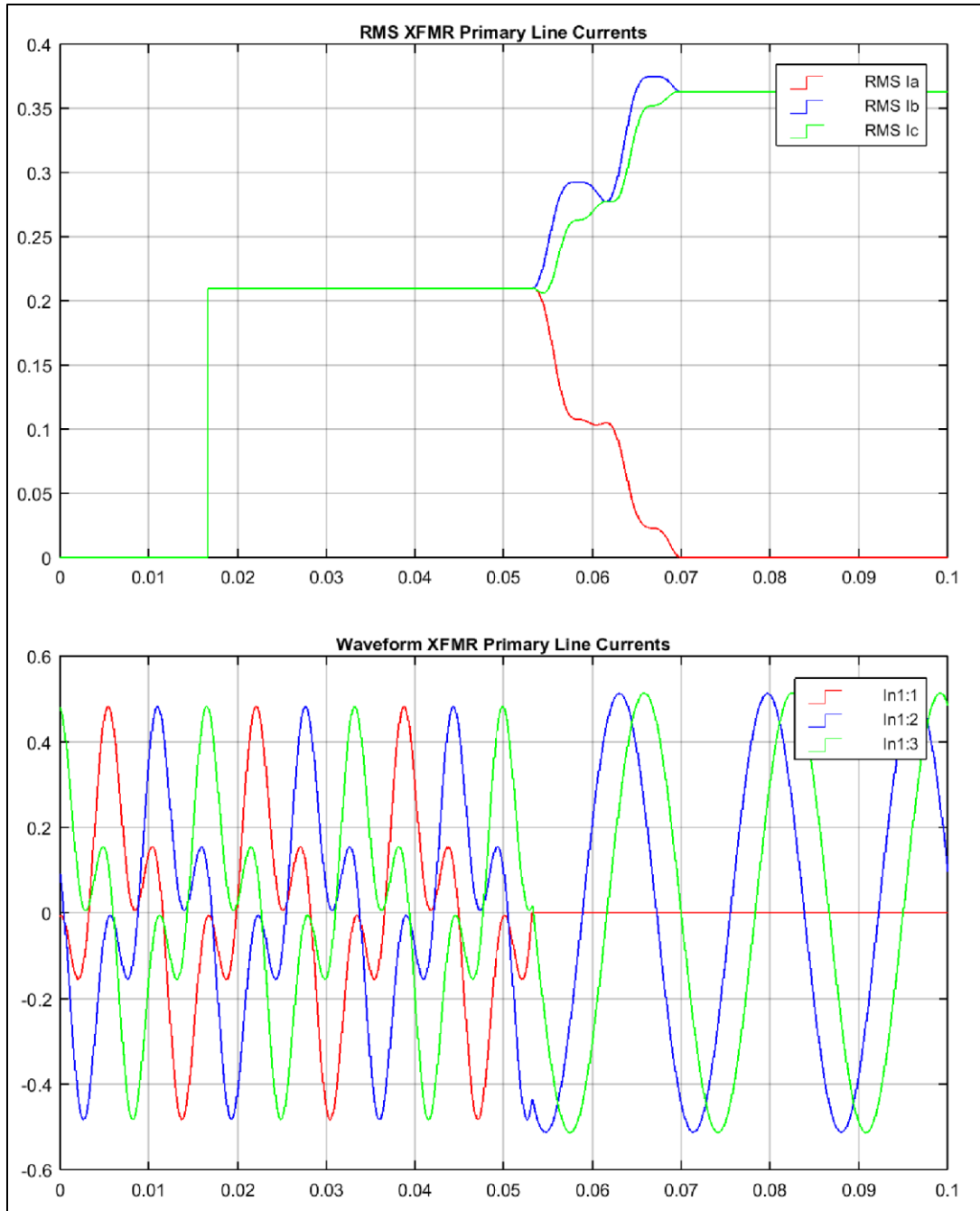


Figure 27: XFMR Primary Side Currents with Current Injection

Following the open phase, voltage dips slightly on the impacted supply phase. However the dip is commensurate with the dip seen in Section 3.2 for an open phase transformer without current injection. Voltages remain relatively balanced. The more

profound effect is for the supply currents and neutral ground currents. As shown in Figures 26 and 27 above, the supply currents shift from a heavily distorted 180Hz wave form to a 60Hz dominant current for the intact phases and zero current for the open phase. RMS current on the intact phases mirrors that of the open phase unloaded transformer in Section 3.2 (approximately 0.36Amps RMS). Neutral ground current follows this change with the post fault dominant frequency at 60Hz and approximately 0.63Amps RMS. Interestingly despite the low level of line and neutral current following the fault, the injected signal produces negligible distortion on the resulting current waveform. This proves that the open phase results in a significant increase in zero sequence impedance between the transformer neutral point and the supply ground which chokes off the injected current. Hence for the unloaded transformer this can be a very effective method of detecting an open phase condition as the change in current signature between the pre fault condition and the post fault condition is so significant.

An injected current at an off nominal frequency and the corresponding distortion of the line current supply raises concerns regarding secondary side effects to the transformer voltage supply. However as shown in Figure 28 below, the RMS and waveform voltages remain completely unaffected by the current injection source. The secondary side voltage is only slightly affected by the open phase in a similar manner as was described in Section 3.2. Hence it is safe to conclude that the injection source will not produce any secondary side voltage effects that may impact sensitive relays or devices. The most significant difference on the secondary side is related to circulating current within the delta connected windings. The windings now show a 180Hz circulating current prior to the open phase fault which mirrors the primary side injected current. This

is expected as any zero sequence current will be reflected as a circulating current in the delta winding. After the open phase fault, the current shifts to a 60Hz dominant current as expected. Secondary side coil currents are shown in Figure 29.

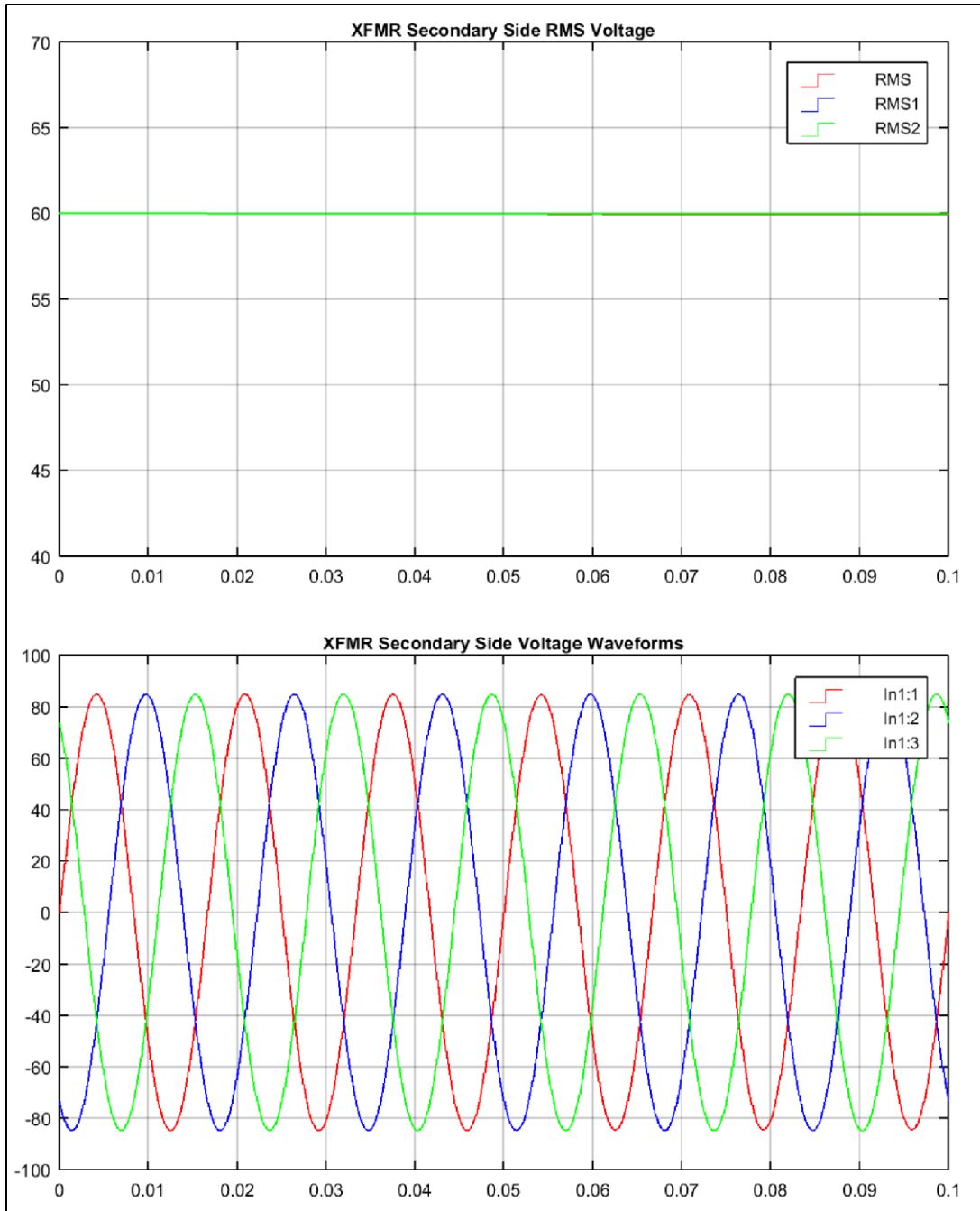


Figure 28: Secondary Side Voltage Traces for Unloaded XFMR with Current Injection

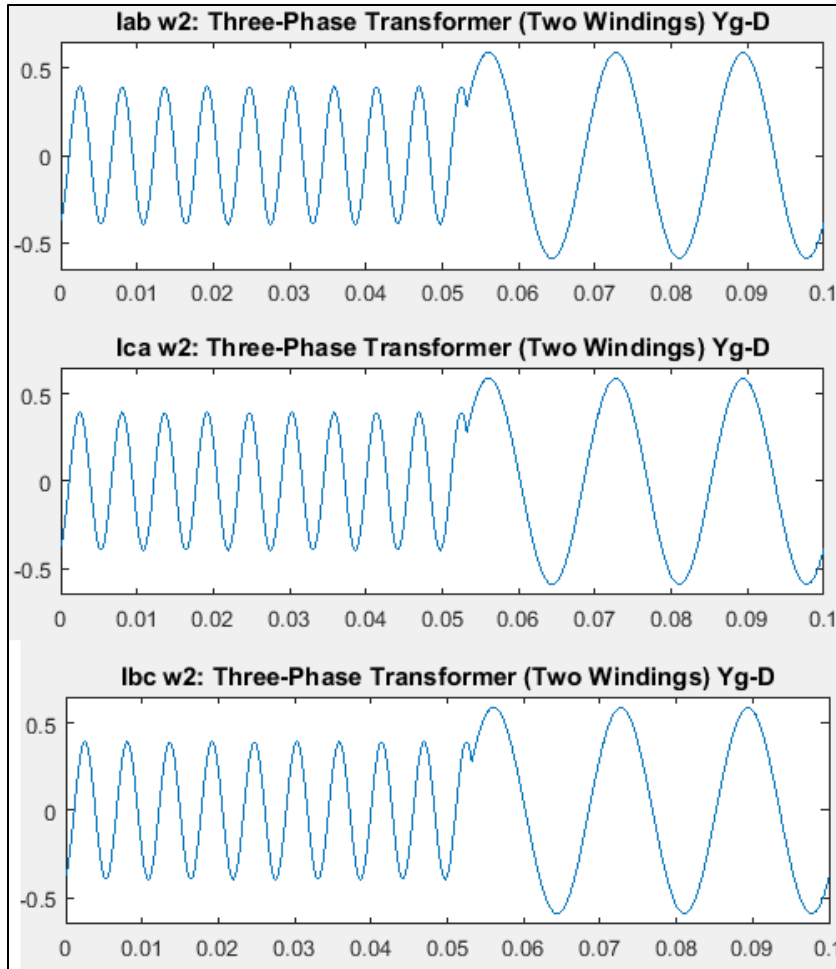


Figure 29: Secondary Winding Coil Currents Unloaded Including Current Injection

The second analysis of this Section will determine if this detection method will still work when the secondary side of the transformer is loaded. Hence the secondary side load breakers are closed and the simulation repeated. For the loaded case, the supply side voltages mirror the loaded run performed in Section 3.2 with voltages well balanced both before and after the fault (Figure 30). Unlike the unloaded condition, the supply side currents prior to the fault do not have the significant 180Hz distortion. Instead they mirror the current conditions for the loaded run in Section 3.2. This is because in the loaded condition, the supply side currents are more than 20x the magnitude of the

injected current and hence it is shadowed by the load current. However Figure 32 shows that the neutral current still carries the 180Hz current prior to the open phase fault. This is again because despite the high level of loading, during the balanced condition, the zero sequence impedance path is very small and still allows the injected signal current to flow easily. It is only after the open phase fault and the significant change in zero sequence impedance that the injected current is choked off and the sensed neutral current becomes dominantly 60 Hz based.

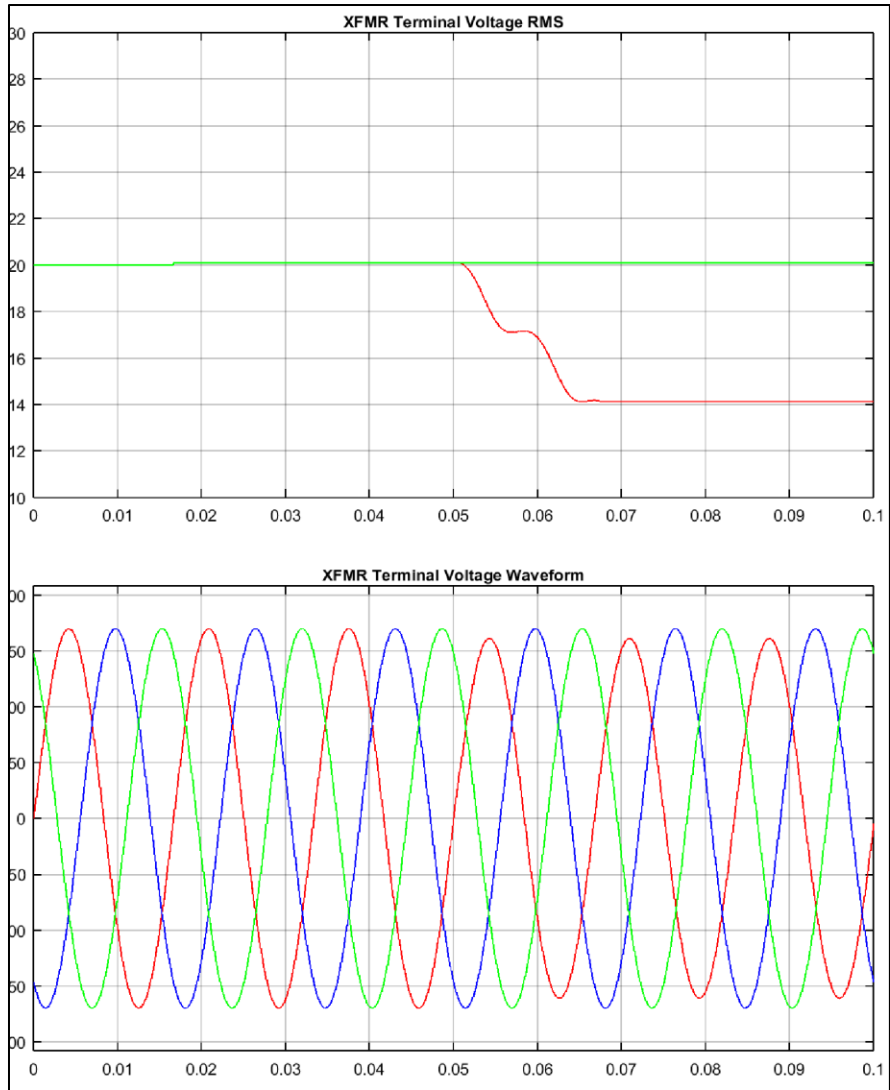


Figure 30: Primary Side Voltages for Balanced 30% Loaded XFMR with Current Injection

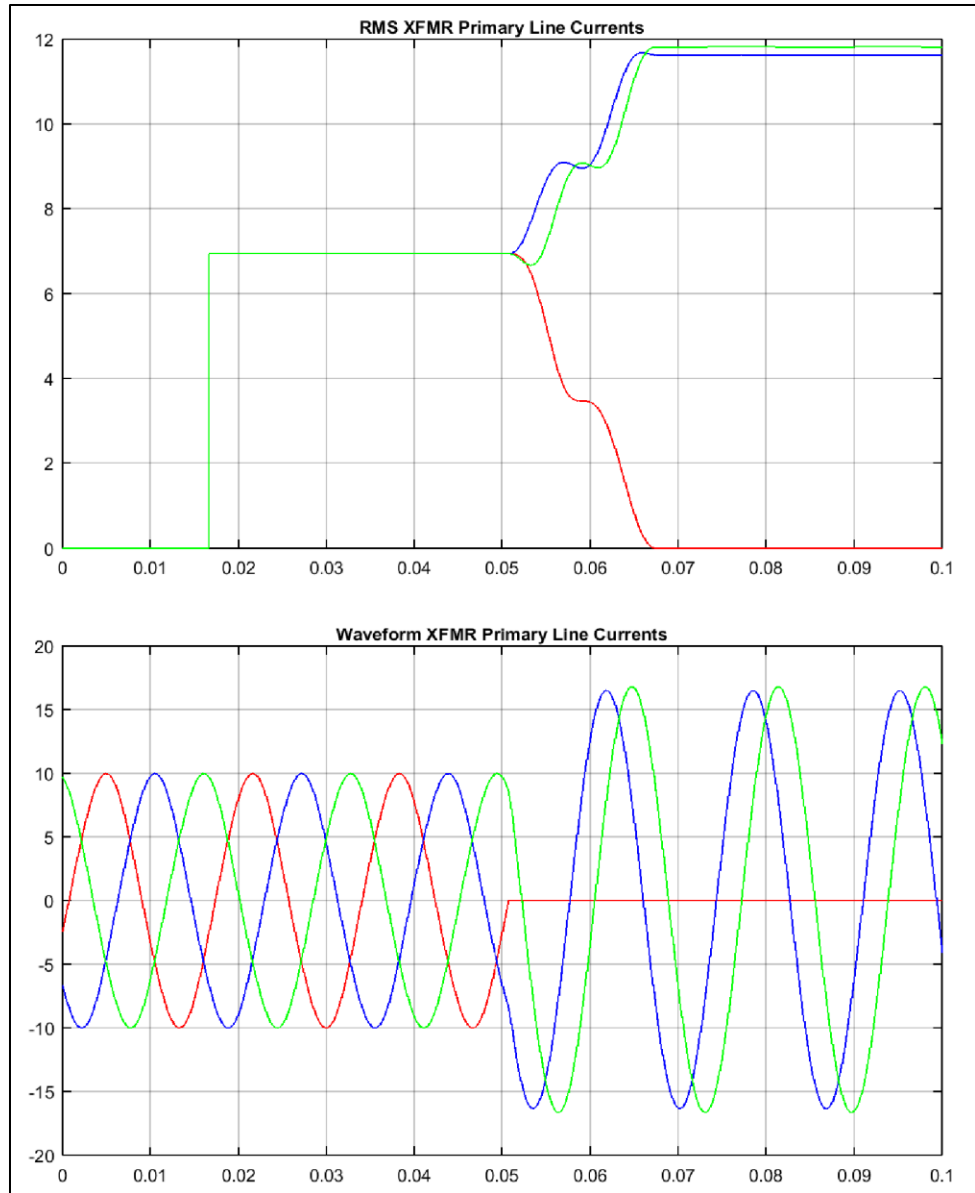


Figure 31: Primary Line Currents for 30% Loaded XFMR with Current Injection

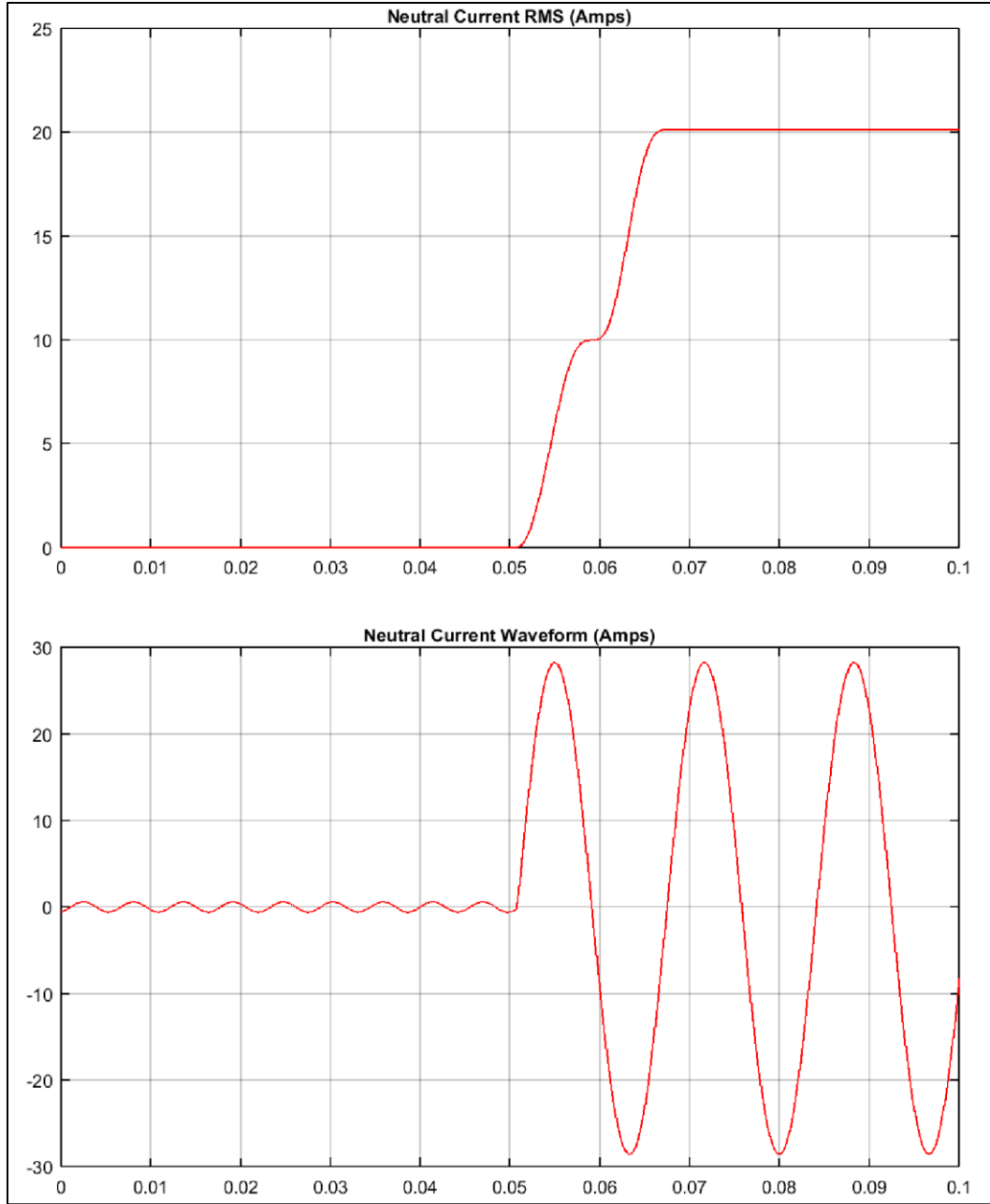


Figure 32: Neutral Injection Current During 30% Loaded Scenario

On the secondary side, line voltage and line currents again mirror the results of the loaded scenario in Section 3.2. They are unaffected by the injection signal both prior to the open phase and after. Load side voltages and currents remaining fairly balanced. Additionally because of the large load currents, the secondary side delta coil currents do

not show the 180Hz circulating current as they are shadowed by the load current. Results are shown below in Figures 33 through 35.

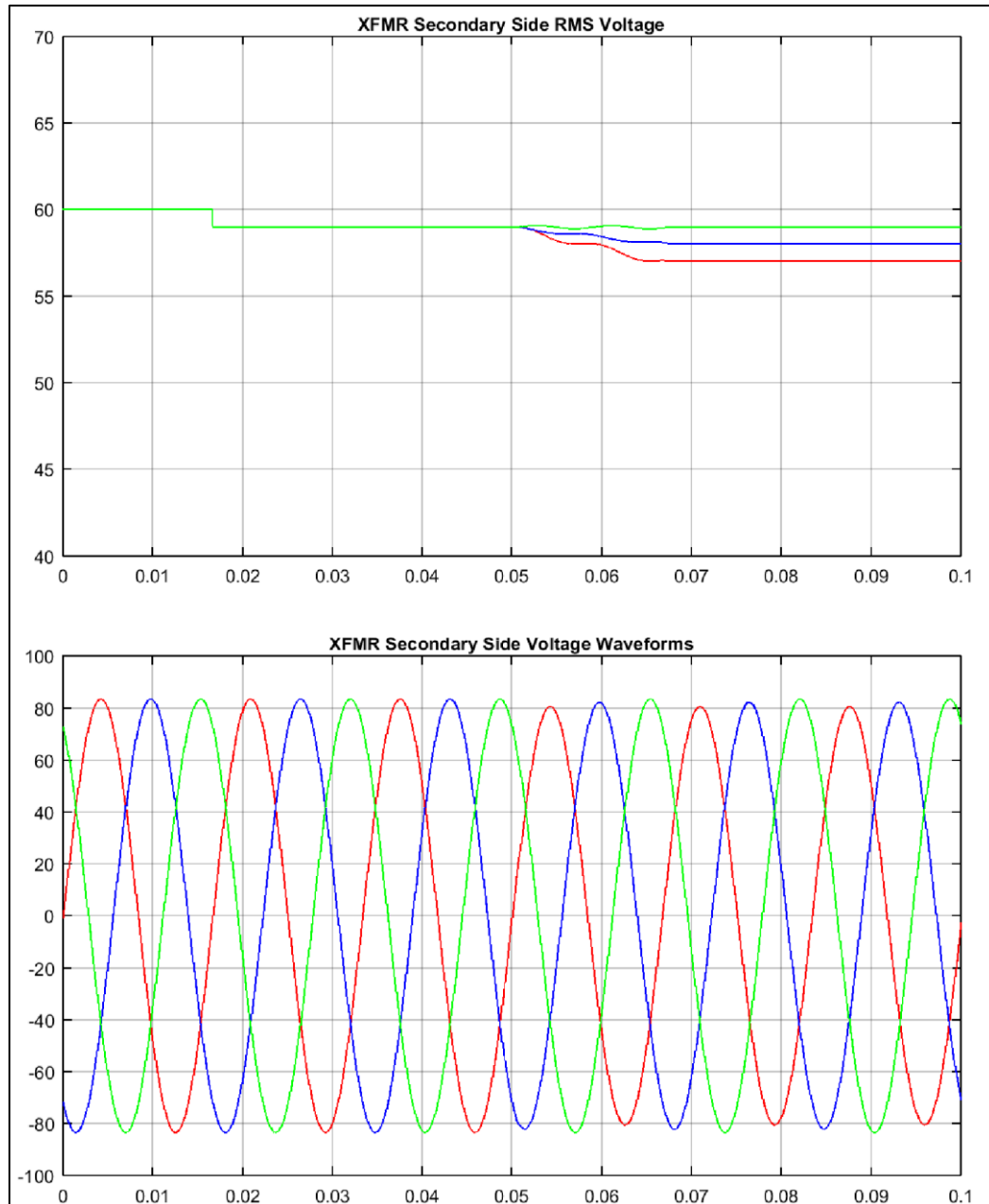


Figure 33: 30% Loaded XFMR Secondary Voltages with Current Injection

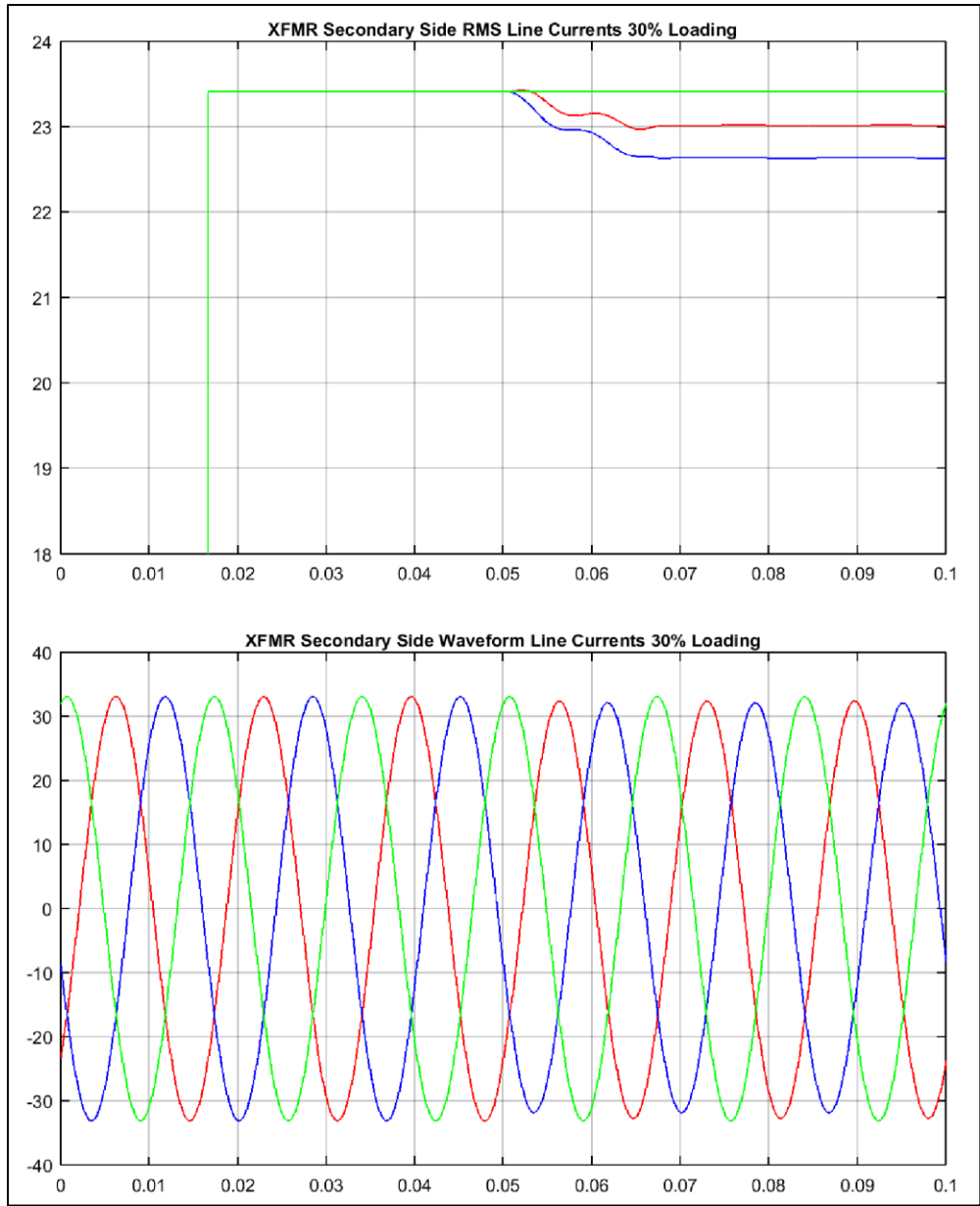


Figure 34: 30% Loaded XFMR Secondary Side Currents with Current Injection

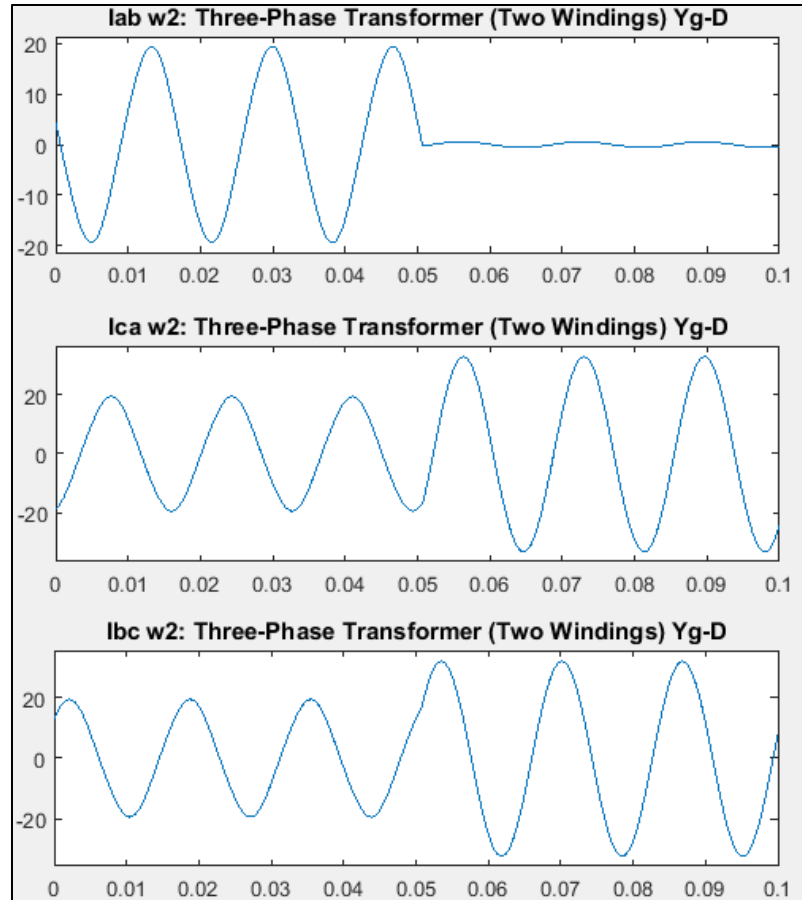


Figure 35: 30% Loaded XFMR Secondary Side Coil Currents with Current Injection

While the results in the two analyses above are very promising with regard to the viability of using current injection as a method of open phase detection, there were concerns regarding the ability of the neutral current injection method to detect when significant secondary side load unbalance presented itself. It is expected that unbalanced loading conditions on the secondary side will present itself as unbalanced current supplies on the primary side which will result in significant neutral current flowing. Hence additional analyses were conducted using unbalanced secondary side loading. For the third analysis, the “A” phase secondary side breaker was maintained open which would

present as zero load on the “A” phase secondary. The 33% loading remained on the “B” and “C” phases. All other conditions from the first two current injection runs above remained the same. The model change is shown in Figure 36 below.

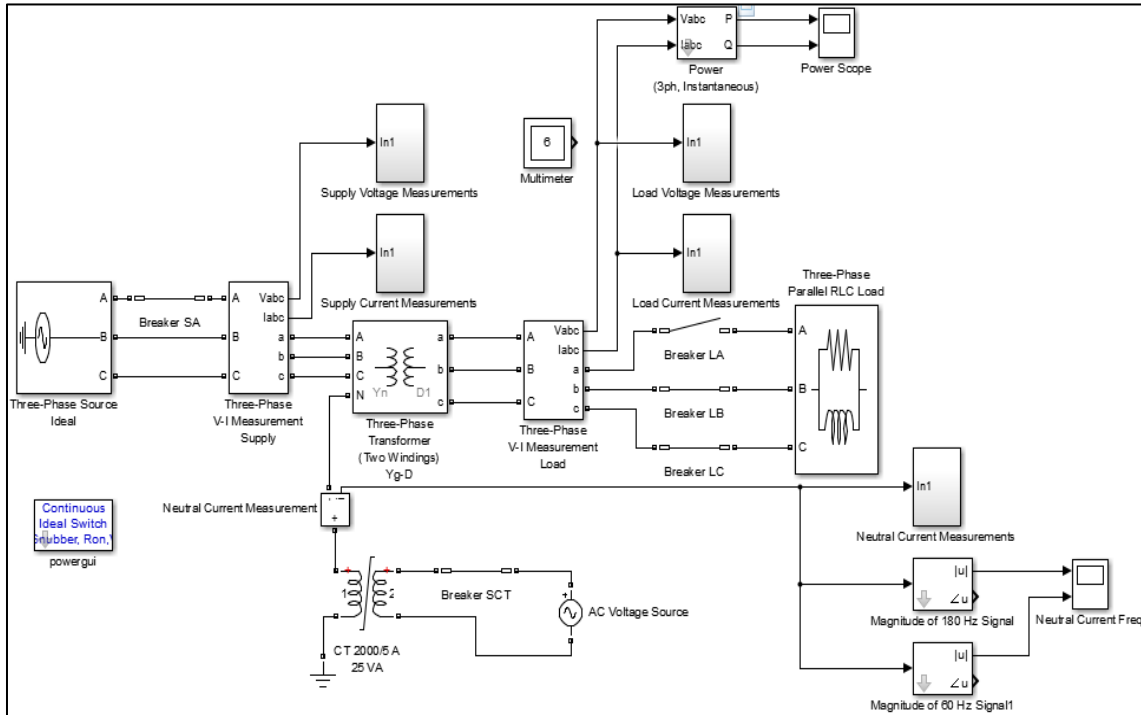


Figure 36: MATLAB Model for Unbalanced Loading (30%) on XFMR Secondary

The results of this run demonstrate that on the primary side, supply side terminal voltage again remains extremely balanced both prior to the fault and after the fault. While the RMS voltage signal for the primary side “A” phase shows a transient at the point of the open phase fault, the waveform trace shows absolutely no disturbance. This discrepancy is attributed to the Simulink RMS calculation blocks need for conditions to be steady for 2 cycles before it can produce reliable results. See Figure 37 for results. More notable are the impacts of the secondary side loading unbalance to the primary side line currents as shown in Figure 38. Prior to the open phase, there is significant unbalance

with the “A” and “C” phase line currents mirroring each other and in phase. The “B” phase current is out of phase from “A” and “C” by 180 degrees and has a magnitude approximately twice that of “A” and “C”. For this reason, the sum of the currents at the neutral point remains zero despite the secondary side unbalance. Following the fault the “A” phase line current drops to zero as expected but surprisingly “C” phase also drops nearly to zero and “B” phase rises to carry the majority of the load current. The significant drop in “C” phase current despite the phase being intact was not investigated further but is most likely due to the magnetic circuit of the transformer attempting to balance itself. Investigation into why this phenomenon occurs is left for future work. While these results show dramatic changes, the final steady state currents still do not rise to the level of potentially tripping a protective relay as they are all still well within the nameplate rating of the transformer primary current rating. The resulting neutral current traces are most encouraging as they continue to show that despite the significant load unbalance on the secondary side, the neutral current prior to the open phase is dominated by the 180Hz injection current and again shifts to a dominant 60Hz current following the open phase.

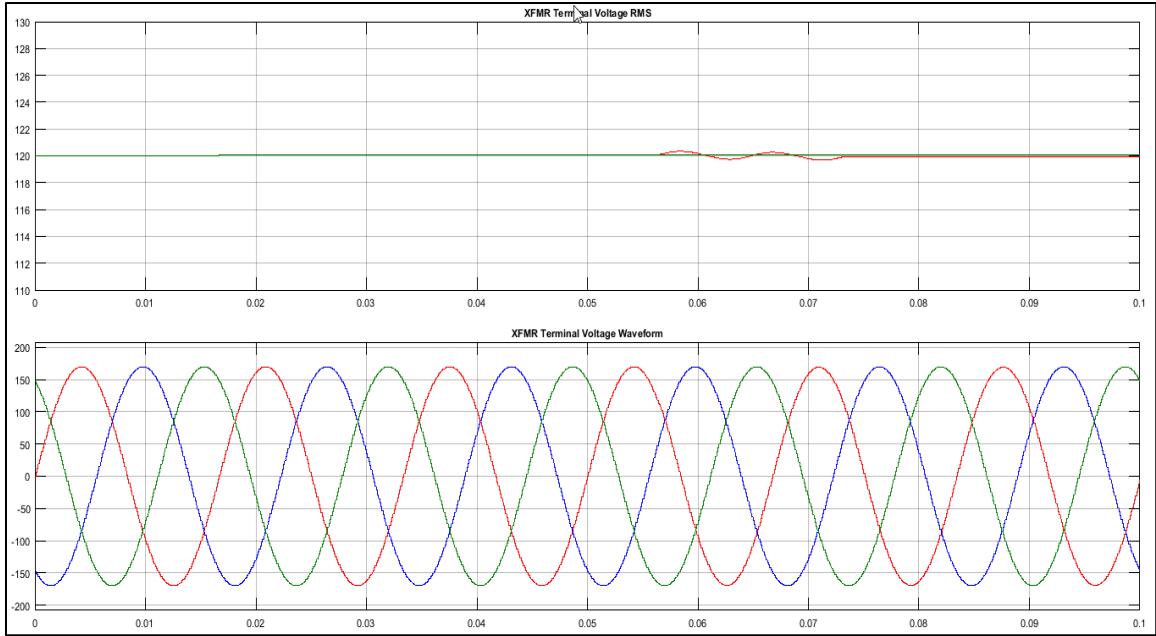


Figure 37: Primary Side Voltages for Unbalanced Loaded XFMR with Current Injection

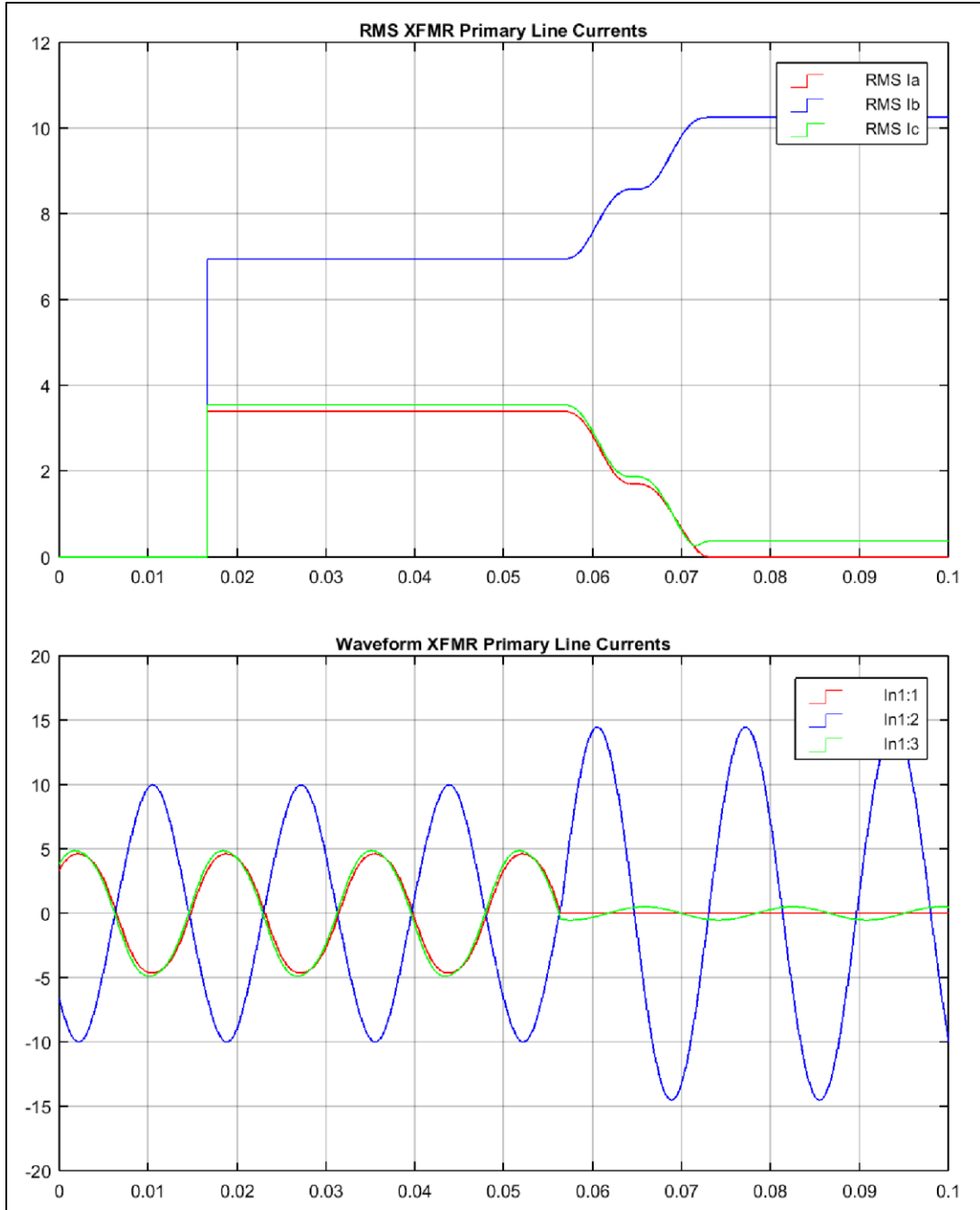


Figure 38: Primary Side Currents, Unbalanced Loaded XFMR with Current Injection

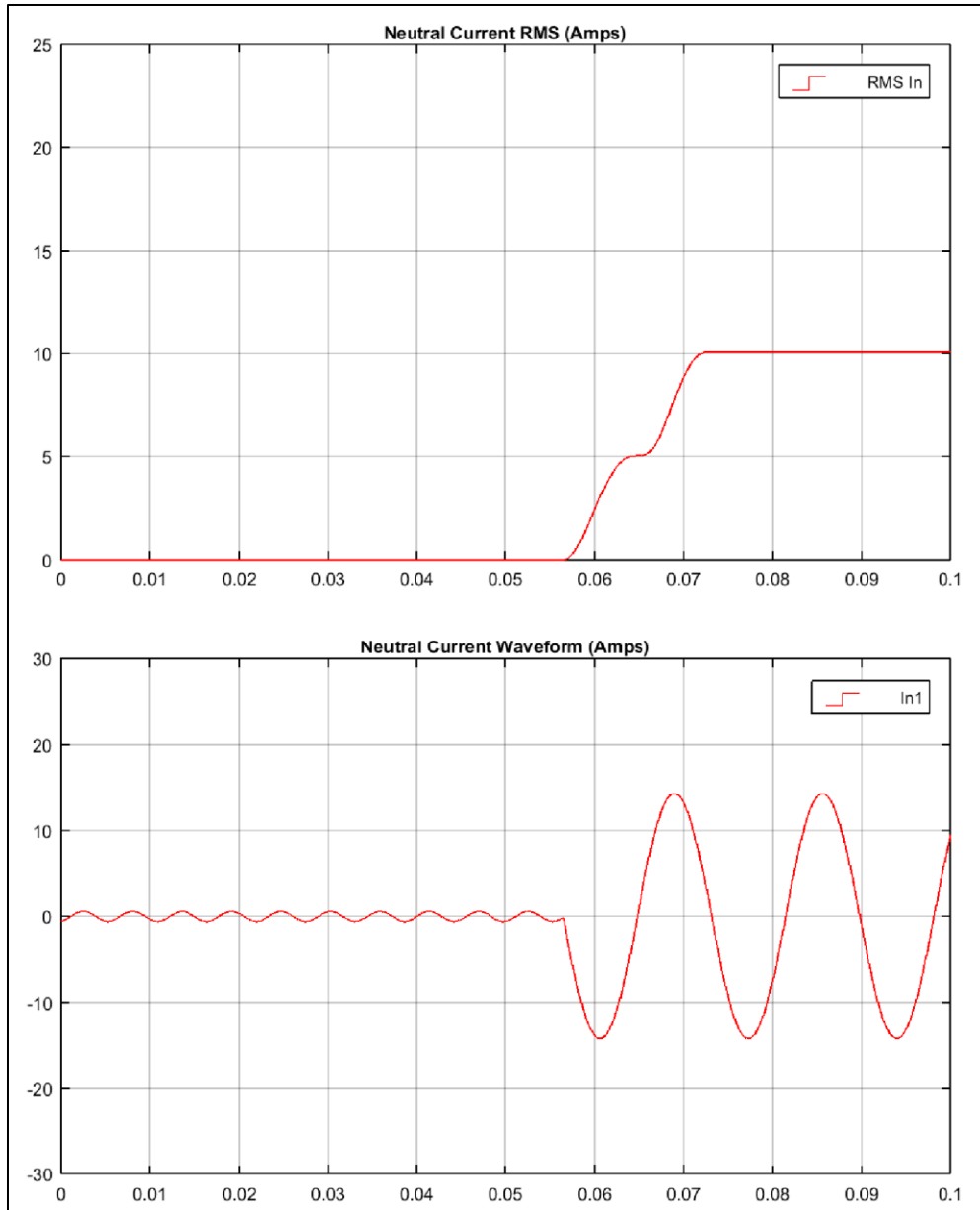


Figure 39: Neutral Injected Current, Unbalanced XFMR Loaded Scenario

Again the secondary side conditions are monitored for any adverse effect from the current injection source and none are identified. As shown in Figures 40, 41 and 42 the secondary side voltages, line currents and winding currents present no signs of the injection signal and are commensurate with the expected results for an unbalanced secondary side loading condition.

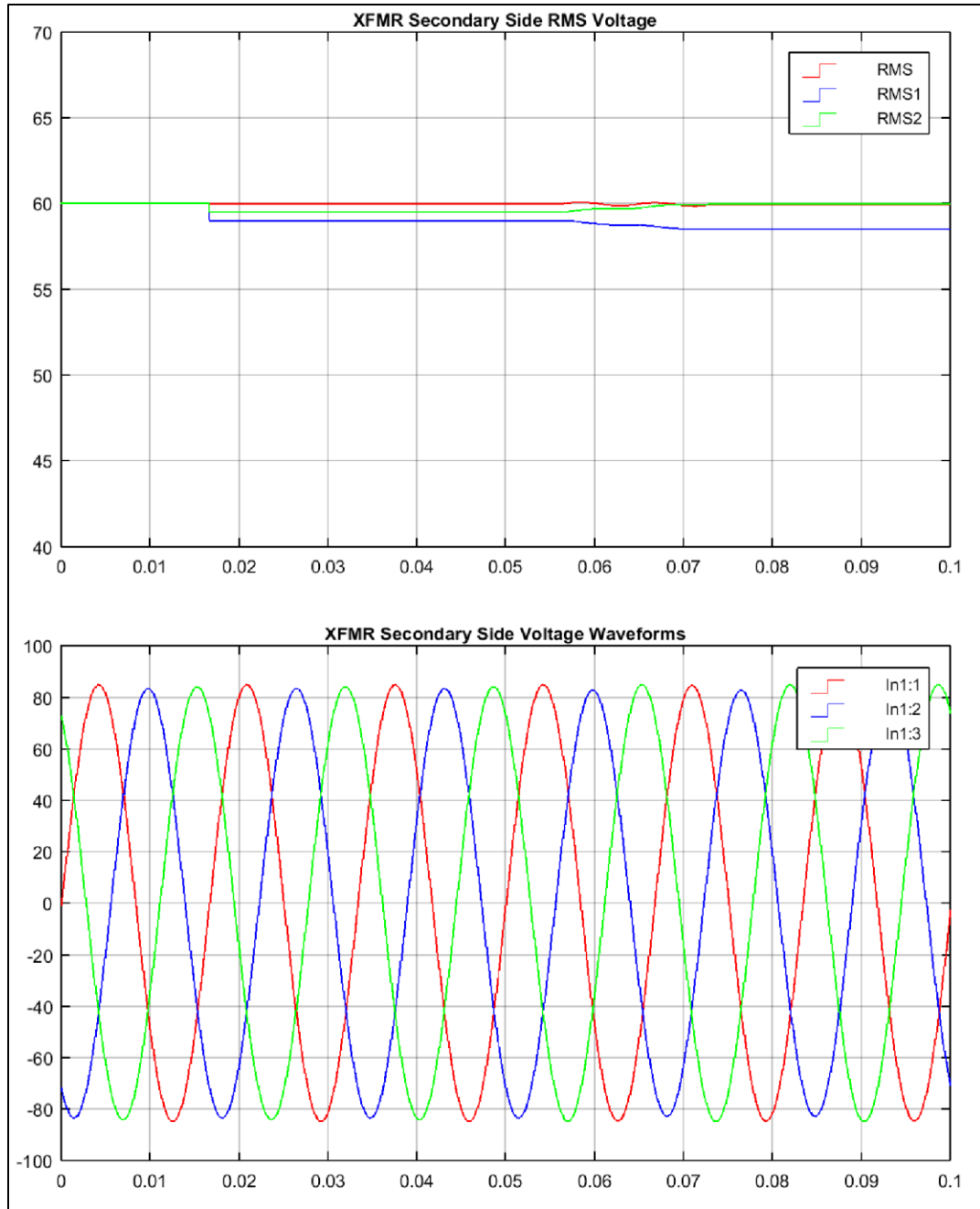


Figure 40: Secondary Side Voltages, Unbalanced Loaded XFMR with Current Injection

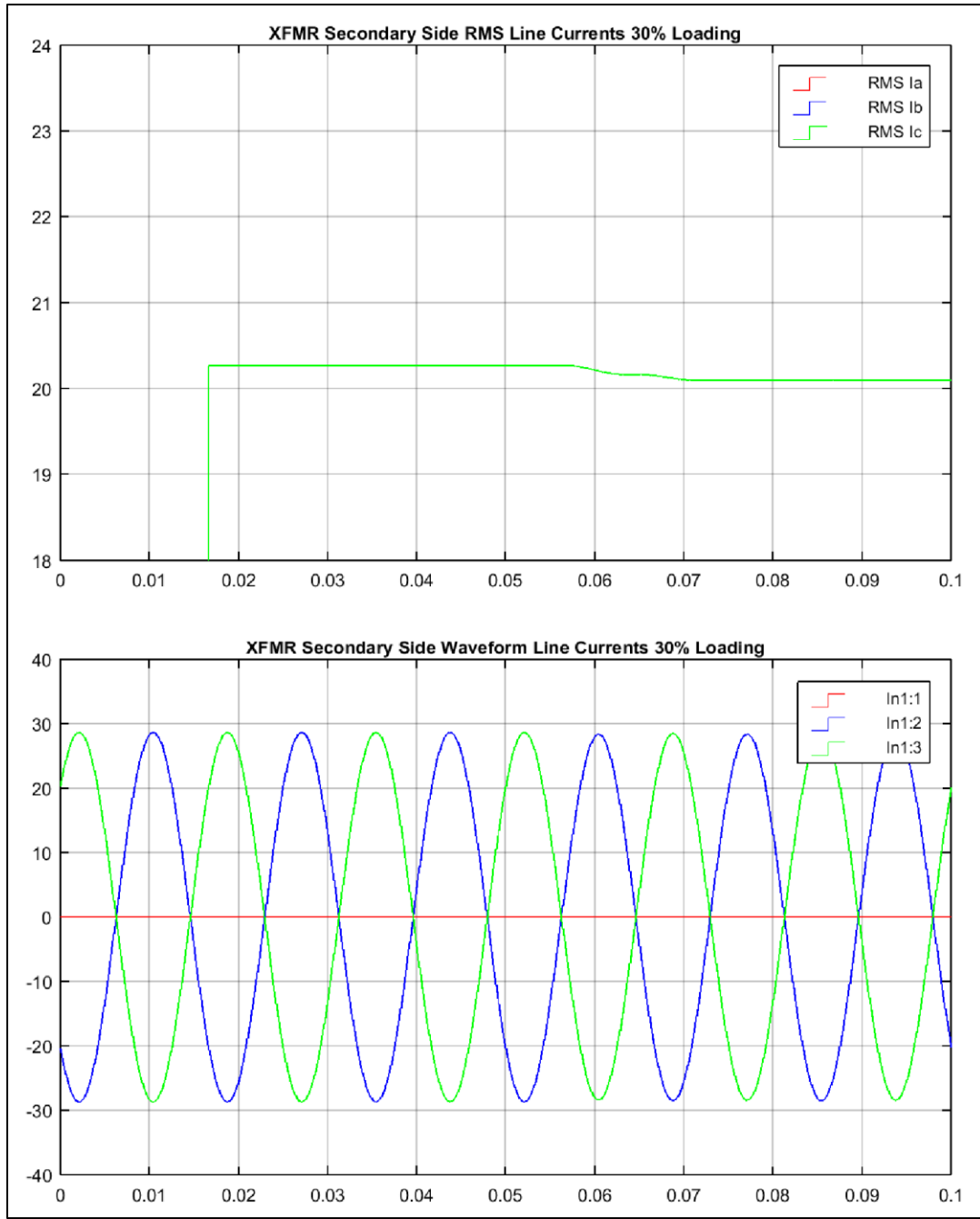


Figure 41: Secondary Side Currents, Unbalanced Loaded Transformer with Current Injection

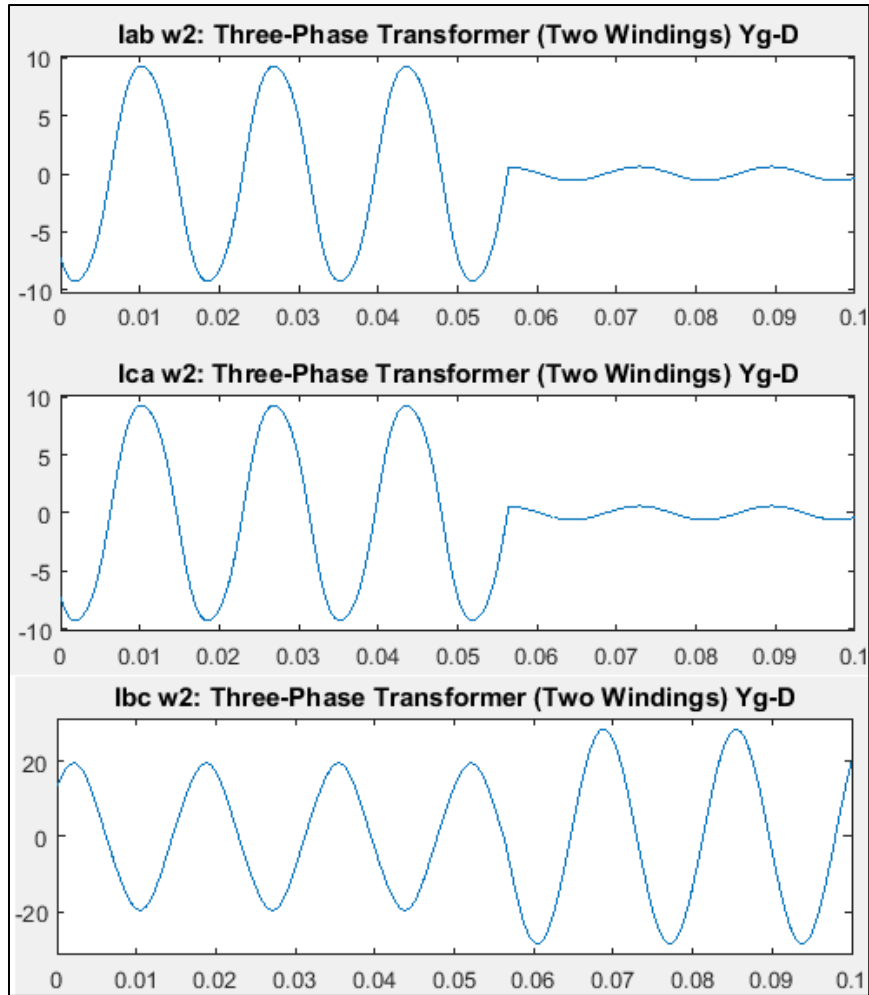


Figure 42: Secondary Side Coil Currents, Unbalanced Loaded XFMR with Current Injection

The unbalanced loading analysis shows that the current injection method is immune to the effects of unbalanced loading. However, it is impractical to test this configuration in the Cal Poly Energy Lab due to the large amount of inductive loading necessary. For this reason a final analysis was performed in MATLAB utilizing 900W of purely resistive load. This configuration could be tested in the laboratory environment utilizing 10 Ohm Rheostat resistors arranged in a delta configuration as demonstrated in Section 4.2. The analysis was performed for both balanced loaded and unbalance loaded conditions. The same model utilized for the 30% loading analysis described above was used; however, the configurable load was changed as demonstrated in Figure 43 below.

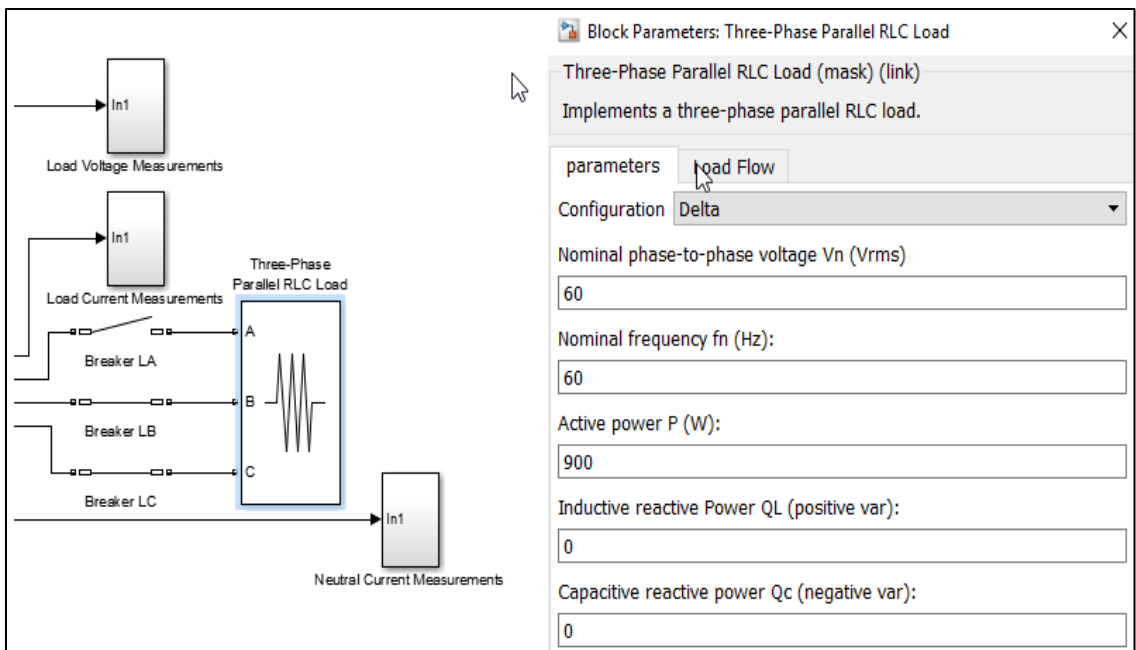


Figure 43: MATLAB Load Change for Balanced Resistive Loading on XFMR Secondary

The results of this run were as expected and very similar to the results for the 30% loaded case. On the primary side, supply side terminal voltage again remains extremely

balanced both prior to the fault and after the fault with a negligible dip on the “A” phase terminal as shown in Figure 44.

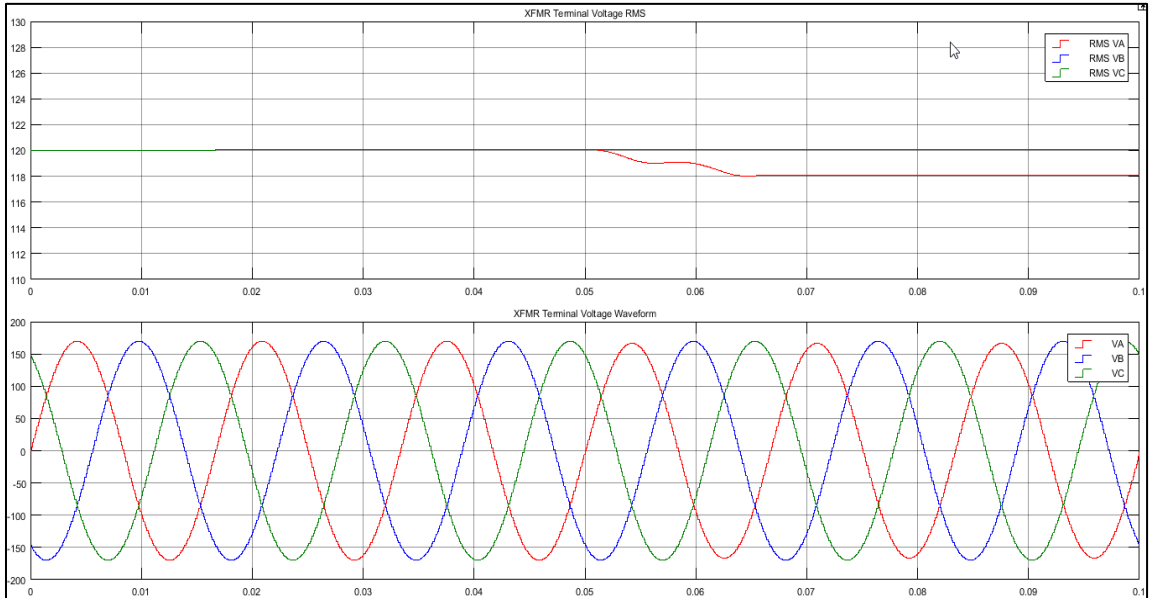


Figure 44: Primary Side Voltages for Balanced Resistance Loading with CI

The supply side current trace also mirrors previous runs with balanced currents of approximately 2.6Amps prior to the fault and unbalanced currents (A phase = 0 Amps, B&C phases = 4.5 Amps) following the open phase (Figure 45).

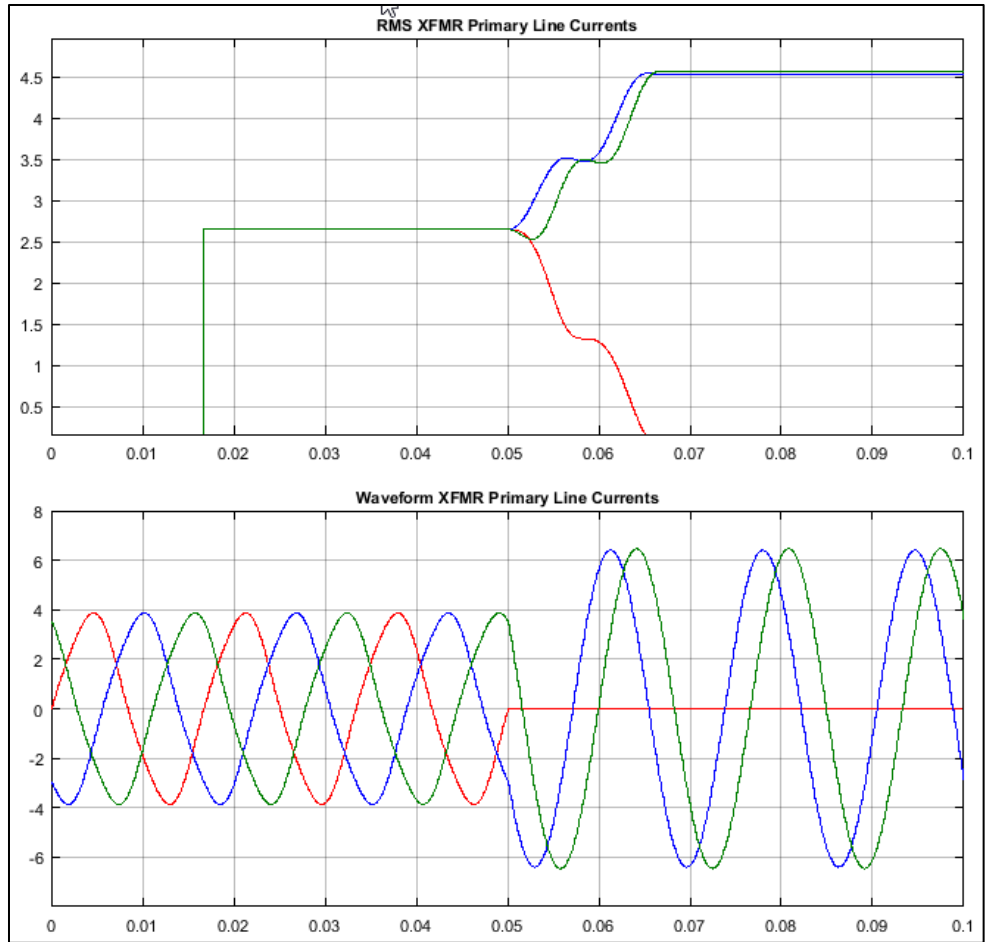


Figure 45: Supply Side XFMR Currents for Balanced Resistance Loading

The injected current mirrored previous simulations with unloaded and loaded cases. As expected the current is dominated by the 180Hz injected current prior to the open phase and then overwhelmed by the 60Hz fundamental unbalanced current following the open phase.

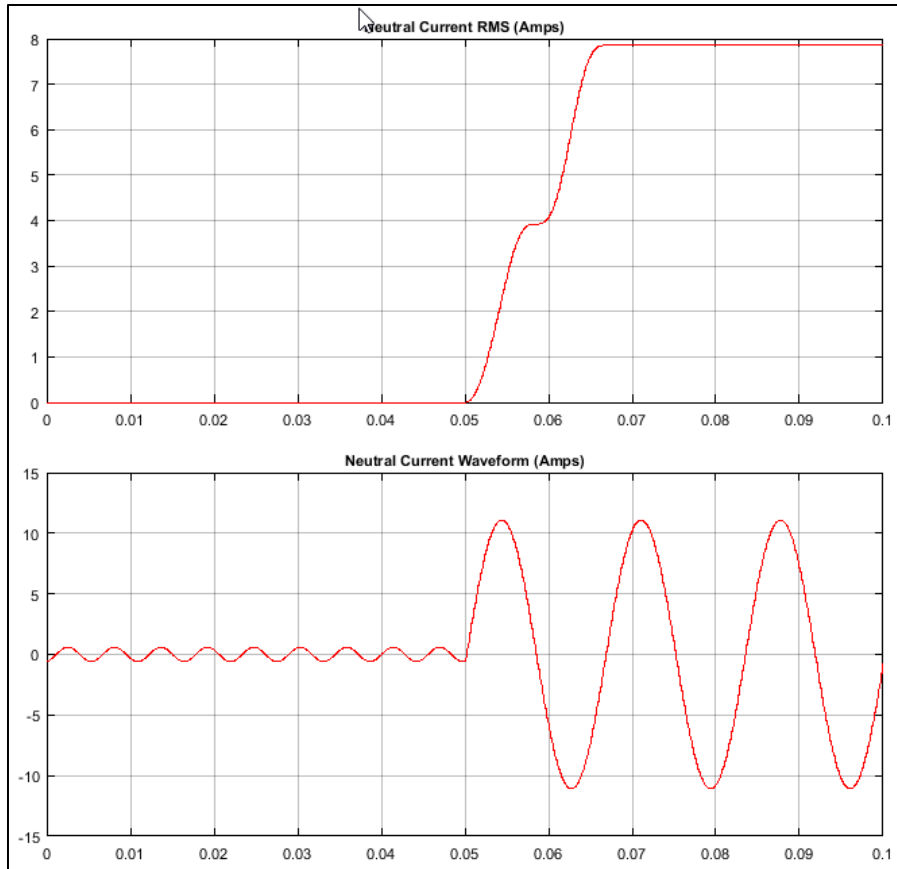


Figure 46: Neutral Injection Current for Balanced Resistive Loaded XFMR (900W)

Secondary side voltages are again re-created almost perfectly and are balanced at approximately 60VAC while currents also remain fairly balanced (Figures 47 and 48). The dip and unbalance in the load currents from a pre-fault value of approximately 8.6 amps to 8.5 amps is attributed to the minor voltage dip that occurs on secondary side windings B&C which carry all the power.

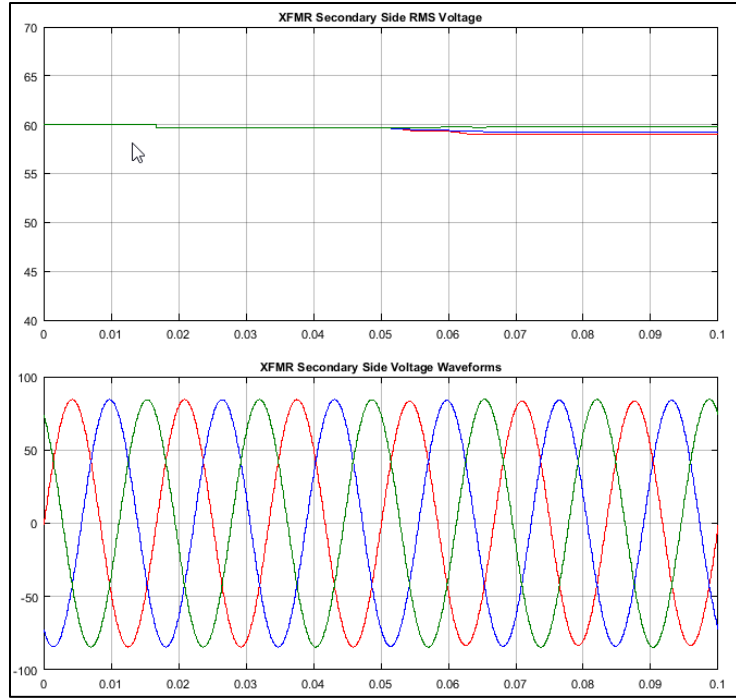


Figure 47: Secondary Side Voltages for Balanced Resistance Loaded XFMR (900W)

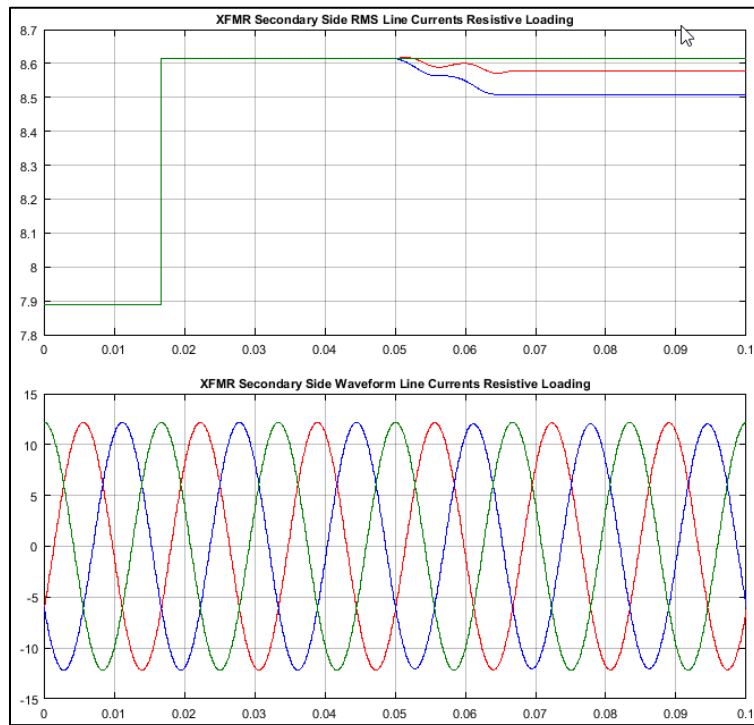


Figure 48: Secondary Side Currents for Balanced Resistance Loaded XFMR (900W)

Finally, an unbalanced resistance loaded analysis was performed as was done for the mixed load (inductive) example previously in this Section. This analysis was performed by opening the secondary side load breaker for phase “A” thereby distributing all the load on only the “B” and “C” secondary side phases. The results were extremely similar to those of the inductive loaded case and are summarized in the Figures 49 through 54 below.

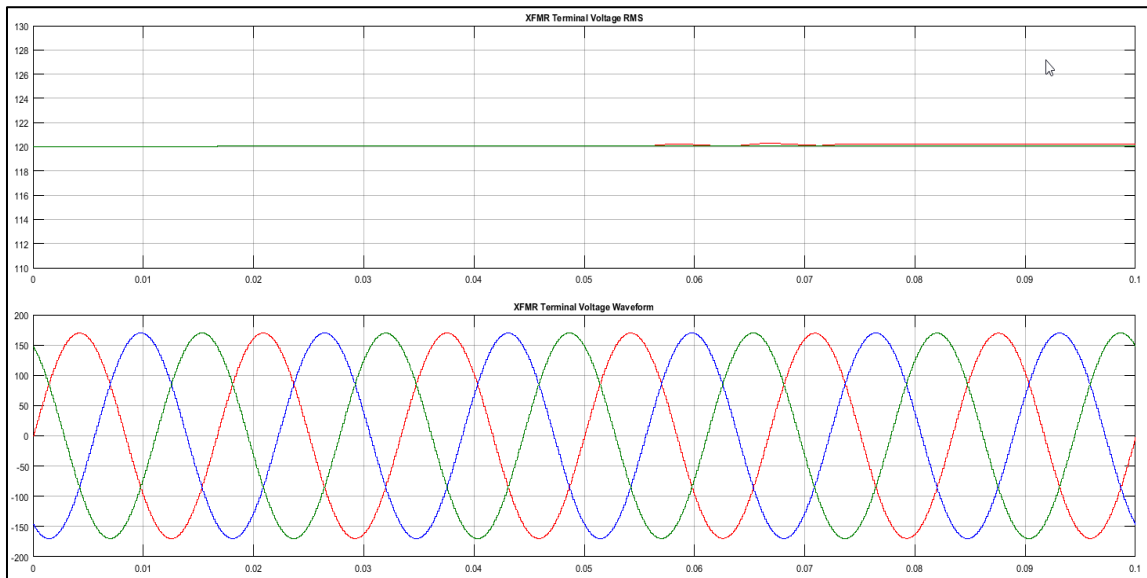


Figure 49: Supply Side Voltages for Unbalanced Resistance Supply Load (900W)

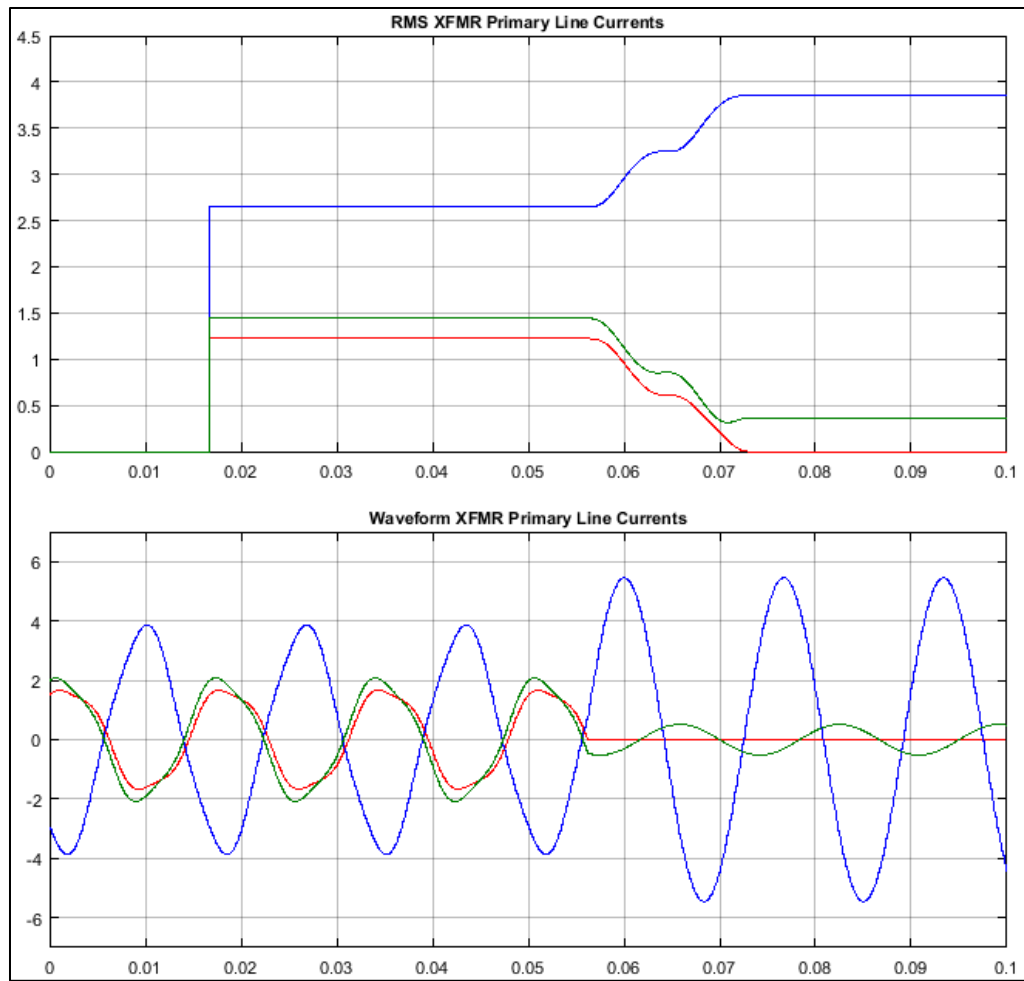
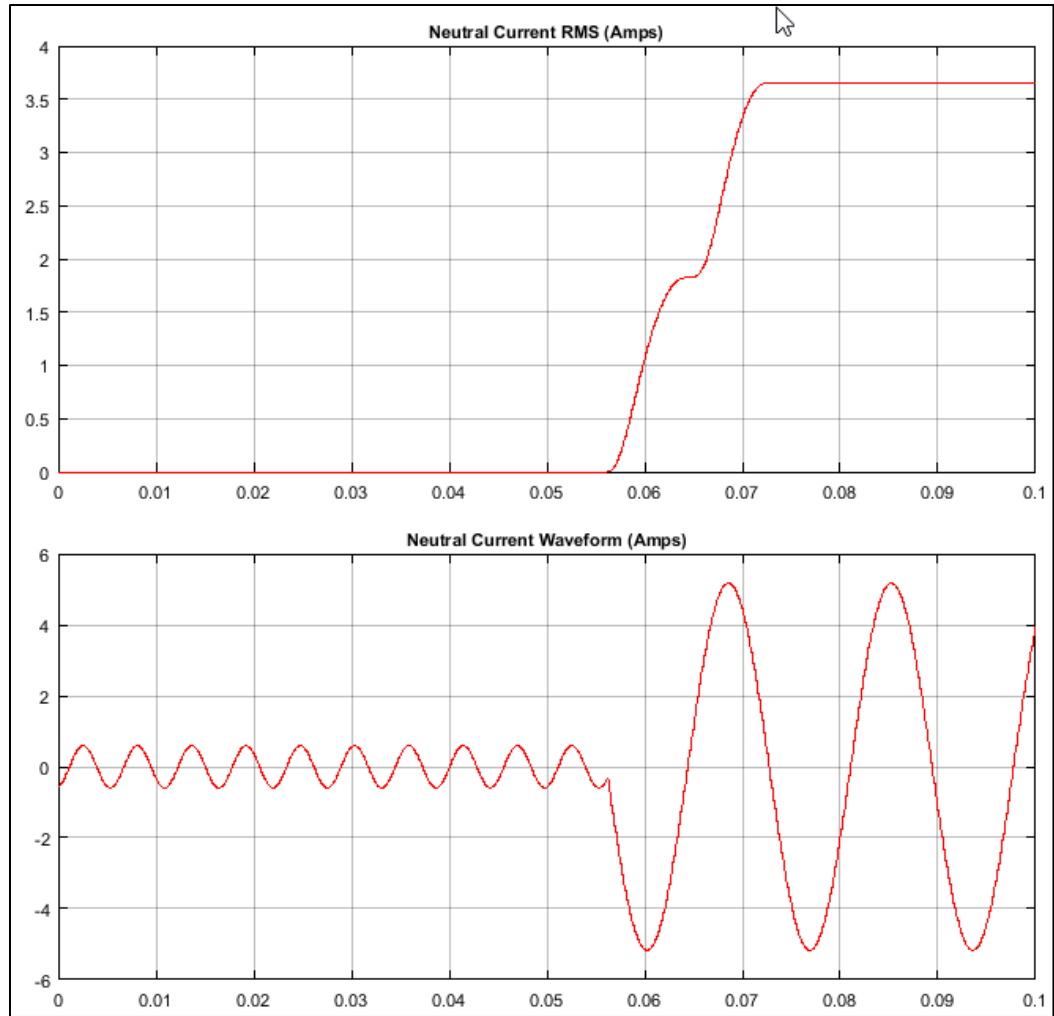
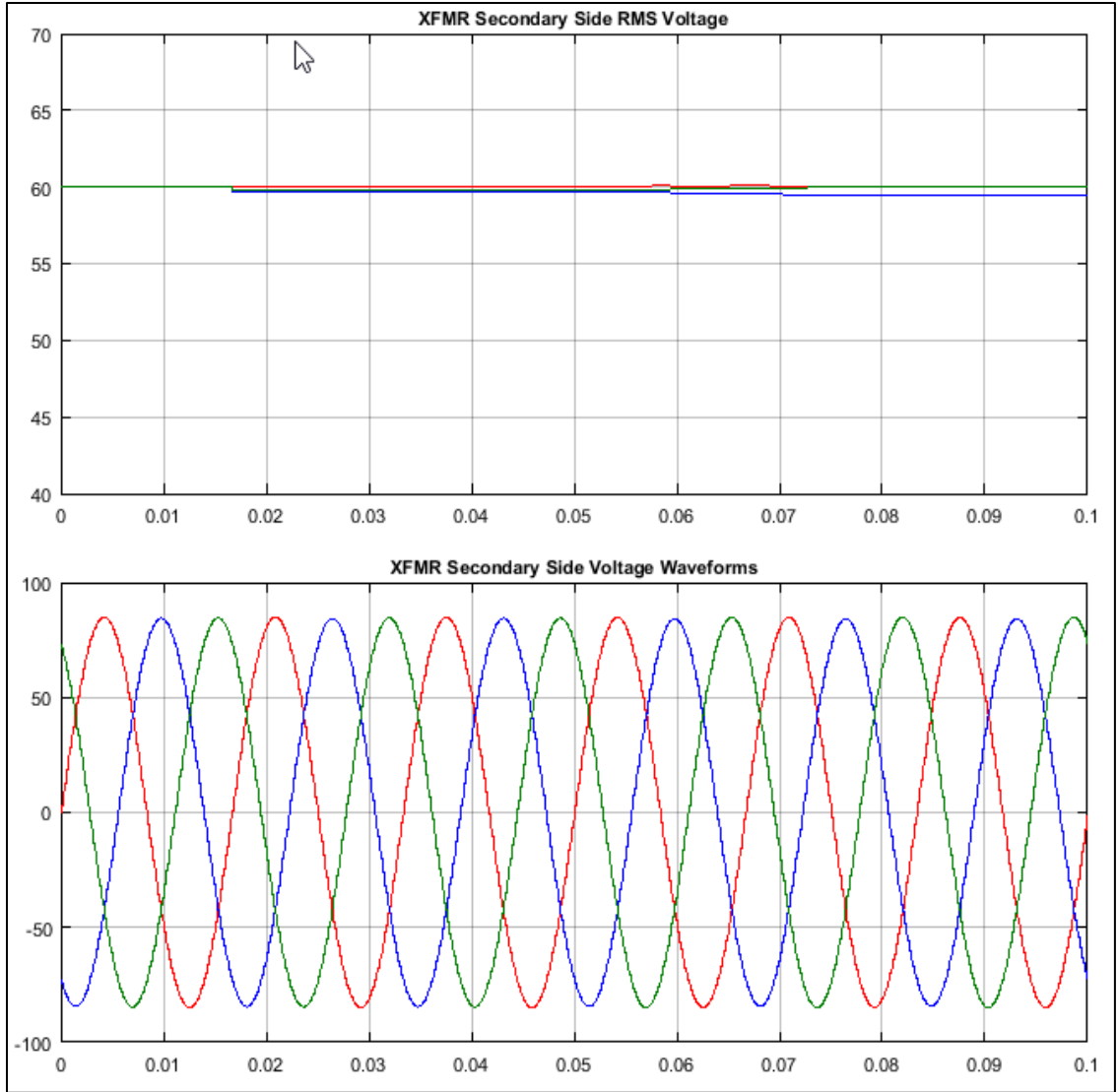


Figure 50: Supply Side Currents for Unbalanced Resistance Loaded XFMR (900W)



**Figure 51: Neutral Injection Current for Unbalanced Resistance Loaded XFMR
(900W)**



**Figure 52: Secondary Side Voltages for Unbalanced Resistance Loaded XFMR
(900W)**

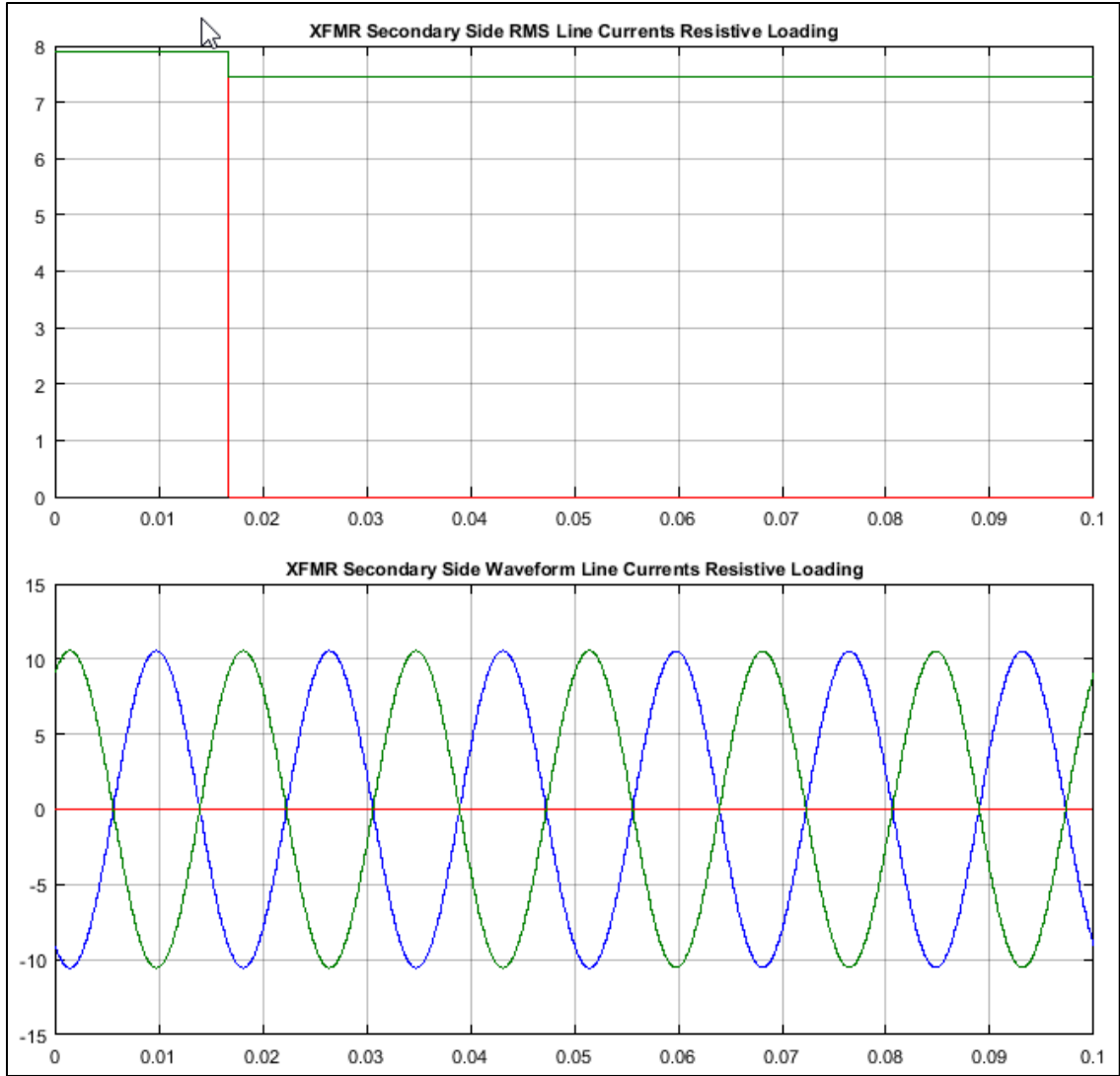


Figure 53: Secondary Side Load Currents for Unbalanced Resistance Loading

3.4 SUMMARY OF ANALYTICAL RESULTS

The analyses presented in this Chapter provide the following findings:

1. Results of the analyses show that standard distribution system protective elements such as overcurrent protective devices, undervoltage devices and differential current devices will not be successful in detecting an open phase condition on the primary side of a Wye-G Delta transformer because the resulting conditions will not approach the typical settings applied to these devices. For all intents and purposes, the transformer can continue operating long term in this condition with no danger to the supply side source or the transformer as long as the loading is of constant impedance.
2. Despite the relatively mild steady state conditions following an open phase condition, the resulting voltage unbalance on the secondary side (though mild) could cause catastrophic negative sequence currents in motors that could go undetected if not protected correctly. The voltage unbalance is caused by the voltage drop in the power transmission coils because they end up transferring the power that the open phase cannot.
3. An open phase results in a significant increase in zero sequence impedance as seen from the transformer neutral looking towards the source.
4. Current injection via an induced current into the primary neutral is a reliable method of detection for an open phase condition. Even during secondary side loading unbalance and for various types of loads, the injection signal signature stands out as long as an off nominal frequency is used.

As a result of these conclusions, a current injection experiment was conducted to validate the simulation results in Cal Poly laboratory equipment. The laboratory set up, experiments and results are described in the following Chapter of this thesis.

CHAPTER 4: SYSTEM TESTING, EVALUATION AND DISCUSSION

This Chapter of the thesis will document the proof of concept testing performed in the Cal Poly energy conversion laboratory. The laboratory experiments were designed to first, demonstrate the validity of the MATLAB simulation and second to demonstrate that the current injection method can be created in a physical model. The analysis results showed that consequential current and voltage levels of the post fault condition were at safe levels for realizing in the laboratory environment without risking damage to laboratory equipment or risking personal safety. The following Sections will detail the equipment used as well as how it was connected for each experiment. The results are compared to the simulation results in the conclusion Section.

4.1 LABORATORY EXPERIMENTS FOR OBTAINING EQUIPMENT PARAMETERS

In order to perform the analyses required in Chapter 3, the parameters necessary for modeling the real world equipment were required. This requirement mainly pertained to the three phase transformer impedances and the characteristics of the current transformer for the purposes of current injection. In order to properly model the three phase transformer open circuit, short circuit and zero sequence tests all needed to be performed.

The first test performed was the open circuit test in order to determine the shunt magnetizing inductance and the core loss resistance. The open circuit test was performed with the laboratory bench transformer connected with a Wye-grounded neutral primary and an ungrounded delta secondary as shown in Figure 54. Three phase voltage at 208VAC line to line was applied to the primary terminals with the secondary side completely open circuited and unloaded. Primary side voltage, line current, power factor and three phase power were all measured and recorded as shown in Appendix 1. The resulting parallel combination impedance for the transformer no load losses is $90.30+j77.70$ pu or in polar coordinates, $119.13\angle 40.7^\circ$ pu.

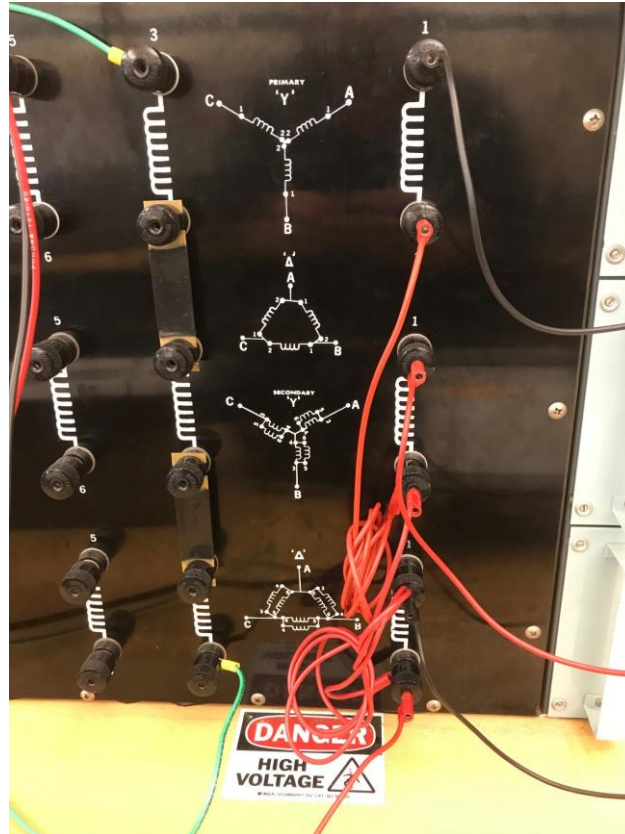


Figure 54: 9000VA Bench Transformer Configured in Wye-G:Delta

The short circuit current test was performed next by shorting the three terminals of the secondary side delta winding together. Supply side voltage and current were measured and supplied through a variac. Voltage is applied initially with the variac turned all the way down and then slowly raised until rated current is applied to the transformer primary. As shown in Appendix 1 the rated current of the transformer primary is 12.5A single phase. Hence the current was only raised to a point slightly above 12 amps. This is acceptable because in this region the series impedance of the transformer is linear. Hence the measurements taken at 12 amps will produce measurements of suitable accuracy for calculating the series impedance. Primary side voltage, line current, power factor and three phase power were all measured and recorded

as shown in Appendix 1. The resulting series combination impedance for the transformer winding is $0.16 + j0.07 \Omega$ pu or in polar coordinates, $0.17 \angle 23.6^\circ$ pu.

The final transformer parameter test performed was the zero sequence impedance test. This test is described in detail in reference [15]. The test is performed by shorting all line side terminals together on the Wye connected primary winding and energizing across the input terminals and the neutral connection with a single phase voltage through a variac. The variac is slowly turned up until rated current is measured at the input. Since the neutral connection is the limiting point of the transformer, rated current is limited to the single phase rating of 12.5A. Again, because of the limitation on the measurement fuses, the current was limited to slightly greater than 12 Amps. Primary side voltage, line current, power factor and power were all measured and recorded as shown in Appendix 1. The resulting zero sequence impedance for the transformer primary side winding is $0.066 + j0.025$ pu or in polar coordinates, $0.071 \angle 20.5^\circ$ pu.

The next set of laboratory tests involved the testing of the current transformer for determining optimal tap selection for current injection. In order to obtain the best possible results for detection of the current injection signal, the current induced had to be as large as possible. Since the function generator can only produce a maximum of 200mA, a current transformer is used to attempt to amplify the current by applying the function generator output to the low side of the current transformer. A General Electric Type JP-1 (model 9JP1FAB2) current transformer with available tap settings of 10:5, 20:5, 50:5, 100:5 and 600:5 was used as shown in Figure 55. Three different experiments were run as summarized in Appendix 3 to determine the optimal tap setting. The first experiment connected the function generator to the low side of the CT and through a bench ammeter

to measure function generator current. The high side tap was shorted through a second bench ammeter to measure the amplified current. High side tap connections were varied between the available tap settings and the resulting low side and high side currents were all recorded. The function generator input signal was provided at max amplitude available with a 180Hz frequency. The maximum amplification was for a 100:5 (20:1) ratio. With function generator current at 82.7mA RMS, the CT output current was 1.208 A RMS for a true current ratio of 14.6:1. While the reason a 20:1 ratio is not achieved is not known, the author of this thesis believes it to be because the CT is rated for 25-125 cycles and the applied signal is at 180Hz therefore additional magnetic losses are experienced. This is left for future work to determine.

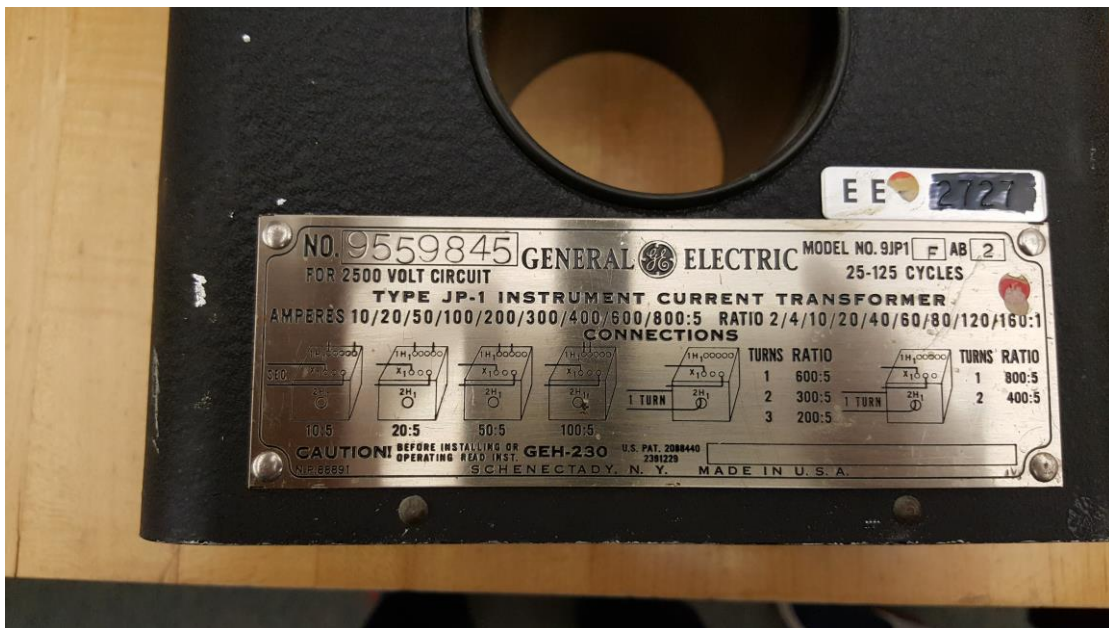


Figure 55: Bench Current Transformer

For the next experiment, the high side of the CT was connected through the primary Wye connected side winding of the transformer with all line side transformer

terminals shorted together and connected to ground through an ammeter. The transformer was left de-energized. Again the high side tap connections were varied between the available tap settings and the resulting low side and high side currents were all recorded. The function generator input signal was provided at max amplitude available with a 180Hz frequency. While the largest amplification ratio was for the 100:1 tap setting (actual ratio 7.6:1), the largest injection current was for a 50:5 (10:1) tap setting. With function generator current at 86mA RMS, the CT output current was 587mA RMS for a true current ratio of 6.8:1. The additional transformer impedance results in a drop in injected current. During this experiment, the secondary side delta circulating current was measured to be 385mA as measured by a FLUKE clamp on ammeter.

The final experiment to classify the CT injection behavior was to determine if the CT experienced increased impedance when injecting through an energized transformer. The line side terminals of the transformer were connected to the 3-phase 208VAC supply. The high side of the CT was connected between ground and the neutral connection of the Wye connected primary side winding. Again the high side tap connections were varied while the high side and low side CT currents were all recorded. Transformer line current was measured at 0.217A RMS balanced three phase. Again the largest injection current was for a CT ratio of 50:5 (10:1). With function generator current at 75.6mA RMS, the CT output current was 513mA RMS @ 180 Hz. The secondary side delta circulating current was measured at 410mA @ 180 Hz. Hence this experiment has demonstrated that the optimal CT ration for current injection is the 50:5 tap and that the injected current sees a negligible increase in zero sequence impedance when the transformer is connected to its balanced 3-phase power supply.

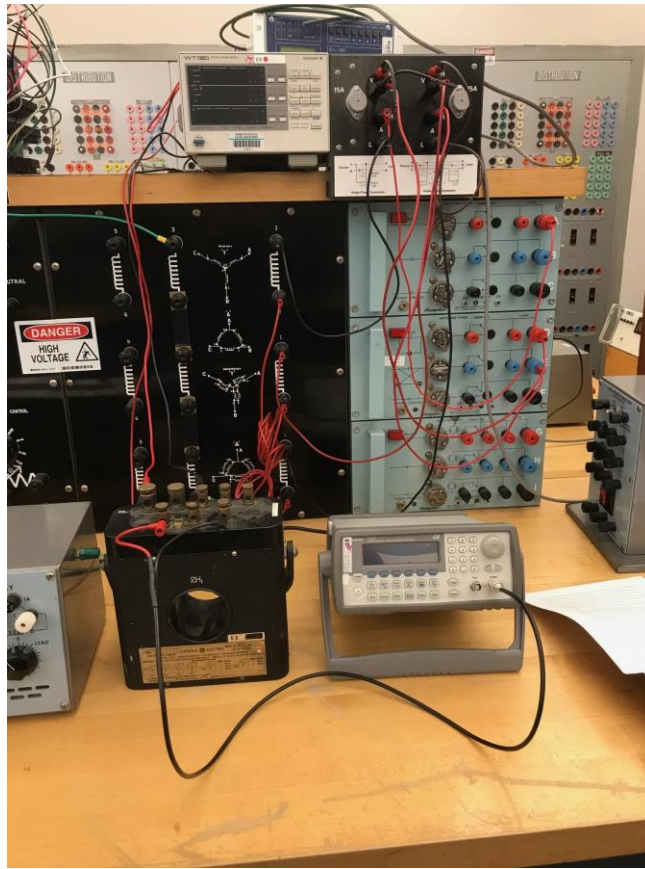


Figure 56: CT Connected for Current Injection and 180Hz Function Generator

Source

4.2 LABORATORY TESTING OF CURRENT INJECTION SYSTEM

This Section of the thesis documents the set up and testing of the current injection system (in accordance with the computer analysis of Section 3.3) in the laboratory environment. The results of the CT ratio optimization experiments in Section 4.1 were used to select the CT ratio of 50:5 with the function generator connected to the low side of the CT and turned to max voltage (10V P-P) at a frequency of 180Hz. The high side of the CT was connected between the neutral point of the bench transformer Wye winding and ground. The line side terminals were connected to a balanced three phase 208VAC supply with the “A” phase connected through a bench switch to simulate the open phase. Excitation of the transformer was initially performed with the “A” phase switch closed. In order to allow switching of a single phase, the “B” and “C” phases were supplied via the “D” and “E” supply switch on the energy lab bench power board.

Three different test cases were run to verify the findings of the MATLAB analyses described in Section 3.3. The first was the case of an unloaded secondary side delta connected winding. The second was for a balanced three phase load of three 10 Ohm 6.8 Amp Rheostat's connected in a delta formation and supplied by the secondary side delta winding (approximately 900 Watts). The third was for an unbalanced load on the secondary side with the same three phase delta load from the 2nd case supplied only by B&C phases. For each test case, the transformer was initially energized with balanced 3-phase supply and the injection source was turned to max function generator voltage at 180Hz. For each case the following parameters were measured initially with all primary side supply phases intact:

Primary side voltage and frequency, primary side line current (for intact phases), primary side power, neutral to ground current magnitude (sensed current) and frequency, secondary side voltage, secondary side delta circulating current, secondary side line current (for loaded cases) and secondary side power (for loaded cases).

Following the recording of all the above parameters for the steady state balanced supply, the “A” phase was opened by throwing the bench switch open. The above parameters were again measured. In accordance with the results of Section 3.3 of this thesis the expectation was for line and load voltages and currents to remain well balanced following the open phase fault. However the neutral current will shift significantly in all cases from a dominant 180Hz signal prior to the open phase to a dominant 60Hz signal following the open phase. Figures 57 through 61 show pictures of the lab set up used to run the three cases. Note that while part of the analyses of Section 3.3 utilized a load of 3000VA with a power factor of 0.8, the laboratory experimentation of this thesis utilizes 900W of purely resistive load due to the limitations of the lab equipment and out of concern for stressing the lab switches during opening due to inductive “kick-back”.

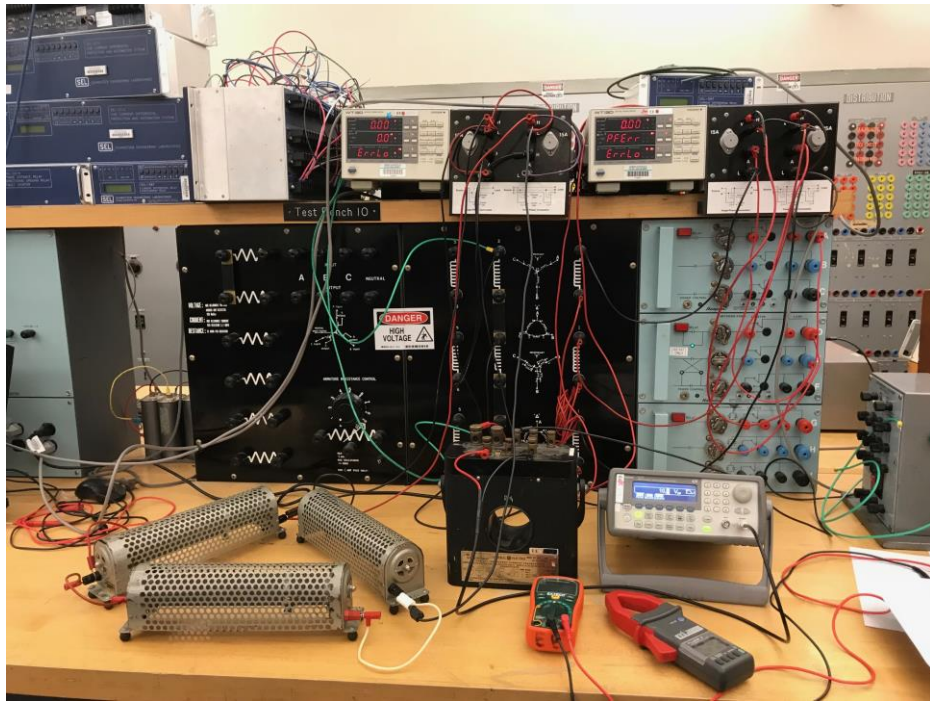


Figure 57: Current Injection Test Set Up

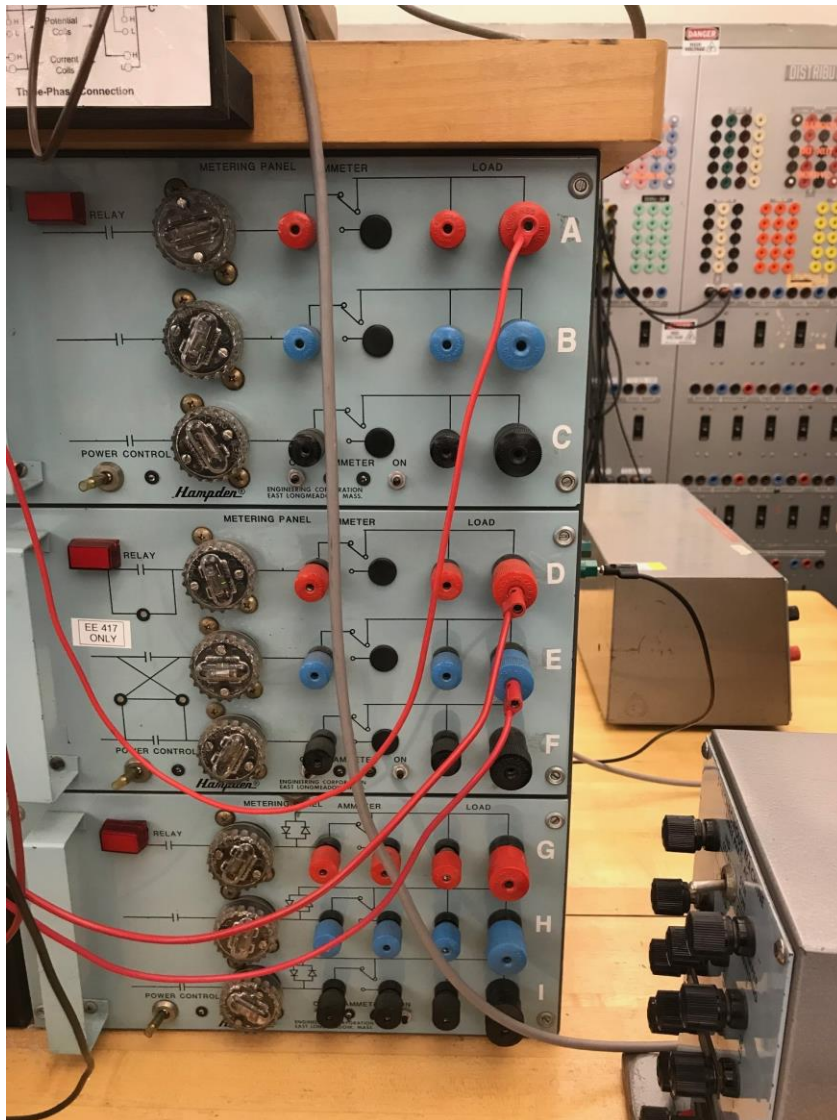


Figure 58: Power Supply through Bench Switches

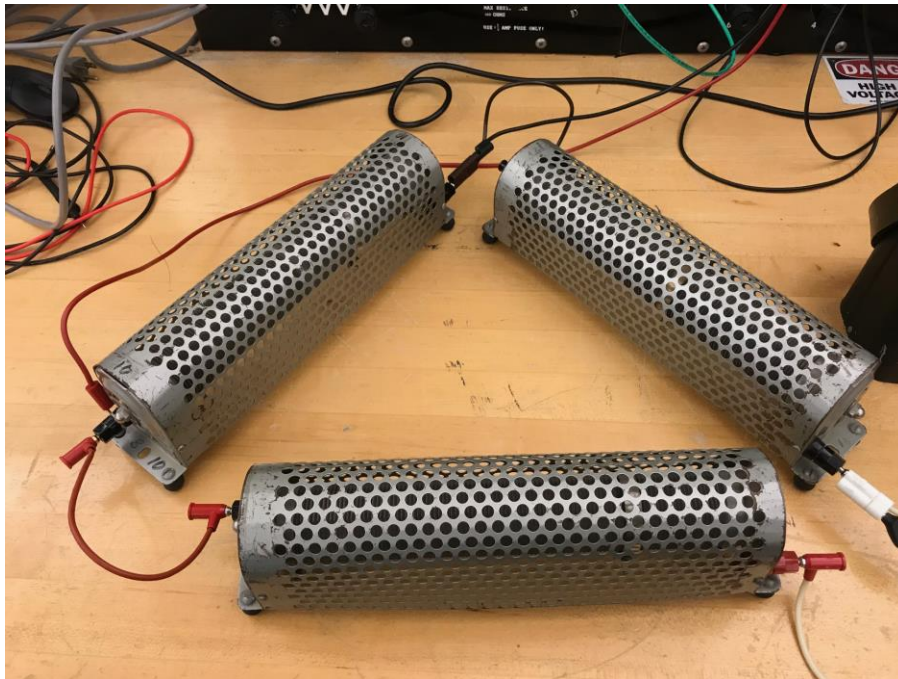


Figure 59: Delta Connected 10 Ohm Rheostat Load



Figure 60: Individual 10 Ohm Rheostat

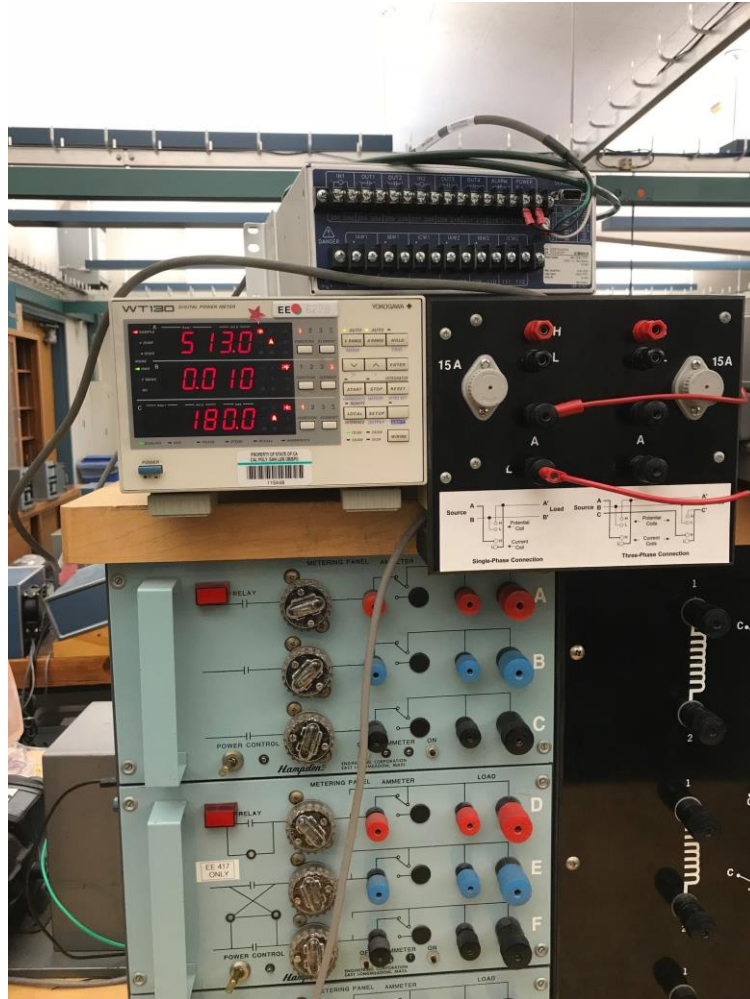


Figure 61: Ammeter Measuring 180Hz Injection Current

Table 1 below shows the results of case 1 (unloaded secondary side). The lab results confirm the hypothesis of this thesis that the current injection method of detection of an ungrounded open phase fault functions well. While results are not an exact match of the simulation results, they do demonstrate many of the simulation findings. It was expected that line current would rise to approximately 1.5 times their initial value for the supply lines left intact (“B” and “C” phases). While they did rise as was expected, they did not rise to such a dramatic magnitude as was predicted by the simulations. Three phase voltages were perfectly re-created both on the secondary and primary sides as predicted

by the simulation models. An unexpected result was the shift in primary side power from a positive value to negative. This is attributed to an error in the metering due to the type of metering used. The use of the two watt meter method utilized in the Cal Poly energy lab for measuring three phase power is not accurate when power is actually delivered by only a two phase source as occurs during an open phase condition. It is left to future work to determine how power is affected by an open phase fault. Neutral to ground current shifted just as expected from a 180Hz dominant current supplied from the current injection source, to a 60Hz dominant current supplied by the unbalanced supply currents. The pre-fault neutral current magnitude mirrored the MATLAB simulations however the post fault current was slightly less (0.44A vs 0.65A). This is again due to the smaller than expected post-fault supply currents but is not of consequence to the thesis findings.

Table 1: Laboratory Results of Case 1 Unloaded XFMR Secondary

Parameter	Pre-Fault Value	Post-Fault Value
Primary Side $V_{\text{Line-to-Line}}$	207.8VAC Balanced	207.7VAC Balanced
Primary Side Frequency	60 Hz	60 Hz
Line Current (for intact phases)	220mA Balanced	259mA Phases B & C
Primary Side Power	36.9W	-13.8W
Neutral to Ground Current	0.482A	0.44A
Neutral Current Frequency	180 Hz	60 Hz
Secondary Side $V_{\text{Line-to-Line}}$	60VAC Balanced	60VAC Balanced
Secondary Circulating Current	0.40A @ 180 Hz	0.14A @ 60 Hz

Table 2 below shows the results of case 2 (balanced load on secondary side). Again the results do not match exactly with the MATLAB simulations documented in Section 3.3. However current and voltage values are very close to the simulation results. The lab results confirm the hypothesis of this thesis that the current injection method of detection of an ungrounded open phase fault functions well for loaded transformer cases. This time with the transformer loaded, line currents did rise to approximately 1.5 times their initial value for the supply lines left intact (“B” and “C” phases). Three phase voltages were again perfectly re-created both on the secondary and primary sides as predicted by the simulation models. The slight dips in voltage that were predicted in the simulations could not be measured by the available lab equipment. Again there was an unexpected shift in primary side power from a pre-fault value of 1kW to a post fault value of 0.385kW. This is due to an error in the metering on the primary side due to the loss of A phase current. This error is verified by the fact that the secondary side power measurements showed power delivered to be approximately the same prior to and following the fault (0.893kW prior and 0.806kW following). It is not possible for the primary side power to be less than the secondary following the fault. Hence this is a metering error. Neutral to ground current shifted again as predicted by the models from a 180Hz dominant current supplied from the current injection source, to a 60Hz dominant current supplied by the unbalanced supply currents. Furthermore the neutral current makes a significant increase in magnitude from 0.534A supplied by the injection source to 7.29A supplied by the unbalanced primary side currents which approximately matches the results of the MATLAB simulation. Also, the laboratory results show that it is not possible to rely on the circulating current signature as both pre-fault and post-fault circulating currents in the

delta winding are dominated by 60Hz fundamental currents. An interesting finding to note during this run was the fact that the function generator injecting into the secondary side of the current transformer experienced an output port voltage overload and shut off the output to protect itself after several minutes of the transformer operating under open phase (see Figure 62). The voltage across the CT secondary was measured at 30VAC RMS using a multi-meter. The function generator output is limited to 10VAC peak to peak. This presents a limitation that will need to be evaluated in future work for the design of function generators that can tolerate the overvoltage presented by open phase conditions on the transformer neutral.

Table 2: Laboratory Results for Case 2 Balanced Load on XFMR Secondary

Parameter	Pre-Fault Value	Post-Fault Value
Primary Side $V_{\text{Line-to-Line}}$	206VAC Balanced	200VAC Balanced
Primary Side Frequency	60 Hz	60 Hz
Line Current (for intact phases)	2.67A Balanced	4.28A Phases B & C
Primary Side Power	1kW	0.385kW
Neutral to Ground Current	0.534A	7.29A
Neutral Current Frequency	180 Hz	60 Hz
Secondary Side $V_{\text{Line-to-Line}}$	57.8VAC Balanced	56.84VAC Balanced
Secondary Circulating Current	4.96A @ 60 Hz	7.6A @ 60 Hz
Secondary Side Line Current	9A Balanced	9A Balanced
Secondary Side Power	0.893kW	0.806kW

Tables 1 and 2 both show significant changes in post-fault primary side power values when compared to the pre-fault value. This is attributed to the metering method used. The method used was the standard two Watt meter approach used in the Cal Poly energy lab. Because this method is utilizing the sum or average of three phases, a significant change in the primary side power is observed following the primary side open phase. However as is seen by the secondary side power measurements, the power remains very close to its pre-fault value. The change on the secondary side is due to the slight voltage unbalance caused by the open phase condition. If we instead calculate the primary side power of the post-fault condition using the phase “B” & “C” currents and the line to line voltage, we get $P = \frac{200V}{\sqrt{3}} * 4.28A * 2 = 988W$. This calculated value more closely matches the pre-fault value of 1kW.

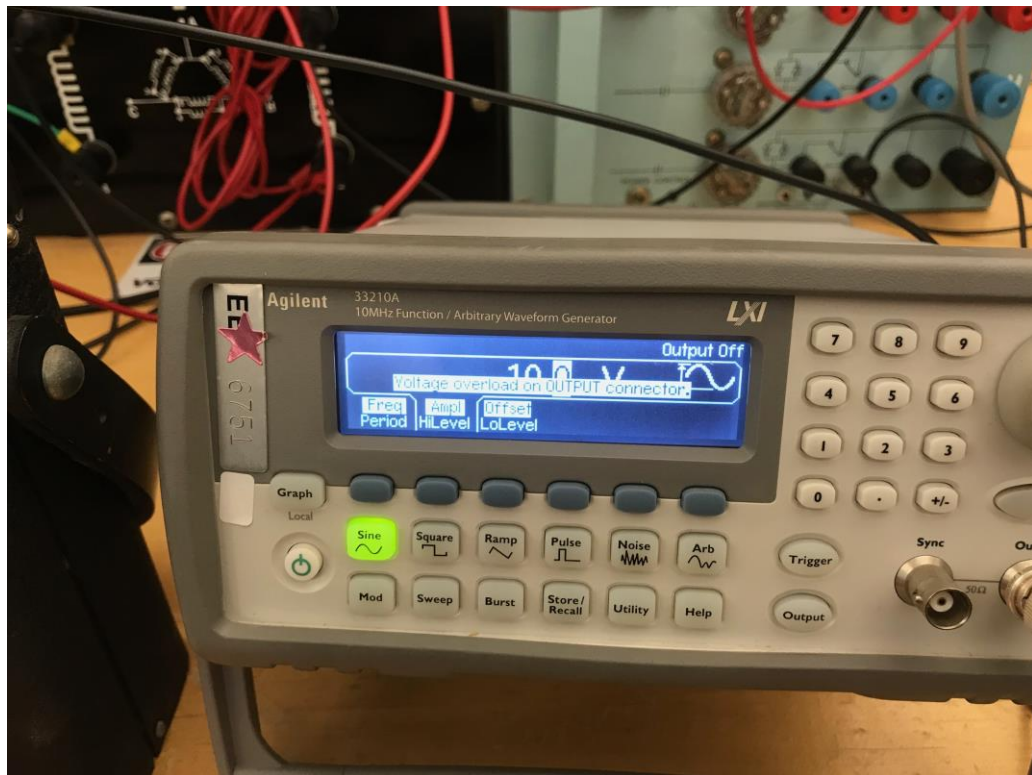


Figure 62: Function Generator Exhibiting Output Overvoltage

Finally, Table 3 below shows the results of case 3 (unbalanced load on secondary side). Again the results closely mirror the MATLAB simulations documented in Section 3.3. The lab results confirm the hypothesis of this thesis that the current injection method of detection of an ungrounded open phase fault functions well for unbalanced loaded conditions as well. This time with the transformer loaded in an unbalanced fashion, line currents shifted dramatically similar to what was demonstrated in the MATLAB simulations. Initially one of the supply side currents “C” phase was significantly larger than the other two “A” and “B”. An oscilloscope was not available to look at waveforms however it is assumed that the currents shifted phase angle similar to the simulation predictions for an unbalanced load. This is because as predicted, the unbalanced supply side currents still cancel out at the neutral such that the current measured at the neutral is dominated by the 180Hz injection source. Also, similar to the simulation results, following the open phase, “A” phase goes to 0 amps, “B” phase is almost zero and “C” phase essentially carries the entire supply side current. As dramatic as the current unbalance is, three phase voltages are again perfectly re-created both on the secondary and primary sides. The slight dips in voltage that were predicted in the simulations could not be measured by the available lab equipment. Neutral to ground current shifted again as expected from a 180Hz dominant current supplied from the current injection source, to a 60Hz dominant current supplied by the unbalanced supply currents following the open phase. Similarly to the balanced case, the neutral current makes a significant increase in magnitude from 0.489A supplied by the injection source to 3.65A supplied by the unbalanced primary side currents. Circulating current in the delta winding is again dominated by 60Hz fundamental currents both prior to and following the open phase.

Table 3: Laboratory Results of Case 3 Unbalanced XFMR Loading

Parameter	Pre-Fault Value	Post-Fault Value
Primary Side $V_{\text{Line-to-Line}}$	207.6 VAC Balanced	208.2 VAC Balanced
Primary Side Frequency	60 Hz	60 Hz
Line Current (for intact phases)	“A”: 1.14A @ 60 Hz “B”: 1.29A @ 60 Hz “C”: 2.57A @ 60 Hz	“B”: 0.1A @ 60 Hz “C”: 3.64A @ 60 Hz
Primary Side Power	0.496kW	0.653kW
Neutral to Ground Current	0.489A	3.65A
Neutral Current Frequency	180 Hz	60 Hz
Secondary Side $V_{\text{Line-to-Line}}$	60VAC Balanced	60VAC Balanced
Secondary Circulating Current	5A @ 60 Hz	7.3A @ 60 Hz
Secondary Side Line Current	“B”: 7.66A “C”: 6.96A	“B”: 6.75A “C”: 7.03A
Secondary Side Power	0.44kW	0.417kW

CHAPTER 5: CONCLUSION

The MATLAB Simulink platform was used to perform intrusive simulations and provide a much better understanding of the consequences and effects of ungrounded open phase faults on the line side of Wye-G:Delta distribution transformers. The Wye-G:Delta transformer was the focus of this thesis as one of the more prevalent configurations present in distribution systems. The simulations effectively showed that for unloaded and moderately loaded distribution transformers, conventional protective devices such as overcurrent relays, undervoltage relays and differential protection relays would not be effective in detecting or protecting against this type of fault. This is primarily due to the fact that voltages on the primary and secondary side of the transformer can be almost perfectly re-created. Literature on this topic demonstrated that this type of fault is least understood amongst the spectrum of faults protected against. While most transformers can operate for long periods of time under a single phase open fault, it can come at the expense of detrimental effects to secondary side loads. This is especially true for motor loads which can experience rotor overheating due to negative sequence currents generated by the secondary side voltage unbalance. Hence a novel protective method was needed.

This thesis performed MATLAB simulation of a solution based on the concept of neutral current injection. The documented simulations provided a detailed look at the impacts an open phase fault has on the ability to inject an induced off nominal frequency current into the neutral point of the high side wye winding. Various cases demonstrated that detection of a shift in current fundamental frequency is effective at providing detection of the open phase condition. The solution was demonstrated to be effective in a

simulated system in the unloaded condition, balanced loaded condition and unbalanced loaded condition. In all cases, initial conditions showed that injected current at 180Hz is the dominant current detected at the neutral point of the transformer. Following the open phase fault, the dominant current is at 60Hz fundamental due to the unbalanced currents entering the transformer. This presents a very high impedance zero sequence path.

Finally this thesis performed laboratory tests to demonstrate that the simulated results present an accurate representation of actual effects in a physical system.

Unloaded, balanced loaded and unbalanced loaded cases were run on a laboratory Wye-G:Delta transformer with injection current injected at 180Hz into the transformer primary. In all cases transformer neutral to ground current was observed to shift from 180Hz dominated current to 60Hz dominated current. Hence this thesis proves that a protection system based on detection of fundamental frequency shift in the neutral current will be an effective method of detecting open phase faults on Wye-G:Delta distribution transformers.

Future work on this topic should be to extend the simulations and laboratory testing on other distribution transformer winding and core configurations. Many permutations exist that may or may not be responsive to this type of detection method. It is the opinion of this thesis author that this method should work for any solidly grounded Wye wound primary side transformer. This is because regardless of the other parameters of the transformer, the zero sequence path will behave in a similar fashion as that demonstrated in this thesis. Additionally, future work can also focus on the development of a protective relaying scheme using either a standard off the shelf relay platform with customizable software or use of other programmable logic solutions. Finally, this thesis

performed work on a small isolated system. The effects introduced by larger transmission systems are not known and should be explored.

REFERENCES

1. Mathew, Roy and Matharu, Singh. "Design Vulnerability in Electric Power System." NRC Bulletin 2012-01: United States Nuclear Regulatory Commission: 1-9. Web. 27 July 2012.
2. Horak, John and Johnson, Gerald F. "A Practical Guide for Detecting Single-Phasing on a Three Phase Power System". *Western Protective Relay Conference (2002)*: 1-54. Web. October 2002.
3. Arritt, R. and Dugan, R. "Nuclear Maintenance Application Center: Development and Analysis of an Open Phase Detection Scheme for Various Configurations of Auxiliary Transformers." *EPRI Technical Report 3002000764* (2013): 1-1 to A-3. Web. May 2013.
4. Norouzi, Amir. "Open Phase Conditions in Transformers Analysis and Protection Algorithm." *Minnesota Power Systems Conference MIPSYCON* (2013): 1-14. Web. 2013.
5. Hwang, Soon-Hyun et al. "Vulnerability Analysis for Open Phase Condition in Electric Power System of Korea's Nuclear Power Generating Station." *International Conference on Circuits, Systems and Simulation* (2017): 185-89. Web. 2017.
6. Cooper III, Preston O et al. "Analysis of Open Phase Fault Events Using ETAP Unbalanced Load Flow Module." *IEEE Power and Energy Society General Meeting* (2016): 1-5. Web. July. 2016.
7. National Electric Manufacturers Association. *NEMA MG-1 Motors and Generators*. (2009): Part 12 p19, Part 14 p10-11. Print.

8. Karrar, Abdelrahman et al. "Influence of Zero Sequence Impedances of Station Auxiliary Transformers on Equipment Performance Under Open-Phase Faults" *Power and Energy Society General Meeting* (2016): 1-6. Web. 17-21 July 2016.
9. Khunkhun, K. J. S. *Station Protection*. Palo Alto, CA: Electric Power Research Institute, 1987. 27-37. Print.
10. Arritt, R. and Franklin, G. "Interim Report: EPRI Open-Phase Detection Method." *EPRI Technical Report 3002004432* (2014): 1-1 to 5-1. Web. October 2014.
11. Arritt, Robert F., Ducan, Roger C., Johnson, Wayne E., Franklin, Gregory A. "Method for Detecting an Open-Phase Condition of a Transformer." *US Patent Application 20170012423* January 12, 2017: 1-11. Web. 2017.
12. Glover, J. Duncan., Mulukutla S. Sarma, and Thomas J. Overbye. *Power System Analysis and Design*. 5th ed. Boston: Cengage Learning, 2012. Print.
13. Blackburn, J. Lewis. *Symmetrical Components for Power Systems Engineering*. New York: Marcel Dekker, 1993. Print.
14. Blackburn, J. Lewis. *Protective Relaying Principles and Applications*. 2nd ed. New York: Marcel Dekker, 1998. Print.
15. IEEE. "IEEE Standard Test Code for Liquid-Immersed Distribution, Power and Regulating Transformers", *IEEE Std C57.12.90*, 2010 Web. 2010.
16. Mohajeryami, Saeed, et al. "An Analysis of Open-Phase Fault in Power Generation Station," *North American Power Symposium*, 2016. Web 2016.

APPENDIX 1: BENCH TRANSFORMER IMPEDANCE DATA

Table 1 below provides the data from performing the open circuit test on the laboratory transformer. Bench 10 of the Cal Poly Energy Lab was used with the transformer connected in Wye g-grounded primary and delta secondary. All measurements were taken on the line side of the transformer primary:

Table 4: Bench 10 Transformer Open Circuit Data

Measured Parameter	3-phase measurement	Sigma Measurement	1-phase Measurement
$V_{\text{line-line}}$ (Volts AC)	207		
I_{line} (Amps AC)	0.217	0.209	0.2
Power (Watts)	24.9	56.8	32
Power Factor	0.55	0.765	0.781

Using the data from Table 1, the following equations were applied to determine the transformer core loss resistance R_L and the magnetizing reactance X_M to determine the shunt transformer impedance \bar{Z}_M . For this calculation the 3-phase line current from the power meter was used and the sigma power was used. First the core loss resistive and the magnetizing portions of the current are calculated.

$$I_L = \frac{\frac{\text{Power}}{3}}{\frac{V_{\text{line to line}}}{\sqrt{3}}} = \frac{\frac{56.8W}{3}}{\frac{207V}{\sqrt{3}}} = 0.158A \quad (8)$$

$$I_M = \sqrt{I_{\text{line}}^2 - I_L^2} = \sqrt{0.209A^2 - 0.158A^2} = 0.136A \quad (9)$$

The currents calculated above are used to determine the R_L and X_M as follows.

$$R_L = \frac{\left(\frac{V_{\text{line to line}}}{\sqrt{3}}\right)}{I_L} = \frac{\left(\frac{207V}{\sqrt{3}}\right)}{0.158A} = 754.4 \Omega \quad (10)$$

$$X_M = \frac{\left(\frac{V_{line\ to\ line}}{\sqrt{3}}\right)}{I_M} = \frac{\left(\frac{207V}{\sqrt{3}}\right)}{0.136A} = 876.7i\ \Omega \quad (11)$$

Table 2 below lists the single phase base parameters from the primary side of the transformer. These are used to convert all of the transformer impedances to per unit.

Table 5: Bench 10 Transformer Base Parameters

S_{Base}	V_{Base}	Z_{Base}	I_{Base}
3000VA	120VAC	4.8 Ω	25A

The parallel combination of R_L and X_M is used to determine the magnitude and angle of the magnetizing impedance \bar{Z}_M in per unit as follows.

$$\bar{Z}_M = \frac{754.4 * j876.7}{754.4 + j876.7} = 433.45 + j372.98\ \Omega \quad (12)$$

$$\bar{Z}_M^{PU} = \frac{433.45 + j372.98\ \Omega}{4.8\ \Omega} = 90.3 + j77.7$$

$$\angle \bar{Z}_M = \cos^{-1}\left(\frac{90.3}{\sqrt{90.3^2 + 77.7^2}}\right) = 40.7^\circ \quad (13)$$

$$|\bar{Z}_M| = \sqrt{90.3^2 + 77.7^2} = 119.13\ PU$$

Hence \bar{Z}_M as expressed in polar coordinates is $119.13\angle 40.7^\circ\ PU$.

Table 3 below provides the data from performing the short circuit test on the laboratory transformer. This was performed on the same Bench 10 transformer by connecting in Wye-G primary with Delta secondary and shorting all secondary side terminals together. Current was restricted to less than the 15Amp rating of the bench power meter. All measurements were taken on the line side of the transformer primary:

Table 6: Bench 10 Transformer Short Circuit Test Data

Measured Parameter	3-phase measurement	Sigma Measurement	1-phase Measurement
$V_{line-SC}$ (Volts AC)	18.27		
$I_{line-SC}$ (Amps AC)	12.96	12.75	12.54
Power (Watts)	135.2	364	229.3
Power Factor	0.57	0.9	0.998

Using the data from Table 3, the following equations were applied to determine the transformer series winding resistance R_S and the series reactance X_S to determine the total series transformer impedance Z_S . For this calculation the 3-phase line current from the power meter was used and the sigma power factor was used.

$$R_S = \frac{\frac{V_{line-SC}}{\sqrt{3}}}{I_{line-SC}} * PF = \frac{\frac{18.27V}{\sqrt{3}}}{12.96A} * 0.90 = 0.75\Omega \quad (14)$$

$$\begin{aligned} X_S &= \frac{\frac{V_{line-SC}}{\sqrt{3}}}{I_{line-SC}} * j\sin(\cos^{-1}(PF)) \\ &= \frac{\frac{18.27V}{\sqrt{3}}}{12.96A} * j\sin(\cos^{-1}(0.9)) = j0.35 \Omega \end{aligned} \quad (15)$$

The series combination of R_S and X_S is used to determine the magnitude and angle of the transformer series impedance \bar{Z}_S in per unit as follows.

$$\bar{Z}_S = 0.75 + j0.35 \Omega$$

$$\bar{Z}_S \text{ PU} = \frac{0.75 + j0.35 \Omega}{4.8 \Omega} = 0.16 + j0.07 \Omega \quad (16)$$

$$\angle \bar{Z}_S = \cos^{-1} \left(\frac{0.16}{\sqrt{0.16^2 + 0.07^2}} \right) = 23.6^\circ \quad (17)$$

$$|\bar{Z}_S| = \sqrt{0.16^2 + 0.07^2} = 0.17 \text{ PU}$$

Hence \bar{Z}_S as expressed in polar coordinates is $0.17 \angle 23.6^\circ \text{ PU}$.

Table 4 below provides the data from performing the zero sequence test on the laboratory transformer. The zero sequence impedance test is described in detail in IEEE standard C57.12.90 [15]. This was performed on the same Bench 10 transformer by connecting in Wye-G primary with Delta secondary and shorting all primary side terminals together. All secondary side terminals were left open circuited. Single phase voltage was applied. Current was restricted to less than the 15Amp rating of the bench power meter. All measurements were taken on the line side of the transformer primary:

Table 7: Bench 10 Transformer Zero Sequence Test Data

Measured Parameter	1-phase measurement
$V_{1-phase}$ (Volts AC)	4.31
I_{line} (Amps AC)	12.75
Power (Watts)	51.4
Power Factor	0.936

Using the data from Table 4, the following equations were applied to determine the transformer zero sequence resistance $R_0/3$, zero sequence reactance $X_0/3$ and total zero sequence impedance $Z_0/3$. Impedance is shown as $1/3$ since the measurements take each phase zero sequence impedance in parallel.

$$\frac{Z_0}{3} = \frac{V_{1-phase}}{I_{line}} = \frac{4.31V}{12.75A} = 0.338\Omega \quad (18)$$

$$\frac{R_0}{3} = Z_0 * PF = 0.34 * 0.936 = 0.316\Omega \quad (19)$$

$$\frac{X_0}{3} = Z_0 * \sin(\cos^{-1}(PF)) = 0.338 * .352 = 0.119\Omega \quad (20)$$

The series combination of $R_0/3$ and $X_0/3$ is used to determine the magnitude and angle of the transformer zero sequence impedance per unit as follows.

$\frac{Z_0}{3} = 0.338 + j0.119 \Omega$ $\frac{Z_0}{3} PU = \frac{0.338 + j0.119 \Omega}{4.8 \Omega} = 0.066 + j0.025 PU$	(21)
$\angle \frac{Z_0}{3} = \tan^{-1} \left(\frac{0.025}{0.066} \right) = 20.5^\circ$ $\left \frac{Z_0}{3} \right = \sqrt{0.066^2 + 0.025^2} = 0.071 PU$	(22)

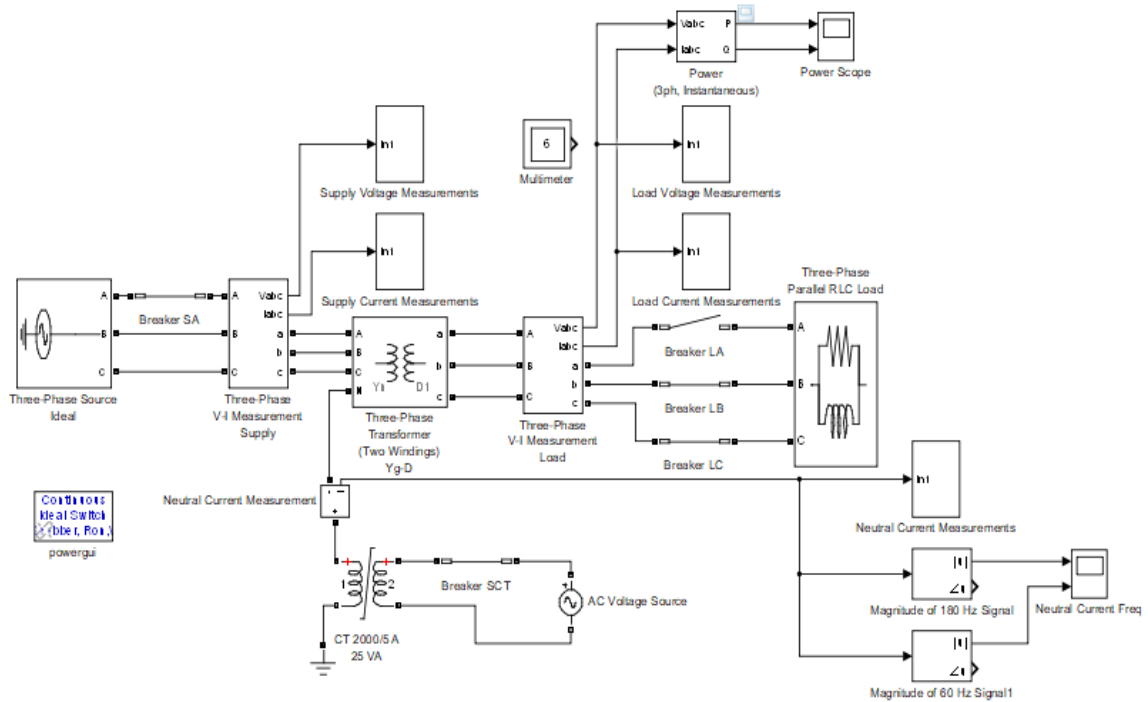
Hence $\frac{Z_0}{3}$ as expressed in polar coordinates is $0.071 \angle 20.5^\circ$ PU.

APPENDIX 2: MATLAB SIMULATION MODEL INFORMATION AND SETTINGS

The following pages contain the entire model print out from MATLAB. MATLAB/Simulink Version 15 Student Edition with SIMSCAPE Power Systems was used for the development of this model. The printout contains the names and types of all blocks used as well as parameter settings and screen shots. Parameter settings were all based on empirical data collected from the laboratory tests described in Chapter 4 of this thesis.

All runs were set up for a 0.1 second real time run with all data channels computing data points at a sample rate of 10,000 samples per second. Switching activity such as the open phase breaker was all programmed to occur at a time of 0.05 seconds (halfway into the simulation).

TM_2_Simple_Open_Phase



Montoya

21-Mar-2018 20:48:54

Table of Contents

[Model - TM 2 Simple Open Phase](#)

[System - TM 2 Simple Open Phase](#)

[System - TM 2 Simple Open Phase/Load Current Measurements](#)

[System - TM 2 Simple Open Phase/Load Voltage Measurements](#)

[System - TM 2 Simple Open Phase/Neutral Current Measurements](#)

[System - TM 2 Simple Open Phase/Supply Current Measurements](#)

[System - TM 2 Simple Open Phase/Supply Voltage Measurements](#)

[Appendix](#)

List of Tables

1. [AC Voltage Source Block Properties](#)

2. [Breaker Block Properties](#)
3. [Current Measurement Block Properties](#)
4. [Fourier Block Properties](#)
5. [Ground Block Properties](#)
6. [MultimeterPSB Block Properties](#)
7. [PSB option menu block Block Properties](#)
8. [Power \(3ph, Instantaneous\) Block Properties](#)
9. [Saturable Transformer Block Properties](#)
10. [Three-Phase Parallel RLC Load Block Properties](#)
11. [Three-Phase Source Block Properties](#)
12. [Three-Phase Transformer \(Two Windings\) Block Properties](#)
13. [Three-Phase VI Measurement Block Properties](#)
14. [Demux Block Properties](#)
15. [Inport Block Properties](#)
16. [Mux Block Properties](#)
17. [RMS Block Properties](#)
18. [Demux Block Properties](#)
19. [Inport Block Properties](#)
20. [Mux Block Properties](#)
21. [RMS Block Properties](#)
22. [Inport Block Properties](#)
23. [RMS Block Properties](#)
24. [Demux Block Properties](#)
25. [Inport Block Properties](#)
26. [Mux Block Properties](#)
27. [RMS Block Properties](#)
28. [Demux Block Properties](#)
29. [Inport Block Properties](#)

30. [Mux Block Properties](#)

31. [RMS Block Properties](#)

32. [Block Type Count](#)

Model - TM_2_Simple_Open_Phase

Full Model Hierarchy

1. [TM_2_Simple_Open_Phase](#)
 1. [Load Current Measurements](#)
 2. [Load Voltage Measurements](#)
 3. [Neutral Current Measurements](#)
 4. [Supply Current Measurements](#)
 5. [Supply Voltage Measurements](#)

Simulation Parameter	Value
Solver	ode45
RelTol	1e-3
Refine	1
MaxOrder	5
ZeroCross	on

[\[more info\]](#)

System - TM_2_Simple_Open_Phase

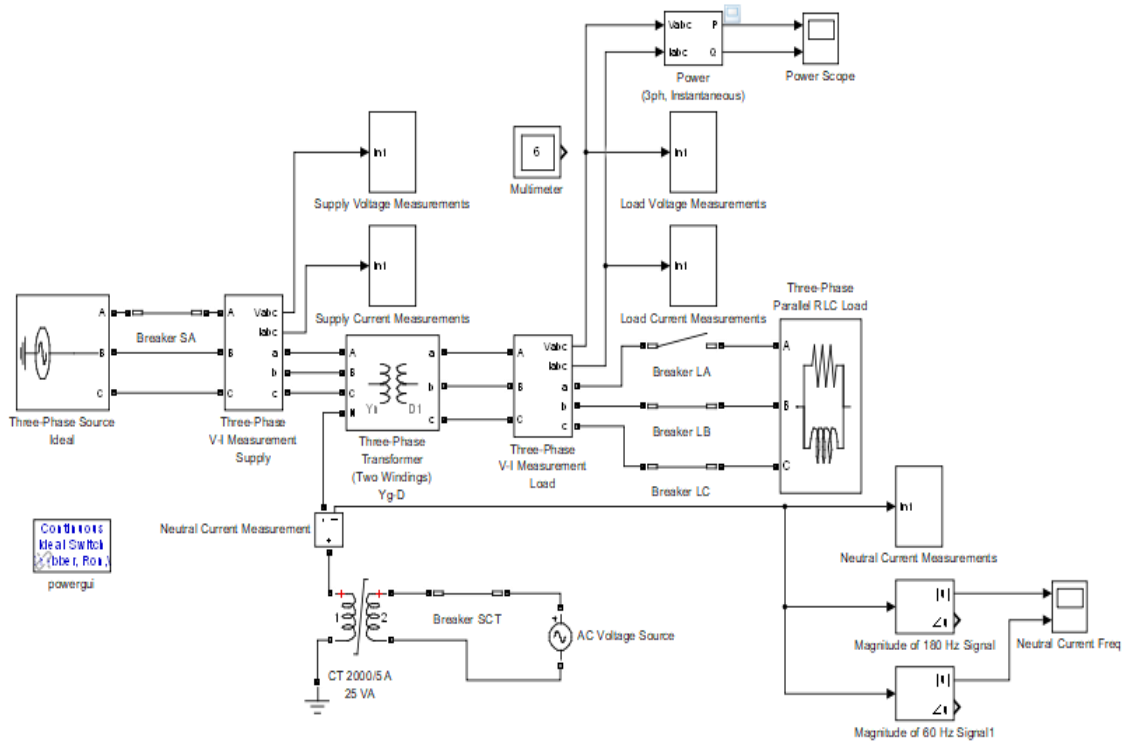


Table 1. AC Voltage Source Block Properties

Name	Amplitude	Phase	Frequency	Sample Time	Measurements
AC Voltage Source	60	0	180	0	None

Table 2. Breaker Block Properties

Name	Initial State	Switching Times	External	Breaker Resistance	Snubber Resistance	Snubber Capacitance	Measurements
Breaker LA	0	0.3	off	0	inf	0	None
Breaker LB	1	0.3	off	0	inf	0	None
Breaker LC	1	0.3	off	0	inf	0	None
Breaker SA	1	0.05	off	0	inf	0	None

Name	Initial State	Switching Times	External	Breaker Resistance	Snubber Resistance	Snubber Capacitance	Measurements
Breaker SCT	1	3	off	0	inf	0	None

Table 3. Current Measurement Block Properties

Name	Output Type
Neutral Current Measurement	Complex

Table 4. Fourier Block Properties

Name	Freq	N	In Init	Ts
Magnitude of 180 Hz Signal	180	1	[0, 0]	0
Magnitude of 60 Hz Signal1	60	1	[0, 0]	0

Table 5. Ground Block Properties

Name	Physical Domain	Sub Class Name	Left Port Type	Right Port Type
Ground	powersysdomain	unknown	p1	p1

Table 6. MultimeterPSB Block Properties

Name	Phasor Simulation	Output Type	Sel	L	Gain	Yselected	Axes Setting	Display	Saved Block Names
Multimeter	off	Complex	[3 4 5 6 7 8]	9	[1 1 1 1]	{'Ian_w1: Three-Phase Transformer (Two Windings) Yg-D', 'Ibn_w1: Three-Phase Transformer (Two Windings) Yg-D', 'Icn_w1: Three-Phase Transformer (Two Windings) Yg-D', 'Iab_w2: Three-Phase Transformer (Two Windings) Yg-D', 'Ibc_w2: Three-Phase Transformer (Two Windings) Yg-D', 'Ica_w2: Three-Phase Transformer (Two Windings) Yg-D'}	[0,0.1,-100,100]	1	-11

Name	Phasor Simulation	Output Type	Sel	L	Gain	Yselected	Axes Setting	Display	Saved Block Names
						Yg-D'};			

Table 7. PSB option menu block Block Properties

Name	Simulation Mode	SP ID	Disable Snubber Devices	Disable Ron Switches	Disable Vf Switches	Display Equations	Interpolation	Function Messages	Echo Messages	Hook Port	Enable Use Of TLC	X0st	Frequency	Pbase	Err Max	Iterations	Units V	Units W
powergui	Continuous	on	on	on	on	off	off	off	off	off	off	blocks	60	9000	1e-4	50	V	kW

Table 8. Power (3ph, Instantaneous) Block Properties

Name
Power (3ph, Instantaneous)

Table 9. Saturable Transformer Block Properties

Name	Three Windings	Hysteresis	Measurements	UNIT S	Nominal Power	Winding 1	Winding 2	Winding 3	Saturation	Core Losses	Break Loop
CT2000/5 A 25 VA	off	off	Flux and magnetization current (Imag)	pu	[25 60]	[5*5/200 0 0.001 0.04]	[5 0.001 0.04]	[5 0.001 0.04]	[0 0 ; 0.01 10 ; 1 10.5]	[100]	off

Table 10. Three-Phase Parallel RLC Load Block Properties

Name	Configuration	Nominal Voltage	Nominal Frequency	Active Power	Inductive Power	Capacitive Power	Measurements	Load Type
------	---------------	-----------------	-------------------	--------------	-----------------	------------------	--------------	-----------

Name	Configuration	Nominal Voltage	Nominal Frequency	Active Power	Inductive Power	Capacitive Power	Measurements	Load Type
Three-Phase Parallel RLC Load	Delta	60	60	2400	600	0	None	constant PQ

Table 11. Three-Phase Source Block Properties

Name	Voltage	Phase Angle	Frequency	Internal Connection	Specify Impedance	Resistance	Inductance	Base Voltage	Bus Type
Three-Phase Source Ideal	208	0	60	Yg	off	0	0	208	swing

Table 12. Three-Phase Transformer (Two Windings) Block Properties

Name	Winding 1 Connection	Winding 2 Connection	Core Type	Set Saturation	Measurements	UNITS	Nominal Power	Winding 1	Winding 2	Rm	Lm	Saturation	Initial Fluxes	Break Loop	Data Type
Three-Phase Transformer (Two Windings) Yg-D	Yn	Delta (D1)	Three single-phase transformers	off	Winding currents	pu	[9000, 60]	[208 0.02 5 0.02 5]	[60 0.02 5 0.02 5]	157.163	182.645	[0 0;0.00 24 1.2;0.9 9999 1.52]	[0.79 999 - 0.79 999 0.69 999]	off	off

Table 13. Three-Phase VI Measurement Block Properties

Name	Voltage Measurement	Set Label V	V _{pu}	V _{pu} LL	Current Measurement	Set Label I	I _{pu}	Output Type
Three-Phase V-I Measurement Load	phase-to-phase	off	off	off	yes	off	off	Complex
Three-Phase V-I	phase-to-ground	off	off	off	yes	off	off	Complex

Name	Voltage Measurement	Set Label V	Vpu	Vpu LL	Current Measurement	Set Label I	Ipu	Output Type
Measurement Supply								

System - [TM 2 Simple Open Phase](#)/Load Current Measurements

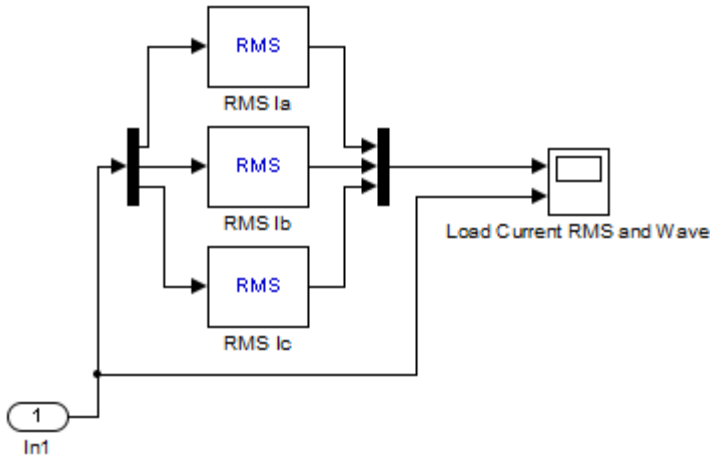


Table 14. Demux Block Properties

Name	Outputs	Display Option	Bus Selection Mode
Demux	3	bar	off

Table 15. Inport Block Properties

Name	Port	Defined In Blk
In1	1	Kv

Table 16. Mux Block Properties

Name	Inputs	Display Option
Mux	3	bar

Table 17. RMS Block Properties

Name	True RMS	Freq	RMSInit	Ts

Name	True RMS	Freq	RMSInit	Ts
RMS Ia	off	60	7.888	0
RMS Ib	off	60	7.888	0
RMS Ic	off	60	7.888	0

System - [TM 2 Simple Open Phase](#)/Load Voltage Measurements

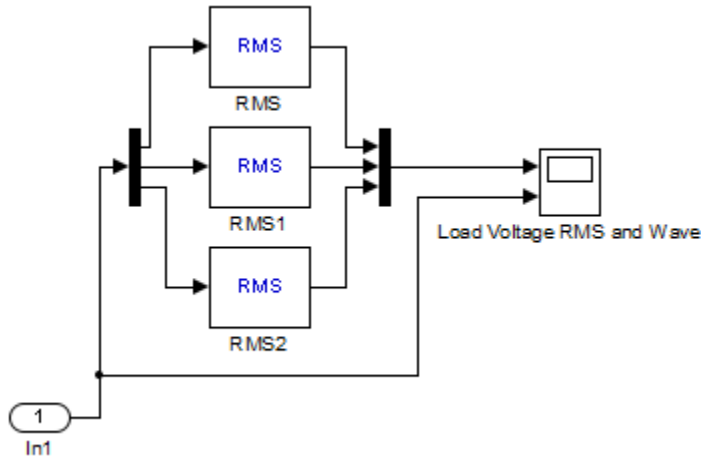


Table 18. Demux Block Properties

Name	Outputs	Display Option	Bus Selection Mode
Demux	3	bar	off

Table 19. Inport Block Properties

Name	Port	Defined In Blk
In1	1	Kv1

Table 20. Mux Block Properties

Name	Inputs	Display Option
Mux	3	bar

Table 21. RMS Block Properties

Name	True RMS	Freq	RMSInit	Ts
RMS	off	60	60	0
RMS1	off	60	60	0
RMS2	off	60	60	0

System - [TM 2 Simple Open Phase](#)/Neutral Current Measurements

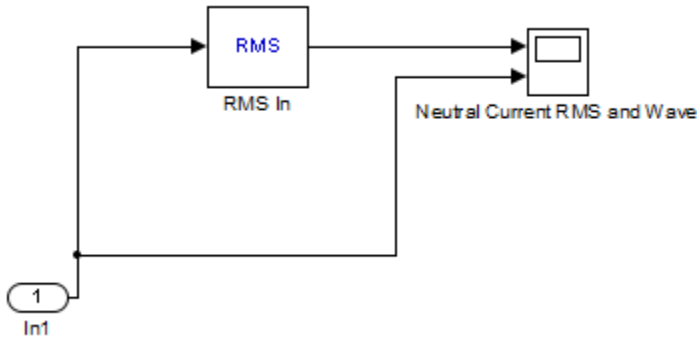


Table 22. Inport Block Properties

Name	Port	Defined In Blk
In1	1	do not delete this gain

Table 23. RMS Block Properties

Name	True RMS	Freq	RMSInit	Ts
RMS In	off	60	0	0

System - [TM 2 Simple Open Phase](#)/Supply Current Measurements

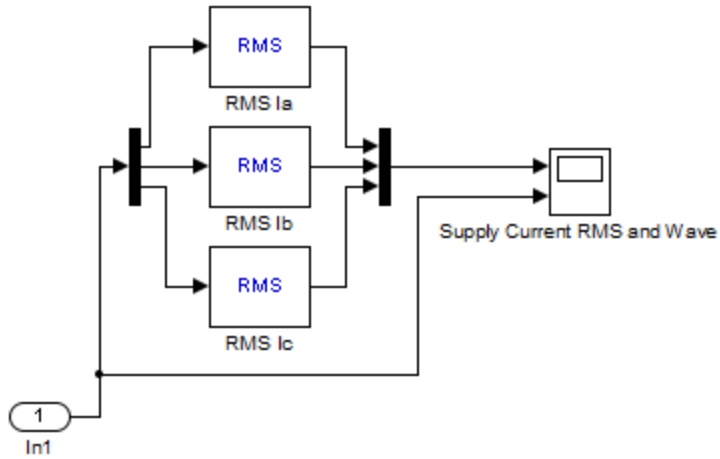


Table 24. Demux Block Properties

Name	Outputs	Display Option	Bus Selection Mode
Demux	3	bar	off

Table 25. Inport Block Properties

Name	Port	Defined In Blk
In1	1	Kv

Table 26. Mux Block Properties

Name	Inputs	Display Option
Mux	3	bar

Table 27. RMS Block Properties

Name	True RMS	Freq	RMSInit	Ts
RMS Ia	off	60	0	0
RMS Ib	off	60	0	0
RMS Ic	off	60	0	0

System - [TM 2 Simple Open Phase](#)/Supply Voltage Measurements

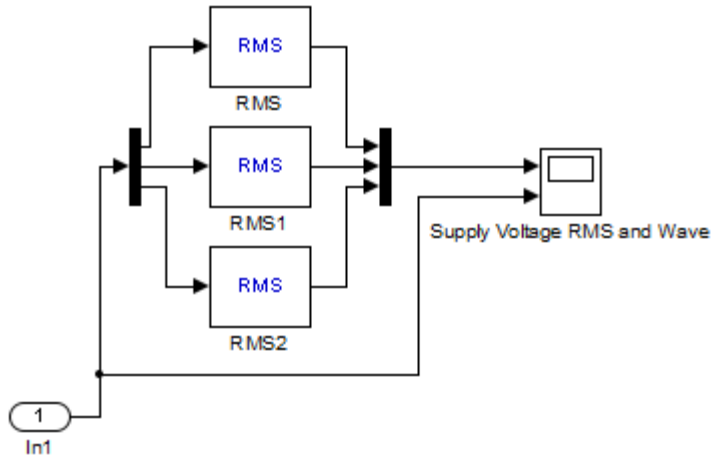


Table 28. Demux Block Properties

Name	Outputs	Display Option	Bus Selection Mode
Demux	3	bar	off

Table 29. Inport Block Properties

Name	Port	Defined In Blk
In1	1	Kv1

Table 30. Mux Block Properties

Name	Inputs	Display Option
Mux	3	bar

Table 31. RMS Block Properties

Name	True RMS	Freq	RMSInit	Ts
RMS	off	60	120	0
RMS1	off	60	120	0
RMS2	off	60	120	0

Appendix

Table 32. Block Type Count

BlockType	Count	Block Names
RMS (m)	13	RMS Ia , RMS Ib , RMS Ic , RMS , RMS1 , RMS2 , RMS In , RMS Ia , RMS Ib , RMS Ic , RMS , RMS1 , RMS2
Scope	7	Load Current RMS and Wave , Load Voltage RMS and Wave , Neutral Current Freq, Neutral Current RMS and Wave , Power Scope , Supply Current RMS and Wave , Supply Voltage RMS and Wave
SubSystem	5	Load Current Measurements , Load Voltage Measurements , Neutral Current Measurements , Supply Current Measurements , Supply Voltage Measurements
Inport	5	In1 , In1 , In1 , In1 , In1
Breaker (m)	5	Breaker LA , Breaker LB , Breaker LC , Breaker SA , Breaker SCT
Mux	4	Mux , Mux , Mux , Mux
Demux	4	Demux , Demux , Demux , Demux
Three-Phase VI Measurement (m)	2	Three-Phase V-I Measurement Load , Three-Phase V-I Measurement Supply
Fourier (m)	2	Magnitude of 180 Hz Signal , Magnitude of 60 Hz Signal1
Three-Phase Transformer (Two Windings) (m)	1	Three-Phase Transformer (Two Windings) Yg-D
Three-Phase Source (m)	1	Three-Phase Source Ideal
Three-Phase Parallel RLC Load (m)	1	Three-Phase Parallel RLC Load
Saturable Transformer (m)	1	CT 2000/5 A 25 VA
Power (3ph, Instantaneous) (m)	1	Power (3ph, Instantaneous)
PSB option menu block (m)	1	powergui
MultimeterPSB (m)	1	Multimeter
Ground (m)	1	Ground

BlockType	Count	Block Names
Current Measurement (m)	1	Neutral Current Measurement
AC Voltage Source (m)	1	AC Voltage Source

APPENDIX 3: LABORATORY DATA ON CURRENT TRANSFORMER

TESTING

Experiment 1: Determine if current transformer amplifies injection current without transformer impedance.

Supplies:

Function Generator

Current Transformer

Leads of various lengths

Current meter

Steps:

1. Set up function generator for maximum voltage output, sinewave at frequency of 180 Hz then shut off.
2. Connect output of function generator to low side of Current Transformer with Ammeter in-line to measure amount of current delivered to CT secondary.
3. Connect high side of current transformer (beginning with lowest current ratio) to Ammeter.
4. Energize function generator and measure function generator injection current and “amplified” primary CT current.
5. Shut function generator down.
6. Repeat steps 3 through 5 by increasing the current transformer ratio by the next level (ensure that the current through the primary of the current transformer will not exceed the ammeter rating).
7. Once the data is collected, determine if CT is correctly amplifying current.

Table 8: CT Experiment 1 Data

Trial	CT Ratio	Function Gen Current (A)	CT Output Current (A)
1	10:5	0.138	0.271
2	20:5	0.131	0.5
3	50:5	0.115	1.03
4	100:5	0.083	1.21
5	600:5	0.047	0.671

Experiment 2: Determine if injection current amplification is impacted by transformer zero sequence impedance.

Supplies:

Function Generator

Current Transformer

Leads of various lengths

Current meter

Bench Transformer connected in Yg primary to Delta secondary

Steps:

1. Set up function generator for maximum voltage output, sinewave at frequency of 180 Hz then shut off.
2. Connect output of function generator to low side of Current Transformer with Ammeter in-line to measure amount of current delivered to CT secondary.
3. Connect high side of current transformer (beginning with lowest current ratio) between ground and neutral point of Yg bench transformer primary.
4. Short A, B, C phases of Yg bench transformer primary together and connect to ground through ammeter.
5. Energize function generator and measure function generator injection current and “amplified” primary CT current delivered to Yg transformer primary.
6. Measure if circulating current exists in secondary Delta and measure value.
7. Shut function generator down.
8. Repeat steps 3 through 7 by increasing the current transformer ratio by the next level (ensure that the current through the primary of the current transformer will not exceed the transformer winding or ammeter rating).
9. Once the data is collected, determine if CT is correctly amplifying current.

Table 9: CT Experiment 2 Data

Trial	CT Ratio	Function Gen Current (A)	CT Output Current (A)	Delta Circulating Current (A)
1	10:5	0.136	0.256	0.16
2	20:5	0.123	0.441	0.29
3	50:5	0.086	0.587	0.39
4	100:5	0.057	0.431	0.28

Experiment 3: Determine if injection current amplification is impacted by energized transformer zero sequence impedance.

Supplies:

Function Generator

Current Transformer

Leads of various lengths

Current meter

Bench Transformer connected in Yg primary to Delta secondary

Bench power leads

Steps:

1. Set up function generator for maximum voltage output, sinewave at frequency of 180 Hz then shut off.
2. Connect output of function generator to low side of Current Transformer with Ammeter in-line to measure amount of current delivered to CT secondary.
3. Connect high side of current transformer (beginning with lowest current ratio) between ground and ammeter input.
4. Connect ammeter output to neutral point of Yg bench transformer primary.
5. Connect A, B, C phases of Yg bench transformer primary to 3-phase power supply of adequate voltage (record voltage).
6. Energize function generator and measure function generator injection current and “amplified” primary CT current delivered to Yg transformer primary.
7. Measure if circulating current exists in secondary Delta and measure value.
8. Shut function generator down.
9. Repeat steps 3 through 8 by increasing the current transformer ratio by the next level (ensure that the current through the primary of the current transformer will not exceed the transformer winding or ammeter rating).

10. Once the data is collected, determine if CT is correctly amplifying current.

Table 10: CT Experiment 3 Data

Trial	CT Ratio	Function Gen Current (A)	CT Output Current (A)	Delta Circulating Current (A)
1	10:5	0.134	0.252	0.17
2	20:5	0.121	0.427	0.26
3	50:5	0.076	0.513	0.41
4	100:5	0.051	0.350	0.26